Investigation of the NOx and PM Emissions from a Diesel Engine Operating on Nanoemulsified Fuels

by

Cornelius O' Sullivan

B.S., Mechanical Engineering
University College Dublin, Ireland
(1997)

SUBMITTED TO THE DEPARTMENT OF MECHANICAL ENGINEERING
IN PARTIAL FULFILLMENT OF THE REQUIREMENTS FOR THE DEGREE OF

MASTER OF SCIENCE IN MECHANICAL ENGINEERING

AT THE

MASSACHUSETTS INSTITUTE OF TECHNOLOGY

September 1999

© 1999 Massachusetts Institute of Technology
All rights reserved

Signature of Author_____
Department of Mechanical Engineering
July 1999

Certified by_____
Simone Hochgreb
Associate Professor of Mechanical Engineering
Thesis Supervisor

Accepted by_____
Ain A. Sonin
Chairman, Departmental Graduate Committee

MASSACHUSETTS INSTITUTE OF TECHNOLOGY
DEC 1 4 1999
LIBRARIES
ARCHIVES

Investigation of the NOx and PM Emissions from a Diesel Engine Operating on Nanoemulsified Fuels

by

Cornelius O'Sullivan

Submitted to the Department of Mechanical Engineering
on July 1st, 1999 in Partial Fulfillment of the
Requirements for the Degree of Master of Science in
Mechanical Engineering

ABSTRACT

Driven in part by concerns regarding global warming, there is a clear trend towards increased usage of compression ignition vehicles running on diesel fuel. Use of diesel fuel has a downside, namely relatively high oxides of nitrogen (NOx) and particulate matter (PM) emissions. Emulsified fuel is a mixture of water and diesel fuel. Quantum Energy Technologies Corporation (QET) have developed nanoemulsified fuels that contain water clusters in the nanometer size range. The main benefits claimed for these fuels are reduced emissions of PM and NOx without any decrease in engine performance levels compared to conventional diesel fuels.

This work investigates these benefits by running different base diesels and nanoemulsions with varying water content in a single cylinder direct injection Ricardo Hydra engine. The effect of water addition on the base diesel is modeled using a previously verified model of the test engine. The experimental and modeling results are compared to published results for conventional microemulsions.

There is no decrease in indicated fuel conversion efficiency for the nanoemulsions. For a 9% water nanoemulsion specific NOx emissions are reduced by 13 – 20% and specific PM emissions are reduced by 15 – 20% compared to the base diesel. However, these fuels do not exhibit any significant emissions improvement over conventional microemulsions.

Thesis Supervisor: Professor Simone Hochgreb

Title: Associate Professor of Mechanical Engineering

ACKNOWLEDGEMENTS

Foremost, I would like to thank my thesis advisor, Professor Simone Hochgreb, for her advice and support throughout this project. Quantum Energy Technologies Corporation (QET) provided the initial sponsorship for this project. Professor John Heywood granted me a teaching assistantship so I could complete my Master's. It was a pleasant and worthwhile experience for which I am very grateful. Without the technical expertise of Brian Corkum, Peter Menard and Professor Wai Cheng, this research would never have been completed. Their patience and support will never be forgotten. The unsurpassed organizational skills of Nancy Cook and Dr. Victor Wong made dealing with the bureaucracy of MIT a simple process.

A special thanks to Alan Shihadeh and Brian Hallgren. At the start of this research, Alan sacrificed considerable time showing me how operate the Ricardo engine, how to run his models and giving me advice on technical problems. Brian assisted me in completing my research and writing my thesis, the Ricardo has now been passed onto him. I greatly appreciated the support and friendship of Mark Dawson, Carlos Herrera, Robert Meyer, Michaela Wiegel and Ertan Yilmaz. I would also like to thank Jim Cowart, David Kayes, Derek Kim, Ioannis Kitsopanidis, Gary Lansberg, Bertrand Lecointe, Helen Liu, Marcus Megerle, Conor McNally, Chris O'Brien, Matt Rublewski, Daisuke Suzuki, Dr. Tian Tian, Benoist Thirouard, Brad VanDerWege and Rik Waero for their friendship and help in various forms during my time in the Sloan Lab.

Outside the lab, Steve Lasher provided expert advice and assistance in trouble-shooting the SMPS system. Everyone involved with the MIT Rugby Club provided a welcome escape from work at MIT. Leslie Regan was a continuous source of help in dealing with the M.E. Department. There is no doubt that the Department would be lost without her. The encouragement of Ruairi Cunningham, Murrough O'Brien and the prayers of Brother Ronan White will be remembered.

Finally, I would like to thank my family, especially my father for his rapid courier service from Ireland of parts for the Ricardo engine. Even though my family is far away, their support has always been with me. I dedicate this thesis to them.

TABLE OF CONTENTS

Page

LIST OF TABLES

LIST OF FIGURES

Page

LIST OF FIGURES

Page

CHAPTER 1

INTRODUCTION

1.1 Background

Driven in part by concerns regarding global warming, there is a clear trend toward increased sales of compression ignition (CI) vehicles running on diesel fuel, in particular light duty vehicles, in many parts of the world. This trend can result in many positive environmental benefits, e.g. low fuel consumption, therefore low levels of CO_2, low levels of gaseous exhaust CO and HC (especially during cold start conditions), and very low levels of evaporative hydrocarbons. However, increased use of diesel fuel has a downside, namely relatively high oxides of nitrogen (NOx) and particulate emissions.

1.2 NOx and Particulate Matter Emissions

The emissions of oxides of nitrogen (NOx) are a concern because of their direct adverse health effects and as a precursor to photochemical smog (ozone). In addition, NOx is a significant contributor to acid precipitation in many countries.

Diesel derived particulates, because of their chemical composition and extremely small size, have raised a host of health and environmental concerns. Particulate matter (PM) consists mostly of three components: soot formed during combustion, heavy hydrocarbons condensed or absorbed on the soot, and sulfates. A schematic of PM composition is shown in Figure 1.1. In older diesel engines, soot was typically 40% to 80% of the total particulate mass. Developments in hardware, for example high-pressure injection, electronically controlled injection and pilot injection have reduced the soot contribution to PM from modern engines considerably. Much of the remaining PM consists of heavy hydrocarbons absorbed or condensed on the soot. This is referred to as the soluble organic fraction of the particulate matter, or SOF. The SOF is derived partly

from the lubricating oil, partly from the unburned fuel, and partly from compounds formed during combustion.

US Environmental Protection Agency standards for PM are based in part on health studies which show a strong correlation between mortality and the mass of fine particles below 2.5 μm [1]. The International Agency for research on Cancer (IARC) in June 1988 concluded that diesel particulate is probably carcinogenic to humans. Other studies have raised concerns about even smaller particles, **ultrafine particles** and **nanoparticles**, which are defined as those smaller than 100 nm and 50 nm diameter, respectively. It has been suggested that these smaller respirable particles could be more detrimental to health through the development of lung cancer. Although modern engines emit low particle total *mass* concentrations they may actually emit larger *number* concentrations than older designs. Most of the particles emitted are in the nanoparticle range on a number basis [2], so a large number concentration implies a large nanoparticle concentration. A recent report released by the Health Effects Institute [3] showed that a modern high-pressure direct injection diesel engine emits at least one order of magnitude higher number concentrations than older technology engines.

1.2.1 Regulations

Many countries are pushing aggressively to reduce diesel emissions. On November 5th 1998, the California Air Resources Board (CARB) adopted a plan to require gasoline-fueled and diesel-fueled light duty vehicles to meet tighter emission standards beginning in 2004. Most notably, vehicles will be required to meet identical standards for CO, HC and NOx regardless of the fuel used. Beginning with the 2004 model year, all light-duty LEVs and ULEVs should meet a 0.05 g/mile NOx standard to be phased in over a three-year period. A full useful life PM standard of 0.01 g/mile will be introduced for light duty diesel vehicles and trucks less than 8500 lbs. gross weight certifying to LEV, ULEV, and SULEV standards.

Table 1.1 California LEV II Light Duty Vehicles (<8500 lbs.) Emission Standards

Category	Mileage for Compliance	NMOG (g/mile)	Carbon Monoxide (g/mile)	Oxides of Nitrogen (g/mile)	Diesel Particulate (g/mile)
TLEV	50,000 miles /5 years	0.125	3.4	0.40	-
LEV		0.075	3.4	0.05	-
ULEV		0.040	1.7	0.05	-
TLEV	120,000 miles /11 years	0.156	4.2	0.6	0.04
LEV		0.090	4.2	0.07	0.01
ULEV		0.055	2.1	0.07	0.01
SULEV		0.010	1.0	0.02	0.01

1.3 Diesel Combustion

Diesel combustion is a complex process. Significant progress has been recently made in furthering our understanding of the diesel combustion process. A recent SAE paper by Flynn et al., [4] proposes a structure for the process based on a combination of previously published and new results.

Initial injection and ignition

Figure 1.2 shows the early stages of diesel combustion as suggested by Dec and Flynn et al., [4, 5]. As liquid leaves the nozzle as a jet it rapidly entrains hot in-cylinder air which initiates fuel vaporization. This leads to the formation of a sheath of fuel-vapor/air in the shear layer along the sides of the jet and leading edge. The vaporizing fuel jet grows and its temperature increases to approximately 750 K. At this temperature, oxidation/breakdown reactions of the high cetane components begin to occur. This process, along with additional hot air entrainment increases the temperature to about 825 K, thereby increasing the oxidation reactions. C_2H_2, C_2H_4, C_3H_3 fuel fragments, CO and H_2O are formed during this process.

The fuel fragments are precursors to the polyaromatic structures that lead to soot. As these partial oxidation products are formed, they are pushed aside by the penetrating jet. At the same time a diffusion flame begins to form as a flame sheath around the periphery of the cloud of partial oxidation products. Figure 1.3 shows the burning jet once quasi-steady processes are established. Now the liquid fuel jet temperature rises from ~350 K (injection temperature) to ~650 K before it enters the region surrounded by the diffusion flame sheath. Inside the diffusion flame sheath the recirculated products of partial oxidation can be entrained in the jet increasing the temperature to ~825 K where oxidation reactions can be completed rapidly. These reactions consume all locally available oxygen and leave a mixture of CO, CO_2, water vapor and fuel fragments at about 1600 K (see Figure 1.4).

Radiative and convective heat transfer from the diffusion flame sheath increases the temperature of the fuel fragments as they are transported through the plume towards the boundary of the diffusion flame sheath. In the diffusion flame the fuel fragments are converted to CO_2 and water vapor, liberating the rest of the heat of combustion. The local temperature rises to ~2500 K in the flame sheath, providing an ideal environment for NOx formation reactions.

1.4 Emulsions

An emulsion is a heterogeneous system, consisting of a least one immiscible liquid intimately dispersed in another in the form of droplets. Microemulsions are a class of emulsions which is distinguished by droplet diameters less than 0.2 microns. They are characterized by inherent stability, optical clarity and minimum work input for formation.

During the past twenty years, research results [6 -11] have shown that diesel engines can effectively utilize an emulsion of water in diesel fuel. Two types of emulsion have been investigated: stable and unstable emulsions. A stable emulsion is one that relies upon the use of an emulsifying agent and some degree of mechanical agitation to produce a clear

liquid, which does not "readily" separate into two layers of immiscible components. An unstable emulsion of water in diesel fuel is one, which uses little, if any, chemical-stabilizing agent but relies almost entirely upon strong agitation to achieve a short-lived uniform dispersion.

An emulsifying agent/surfactant is employed in the water emulsion formulation to increase the ease of formation and/or promote the stability of the emulsion. Emulsion formation is aided by the emulsifying agent by reducing interfacial tension and allowing the formation of a greatly enlarged interfacial area with minimum energy input via mechanical agitation. Surfactants are usually quite complex organic materials, e.g. carboxylic acids, esters, and amines.

1.4.1 Combustion of Emulsified Fuels

When water is introduced, fundamental changes in the combustion maybe associated with the "microexplosion" phenomenon investigated by Dryer et al [12] and Sheng et al [13]. In this phenomenon, small droplets of dispersed water in a larger emulsion fuel droplet are subject to rapid vaporization when the droplet is placed in a high temperature environment after injection. This early vaporization can be so disruptive as to shatter the emulsion droplet into a large number of small fragments. The resulting increase in evaporation surface and improvement in fuel atomization and mixing is hypothesized to be responsible for an observed increase in the burning rate [8] and reduction in the PM of emulsions relative to neat diesel. Further reduction may occur due to improved soot oxidation by OH radicals resulting from partial dissociation of the water. Raising chamber pressure has little effect on the occurrence of the explosion, but the penetration of the droplet fragments will be much shorter due to higher gas density, which weakens the effect of the explosion. Increasing the water content of the emulsion fuel droplet enhances the rapidity and violence of the microexplosions and results in a faster burning rate.

From a thermal aspect, the incorporation of water in an emulsion with the diesel fuel acts as a charge diluent, resulting in lower local flame temperatures as well as lower oxygen concentration. The high latent heat of vaporization reduces cylinder temperature and pressure. These effects reduce the rate of NOx formation, which is highly temperature dependent. Counteracting these effects is the higher burning rate due to better mixing caused by microexplosions and greater air entrainment.

1.4.2 Effect on Emissions

Most investigators have found a reduction in NOx and some have found significant reduction in PM/smoke with the use of water-based emulsions in CI engines. Andrews et al [10] found a 15% reduction in NOx with 5% water by mass* and a 40% reduction with 10% water at high load conditions. There was also a 70% reduction in PM (mass basis) with 10% water. Murayama et al [6] reported a 20% NOx reduction with 15% water by mass and a 55% reduction in smoke with 25% water. Crookes et al [8, 9] reported a 12% NOx reduction and no significant reduction in smoke for a 10% water emulsion in a single cylinder Gardner engine. For a multi-cylinder DI Ford engine they found a 20% reduction in NOx but an increase in smoke number for 10% water. In a U.S. DOE assessment of emulsion technology [11] an IDI Deutz engine achieved a 25% reduction in NOx for a 10 % water emulsion, however the operating conditions was not reported.

1.4.3 Performance

When compared directly on a mass of emulsified fuel vs. fuel basis the brake specific fuel consumption is obviously better for the neat diesel since water has zero heating value. However, when comparing energy input small improvements (ca. 5%) in thermal efficiencies have been reported [7, 14].

---

* The water content is always by mass unless otherwise stated.

The improvement in efficiency may be caused by the following,

- The microexplosion effect resulting in better air-fuel mixing.
- Increased air-entrainment in the spray due to increased spray momentum.
- Increased local excess air ratio in the spray due to water substituted in the fuel.
- Decreased cooling loss due to lower combustion temperature and a less luminous flame.
- Suppression of thermal dissociation during combustion due to lower combustion temperature.

Table 1.2 Specifications of Test Engines Utilized in Emulsion Studies*

Investigator	Tsukahara [6]	Andrews [10]	Crookes [8]	Crookes [8]
Engine	Kubota – LC Marine Single Cylinder	Petter Type Single Cylinder	Gardner IL2 Single Cylinder	Ford 4-cylinder
Displacement per Cylinder (cc)	1425	533	1510	625
Compression Ratio	17.4	19	14	19
Test Speed (rpm)	1200	1500	1500	2500
Injector Opening Pressure (MPa)	29.4	n/a	16.2	24.3
Type of Injection	DI – Bowl in Piston	DI	DI 4-nozzle	DI 4 -nozzle

* Note: It is generally accepted that engine design has a greater influence on emissions levels than diesel fuel quality or additives. In particular the responses of light duty vehicles and heavy duty to changes in fuel properties or addition of water are different. Thus it is difficult to draw general conclusions on how changes in any single fuel property or addition of water will influence emissions from a wide range of engines.

1.5 Alternative Methods of Water Addition

It is worth comparing emulsions to other methods of water addition, which also utilize the heat of vaporization of water for reducing the combustion chamber and flame temperatures, thereby reducing NOx formation.

Alternative methods utilized are:

1. Stratified diesel fuel-water-diesel fuel (DWD) injection by means of a specially modified nozzle [15].
2. Water injection into the combustion chamber by means of a separate nozzle.
3. Water injection into the inlet manifold (fumigation).

In order to achieve the maximum NOx reduction from a minimum amount of water addition, the water must be brought to the correct spot at the correct time, namely to those areas in the combustion chamber where the highest temperatures prevail for considerable periods of time, i.e. the post-flame areas. For this reason it is essential to introduce the water in intimate contact with the diesel fuel. This is the case when diesel fuel-water emulsions are injected as well as with the DWD injection method. The other methods, (2) and (3), are unfavorable as they supply water to areas where it is ineffective or even harmful in other respects. Thus, the amount of water required for a certain NOx reduction is much greater than with an emulsified fuel. This excessive quantity of water reduces the temperature level all over the combustion chamber to the extent that soot oxidation is impeded and HC emission increased, resulting in an increased PM emission. In addition, lubricating oil dilution, corrosion and increased wear are also observed with methods (2) and (3).

The DWD method has the advantage compared to the diesel emulsion injection that the amount of water injected can be quickly varied depending on engine load and speed, which is very important in view of transient operating conditions and during cold start.

Moreover, since in the DWD method only diesel is injected at the beginning of the cycle, the ignition delay is not increased, avoiding the engine noise and retarded combustion associated with emulsions [16]. The disadvantages of this system are the large expenditure for the injection nozzle and water supply system and the technical issues relating to an anti-freeze system and a water quantity control method.

Table 1.3 Comparison of water addition methods

	Inlet manifold water injection	**Direct water injection with separate nozzle**	**Stratified diesel-water-diesel injection**	**Diesel fuel-water emulsion**
Relative NOx reduction	Poor	Poor	Best	Good
Effect on PM emissions	Poor	Poor	Best	Good
Variability of water addition	Good	Good	Poor	Good
Lubricating oil dilution	High	High	Low	Low
Expenditure	Low	High	Average	High

1.6 QET Nanoemulsified Fuels

1.6.1 Background

Quantum Energy Technologies Corporation (QET) have developed nanoemulsified water/diesel fuels, which contain water clusters in the nanometer size range. The main benefits claimed for these fuels are reduced emissions of particulates (typically 30 – 50%) and NOx (typically 20 –50%) whilst maintaining engine performance at close to conventional diesel fuel levels. It is suggested that the reduction of PM is not only due to the thermal and physical effects discussed in Section 1.4, but perhaps also due to the "catalytic" effects of the nanoclusters present in the emulsion. A mechanism for this has been postulated by QET, involving the molecular orbital interaction of water clusters

with aromatic and polyaromatic soot precursors leading to catalysis of the oxidation of these precursors in-cylinder. Little is known about this postulated phenomenon. The detailed theory is beyond the scope of this research. The objectives of the current study, as described in Section 1.7 were to test whether current understanding of the expected effects could explain the behavior of nanoemulsified fuels in a CI engine.

1.6.2 Nanoemulsified Fuel Composition

The exact emulsion compositions are QET proprietary information, however each emulsion was made up of the following components:

1. A base diesel fuel
2. Water (6% - 12% Range)
3. A surfactant which is usually a naturally occurring fatty acid.
4. A co-surfactant which is usually a relatively low molecular weight alcohol.
5. A neutralizer, either ammonia or monoethanolamine, which partly neutralizes the surfactant.

A cetane improver, ethyl hexyl nitrate was added to some of the fuels.

1.7 Objectives

The objectives of this investigation were:

1. To determine the effect of nanoemulsions with different chemical and structural properties on NOx, particulate matter (PM) and fuel consumption
2. To determine the effect of nanoemulsions with varying amounts of water and different base fuels on NOx, particulate matter (PM) and fuel consumption
3. To determine the effect of running an engine with nanoemulsified fuels on engine operation, corrosion, and wear.

4. To provide an interpretation of the data regarding the contribution of thermal, chemical and potential quantum effects on the engine performance and emissions.

Test Matrix

Originally a test matrix was proposed to span a range of different compositions to be compared. The reasoning behind this was to quantify the effect of each composition variable, e.g. water content, surfactant to water ratio, while attempting to keep other composition variables constant. Normal non-nanostructured emulsions with similar water content and composition were also to be tested to quantify the catalytic phenomenon proposed by QET.

However during the project QET changed the base fuels to fuels being used in similar testing performed at Statoil (in Norway) in order to compare results. Then the number of tests performed was later reduced due to financial constraints experienced by QET. Therefore, only the water content and type of base fuel was varied and even then the test matrix was not complete due to a lack of sufficient test fuels.

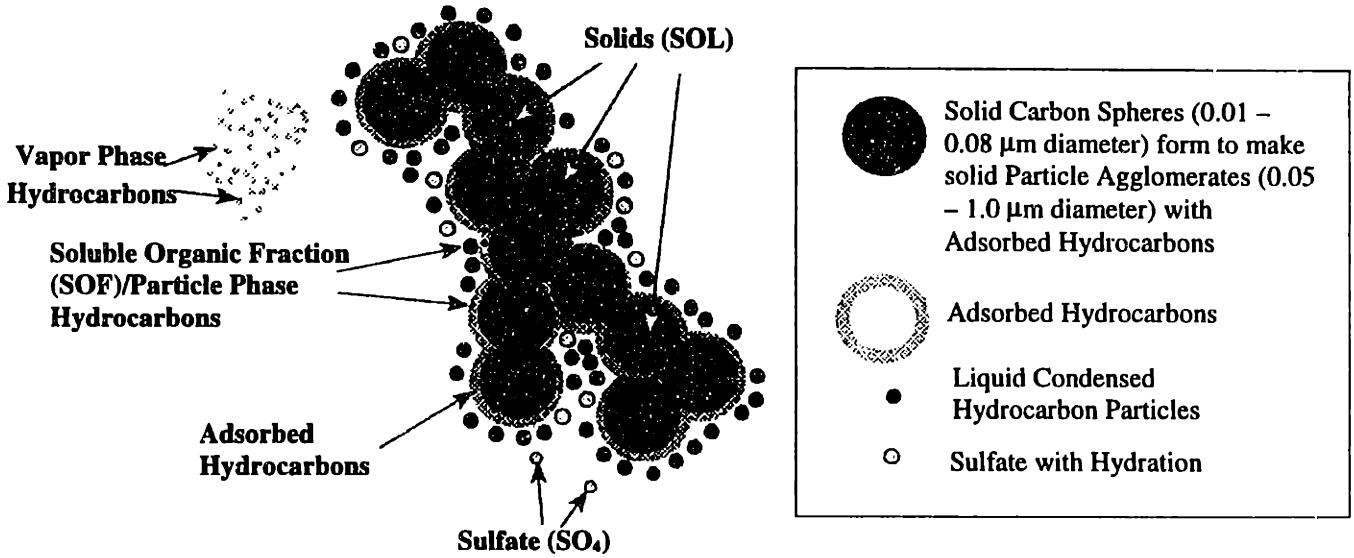

Figure 1.1 Schematic of Diesel Particulates and Vapor Phase Compounds

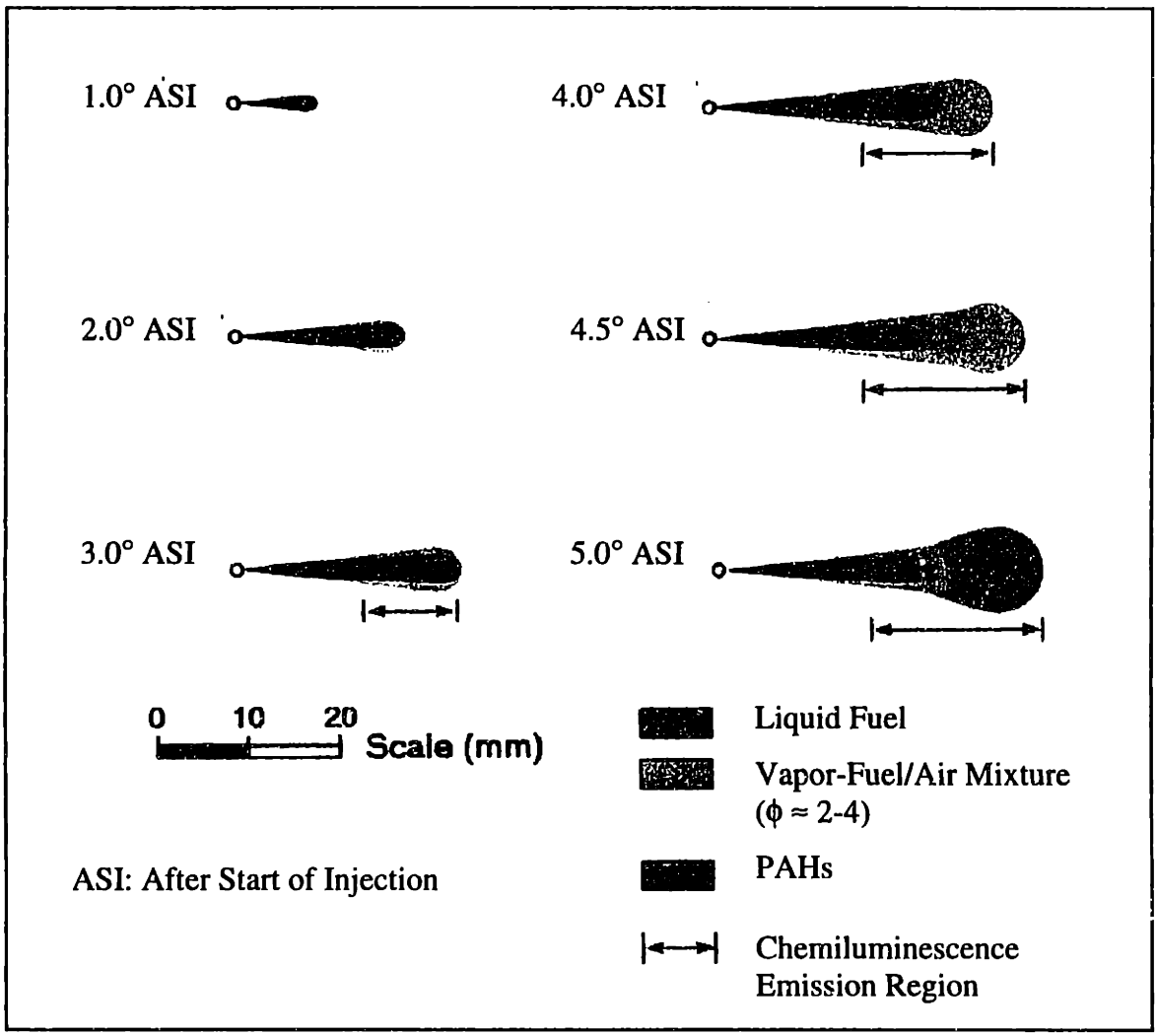

Figure 1.2 Schematic of Developing Spray and Flame

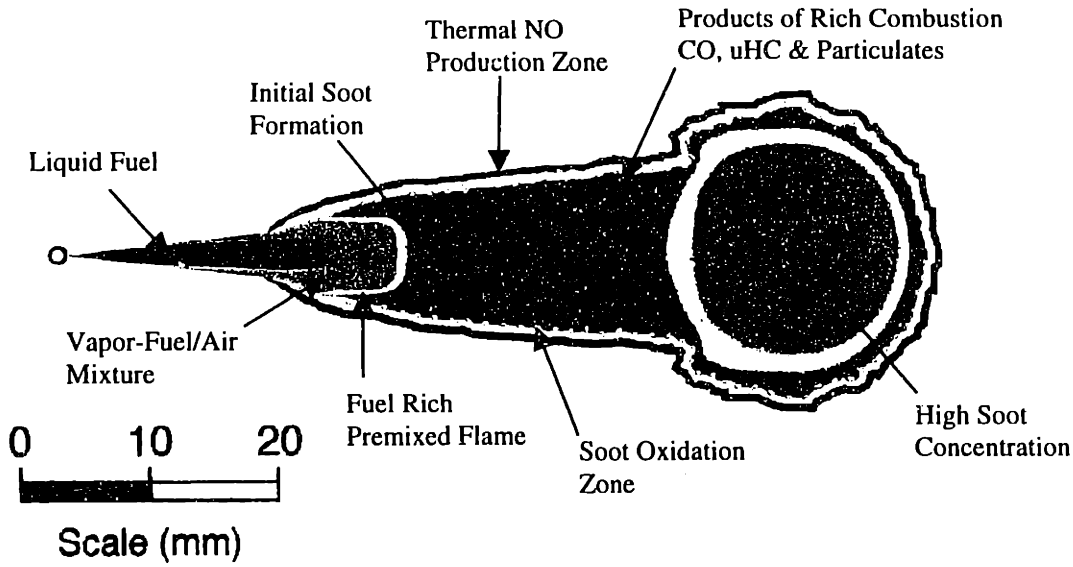

Figure 1.3 Composition of Burning Jet (after Flynn et al., [4])

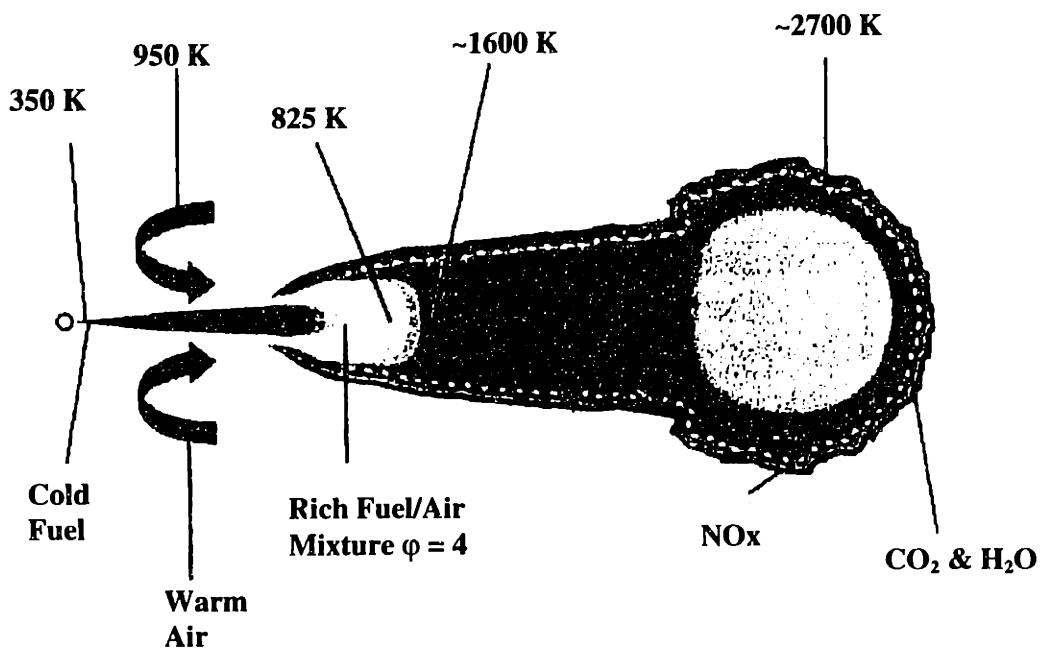

Figure 1.4 Temperatures in Burning Jet (after Flynn et al., [4])

CHAPTER 2

EXPERIMENTAL SETUP

2.1 Test-Engine

The experimental engine used was a single cylinder direct injection Ricardo/Cussons standard Hydra engine connected to a Dynamatic Model 20 AC Dynamometer with a Digilog controller.

Engine specifications are shown in Table 2.1. The fuel injection system utilizes a Bosch type A in-line fuel pump and a four-hole injector nozzle which opens at 250 bar, the fuel pump delivering a maximum pressure of 600 bar, which is low, compared to modern high speed diesels. The fuel flowrate is varied using a servomotor acting as the rack actuator. Injection timing is varied by rotating the fuel pump relative to the crankshaft through an electronic actuator. The engine achieves rapid air fuel mixing by utilized a toroidal bowl in the piston. Its bore/stroke ratio and operating speed are typical of modern light-duty diesel engines.

2.2 Measurement Equipment

2.2.1 Cylinder Pressure Transducer

Cylinder pressure was measured using a flush-mounted Kistler 6125 piezo-electric transducer inserted into the head opposite the injector. The transducer signal is converted to a voltage and amplified using a Kistler model 504 charge amplifier. Using a shaft encoder as the clock the pressure signal is taken every crank angle with a PC based data acquisition system and bottom center of compression is superimposed on the signal by a 2 volt spike triggered by the shaft encoder.

The transducer calibration drifted between calibrations, so it was replaced with a new one. To check the transducer linearity and the engine compression, motoring pressure

data was acquired and log P vs. log V plots were made. This was compared to data in the Ford Standard Manual [17] and the polytropic compression exponent of 1.31 was within the recommended range (1.24 – 1.35). This confirmed that blowby or valve leakage was not excessive.

2.2.2 Needle Lift Indicator

The injector body has a Wolff Controls Corp. Hall-effect proximity sensor in it. The sensor delivers a differential voltage signal via a signal conditioner. The indicator was used to show the actual start of injection and to check that the injection profile was normal. Needle lift and pressure data were acquired simultaneously over 100 cycles using Global Lab data acquisition software. A FORTRAN program used this data to calculate average imep, average peak pressure, peak pressure location, and start of injection (SOI) over 100 cycles.

Table 2.1 Test Engine Specifications

Model	Ricardo Hydra Mark 4	
Number of Cylinders	1	
Bore (mm)	80.26	
Stroke (mm)	88.9	
Displacement (liters)	0.4498	
Compression ratio	19.8	
Valve Timing	IO – 10 DBTC	IC – 41 DABC
	EO – 58 DBBC	EC – 11 DATC
Maximum Speed (rpm)	4500	
Maximum Power (kW)	8	
Oil Outlet Temperature (°C)	85	
Coolant Outlet Temperature (°C)	85	
Injector Nozzle	4 hole x 0.21 mm dia x 155° cone angle	
Pump Type	Bosch A-type (max. pressure = 600 bar)	

2.3 Fuel Metering System

The complete fuel system is shown in Figure 2.1. A secondary fuel metering system was set up for the emulsion and base test fuels for the following reasons:

1) To minimize contamination of the main line with emulsion fuel and to reduce the amount of time to be reasonably confident that the previous test fuel is purged from the system. This saved time and fuel.

2) To enable operation of the engine on the baseline diesel at the beginning and end of a test so as to check baseline conditions.

3) To purge the emulsion fuels from the fuel pump, injector and fuel system after testing to minimize corrosion effects due to these components soaking in the emulsion over a long period.

4) To utilize a gravimetric fuel measuring system (electronic balance) in place of the less accurate MAX™ Rotary Flowmeter on the main fuel system.

This system was configured to allow on-line switching while running the engine in order to keep the engine at steady state operating temperature when switching between test fuels. Heat exchangers were utilized to maintain the fuel temperature constant at ~ 30 °C at the pump inlet and to avoid separation of the emulsions. Stainless steel mesh filters were used in the circulation system to prevent particles causing wear in the pump or the injector. A check valve was used on the test fuel line to prevent return line flow interfering with the test fuel flow measurement.

2.4 Measurement of Particulate Matter

2.4.1 Mini-Dilution Tunnel

The particulates were collected using a mini dilution tunnel. For regulatory purposes, diesel particulates are defined as all solid or liquid matter that collects on a filter in a diluted exhaust stream at temperatures equal to or less than 52°C. So the purpose of the dilution system is to simulate approximately the atmospheric dilution process and cool the exhaust to an ambient temperature less than 52 °C. This is the temperature mandated by the EPA. A schematic of the system is shown in Figure 2.2. Clean, oil-free compressed air is supplied from a 100-psig compressor. A 2" Balson A15/80-DX filter is installed in the line to remove moisture and any particles from the dilution air. It is 93% efficient at 0.01 μm. After the filter the dilution air enters the 2" diameter tunnel and passes through a venturi contraction. This causes a below atmospheric pressure drop, which draws a continuous exhaust sample into the tunnel through the exhaust transfer tube which connects the tunnel to the 2" diameter main exhaust line. The original transfer tube used in previous research [18] was a long flexible U-shaped section. This was replaced with a shorter straight section with a flexible coupling to avoid build-up of particulates in the line and simplify cleaning of the tunnel.

The dilution air and exhaust mix over approximately 33" before sampling. An effective length greater than ten times the diameter is recommended to ensure complete mixing [19]. A sample of the diluted exhaust is drawn from the tunnel using a critical flow orifice and vacuum pump. Initially, a wet test gas flow meter was used in previous research. However, the flowrate used was 3-4 times the recommended maximum flowrate for the wet test meter and therefore the set-up was replaced with a critical flow orifice. The sample line is 3/8" 316 stainless steel tubing. The sample is drawn through 47 mm filters mounted in a BGI stainless steel 47 mm filter holder, then through an O'Keefe Controls precision orifice. Pressure on either side of orifice was monitored to ensure choked flow in the line. In order to have choked flow the downstream-to-upstream absolute pressure ratio across the orifice must be less than 0.528. As particulate built up

on the filter the pressure downstream of the filter (upstream of the orifice) decreased and although the volume flowrate through the orifice was constant, the mass flowrate decreased. The sampling pump was switched off and the sampling line closed before the upstream pressure dropped too low and flow was no longer choked. The upstream pressure was recorded periodically and an average sample mass flow was calculated for each filter sample.

In order to calculate the dilution ratio for the tunnel, volume $\%CO_2$ (on a dry basis) was measured in the main exhaust line and the tunnel. The background volume $\%CO_2$ in the dilution air was also measured. The dilution ratio, r_d was calculated using the following formula.

$$r_d = \frac{[CO_2]_{exh} - [CO_2]_{bg}}{[CO_2]_{dil} - [CO_2]_{bg}} - 1 \tag{2.1}$$

Where r_d is the ratio of dilution air to raw exhaust (on a molar basis),
$[CO_2]_{dil}$ is the volume $\%CO_2$ in diluted exhaust, $[CO_2]_{exh}$ is the volume $\%CO_2$ in raw exhaust, and $[CO_2]_{bg}$ is the volume $\%CO_2$ in pure dilution air. (See Appendix A).

2.4.2 Filter Handling, Conditioning and Weighing

EPA recommended Pallflex TX40H120WW Teflon filters were used. These are recommended for critical sampling tests where purity and non-hygroscopic properties of Teflon are needed, e.g. diesel exhaust measurements [20]. The filter efficiency at 0.3 μm is 99.9% at a filter face velocity of 320 cm/s. EPA guidelines were followed when conditioning, handling and weighing the filters. Each set of filters was conditioned for 24 hours before initial weighing and 20 ± 4 hours after testing before final weighing. In the time period between October and December when a set of filter measurements were made the conditioning room temperature was 25 ± 3°C and humidity was 35 ± 5%. These values were within the EPA specified range. Temperature and humidity were measured using a Cole-Palmer Thermohygrometer.

An Ohaus Explorer E11140 microbalance was used for filter weighing; it is accurate to 0.05 mg [21]. This was the largest source of error in the filter measurements. The average mass collected on the filter was ~ 2.5 mg and each filter was weighed before and after leading to an accuracy of ± 0.1 mg. Therefore, there is on average a 4% error in the filter measurements. To reduce this error a higher mass could have been collected on the filter. However, this would have required either a longer sampling time and/or a higher sample flow rate. The average sampling time at a flow rate of 25 liters per minute was 20 minutes per filter. Two filters were taken for each point and taking into account the time to place and remove the filters and the time to reach steady state conditions for the tunnel and engine, the time to take a point was approximately one hour. A higher sample flow rate would have required a larger flow orifice and therefore a larger vacuum pump. Taking these factors into consideration an error of 4% was acceptable.

Effect of Dilution Ratio and Sampling Flowrate on Mass Collected

As dilution ratio increases, mixture temperature decreases and particle concentration decreases. Decreasing temperature increases the propensity for condensation and adsorption, however this is offset by decreasing concentration reducing the number of collisions. At low dilution ratios the temperature effect dominates causing PM to increase with dilution ratio. At high dilution ratios the opposite is the case. There is an optimum range of dilution ratios where the sensitivity to dilution ratio is minimized. Modeling work by Amann et al. and MacDonald et al. and experimental work by Kayes [22, 23, 24] suggest a ratio in the range of 10 – 20.

Therefore a dilution ratio of 15 was chosen for filter measurements. This was checked by taking two sets of filter measurements at dilution ratios of 13, 15 and 17. The total PM measurements, when corrected for dilution ratio, had at most a difference of 6%. This was between one filter at 15 and one at 17.

Hirakouchi et al. [19] found that when the sampling flowrate was increased from half isokinetic flow to three times isokinetic there was no significant change in PM measurement. To verify this for the sampling setup, three different critical flow orifices were used, with nominal flows of 20, 25 and 38 liters per minute. However it was found that for the 38-lpm orifice the PM measurements were 8-10% lower than the other two orifices. This may have been due to the fact that the ratio of the pressures across the orifice was close to the critical ratio for choked flow and the flow may not have been choked for the whole sampling period. The PM measurements for the two lower flowrates were within 3% and a flowrate of 25 lpm was chosen for running tests since it gave shorter sampling times.

In order to check the effect of tunnel build up and the purity of the dilution air, dilution air was sampled for fifty minutes with the exhaust line closed off. No increase in pressure drop across the filter was observed. When removed the filter was slightly gray and the mass deposited was 0.1 mg, which is within the error range of the weighing system. Therefore once the transfer tube was cleaned regularly tunnel build up could be neglected.

2.4.3 Scanning Mobility Particle Sizer

Scanning Mobility Particle Sizer (SMPS)

A SMPS (TSI Inc. no. 3071) is used to measure particle size distributions and concentrations. A schematic diagram is shown in Figure 2.3. It consists of a neutralizer/charger, a mobility section, a particle detection instrument and a computerized control and data acquisition system. A sample of diluted exhaust is drawn from the dilution tunnel through an impactor, which separates out larger particles (See Table 2.1) and into the Electrostatic Classifier. The particles in the sample/polydisperse-flow pass through a radioactive source (Krypton 85) bipolar ion neutralizer. This brings particle charge distribution level to a minimum Boltzmann's distribution of charge. The flow

then enters the mobility section close to its inner surface. Clean sheath air flows close to the central rod. When the scan voltage is applied to the rod, positively charged particles move in the radial direction at a rate dependent on their size and the scan voltage. Particles with too little aerodynamic drag are drawn toward the charged tube so rapidly that they do not reach the holes for the monodisperse flow. Particles with too high a drag (large aerodynamic diameter) are not drawn in sufficiently to reach these holes. Therefore at a specific voltage and flowrate only a particular size range of particles flows to the Condensation Particle Counter.

Condensation Particle Counter (CPC)

The CPC (TSI Inc. no. 3010) measures particle concentration downstream of the SMPS. A schematic of the system is shown in Figure 2.4. It consists of a saturator, condenser, particle sensor, flow control orifice, and pump. The aerosol entering the instrument is first saturated with alcohol and then cooled in the condenser tube. During the cooling process alcohol condenses on the particles and then they flow into a particle sensing region. A laser light source is focused on a narrow volume in this region. The individual particles generate pulses as they pass through. These pulses are counted by the CPC, which has 50% detection efficiency at 10 nm diameter. It operates in single count mode up to 10,000 particle/cm^3. An automatic correction scheme accounts for the probability of having more than one particle in the view volume simultaneously.

Table 2.2 SMPS Test Range

Test Range	Polydisperse Flowrate (lpm)	Sheath Air Flowrate (lpm)	Impactor Orifice Size (cm)	50 % Number Cut-off Diameter (μm)	SMPS Scan Range (nm)
1	0.7	7	0.0457	0.503	9.0–379
2	0.2	2	0.0508	1.006	19.8 –965

Initial SMPS Setup

There were some initial problems when operating the SMPS. It was configured to operate in underpressure mode i.e. the polydisperse flow is at or below atmospheric pressure. However the tunnel operates above atmospheric pressure (~ 1.3 bar absolute) since it is supplied from a compressor. Following recommendations from TSI [25], the Tygon sample line was opened to atmosphere thus bringing the pressure down to 1.05 bar just upstream of the impactor. Flowrates for monodisperse, excess and sheath air were set by turning valves until a voltage that corresponds to the desired flow was reached. These flowrates and their corresponding voltages are listed in the Classifier manual [26]. However it was discovered when comparing the SMPS to a second SMPS in a different lab that the actual flowrates were higher than those set, leading to higher particle counts. This was due to particle build-up in the monodisperse hot wire flow meter. This problem was corrected by cleaning the sensor and recalibrating the flows with an A.P. Buck bubble flowmeter.

Dilution Ratio for SMPS

Abdul-Khalek et al [2] used a dilution ratio of about 1000 in their studies of diesel exhaust particulates. The reasoning for this is based on simulating the emission from the tailpipe into air from a moving car as well as preventing saturation of the CPC and reducing the rate of soot build up in the classifier. For this research, due to limitations in the range of the CO_2 analyzer and inaccuracy of the NOx analyzer at low concentrations, a dilution ratio of around 50 had to be used as a compromise between satisfactory accuracy and prevention of saturation of the CPC (< 10,000 particle/cm^3). Build up was minimized by only connecting the sample line to the tunnel when taking scans and drawing room air when not scanning, instead of continuously pulling an exhaust sample through it.

SMPS Measurements

Test cell air, dilution air and baseline diesel fuel number and volume measurements were taken at the beginning and end of each set of tests. The average test cell air particle content was 2.0 x 10^4 particles/cm^3 at the beginning and 4.1 x 10^4 particles/cm^3 at the end of the tests. This increase was due to exhaust from the trench mixing with the cell air. Average number concentration for the dilution air was 1.8 x 10^2 particles/cm^3, indicating that the dilution air is over 100 times cleaner than the lab-cell air.

The average baseline diesel number concentration was 2.1 x 10^6 particles/cm^3 at a dilution ratio of 50. Therefore the concentration of the undiluted exhaust was 1.05 x 10^8 particles/cm^3. The maximum variation between any two days was 20% and the maximum variation on a given day was 7%. The average day to day variation was 10% and the average variation between the beginning and end of tests was 5%.

2.5 Emissions Measurement

Percentage CO_2 on a dry basis was measured using a non-disperse infrared analyzer (Rosemount Analytical Model 880A). A 10% range was used for main exhaust and a 1% range for the diluted exhaust. Fourth order polynomial calibration curves were determined for the ranges using calibration gases and a gas divider with nitrogen as the dilution gas. NOx (ppm dry) was measured using a chemiluminescent NOx analyzer (Thermo Environmental Model 10A). This device operates on a linear scale, so a single 990ppm NO span gas was used for calibration.

Problems with the NOx Analyzer and Exhaust Sampling Method

During the initial emulsion tests it was observed that the NOx readings were very low for the given operating condition (~200 ppm for a 12% water emulsion). To check the sampling system the NOx analyzer was calibrated with the 990 ppm span gas. The span gas was then connected to the sample line upstream of the sampling pump. The analyzer

read 550 ppm instead of 990 ppm, indicating a problem with the sampling system. After referring to the manual, it was discovered that the analyzer sampling bypass pump was not operating. This bypass pump is necessary to maintain a constant flow through the reaction chamber of 40 cc/min. The diaphragm in the pump was replaced and an accumulator was connected to the line between the analyzer and the pump to dampen flow fluctuations.

The system was tested again and the span gas of 990 ppm gave a reading of 810 ppm. The entire sampling system was leak tested with pressurized nitrogen and several leaks were discovered, leading to replacement of the air filter, dessicator line and pressure regulator. Now the span gas gave a reading of 920 ppm. This discrepancy was corrected by replacing the piston-type sampling pump with a diaphragm pump. The final reading was 980 ppm, which is within the expected accuracy of the instrument.

2.6 Test Procedure

2.6.1 Test Conditions

Before testing a particular fuel, the baseline condition was run each time in order to warm up the engine on diesel fuel and to check the measurement equipment, in particular the NOx analyzer and SMPS. The fuel used was Ultra Low Sulfur Type 2 Diesel supplied by Phillips 66 (See Appendix B for certificate of analysis).

Table 2.3 Baseline Conditions

Speed	2400 rpm
Indicated Mean Effective Pressure	5.5 – 5.6 bar
Start of Injection	6 DBTC *
Coolant temperature	85 °C
Oil temperature	85 °C

* Crank angle degrees before top center.

The test condition for the test fuels (i.e. base diesel and emulsions) was at the same speed and temperatures. The indicated mean effective pressure (imep) range was wider because of difficulties in obtaining a stable operating point (Section 3.1.1). The speed was the same as that used by Shihadeh [27] in previous research and the load was 2/3 of maximum load for the engine. For this load the engine operated at an equivalence ratio of 0.5. This equivalence ratio was sufficient to produce reasonable soot formation conditions for filter measurements.

Table 2.4 Test Fuel Conditions

Speed	2400 rpm
Indicated Mean Effective Pressure	5.4 – 5.6 bar
Start of Injection	Range from 2 – 10 DBTC

2.6.2 Experimental Procedure

1) One hour before running, the dyno controller, the SMPS, the dilution air compressor, and the NOx analyzer system are switched on. The engine oil and coolant levels are checked.

2) The SMPS flowrates are set to the correct range and scans of the tunnel dilution air and test cell air are performed. The NOx and CO_2 analyzers are calibrated and the sampling system is leak checked.

3) The engine is started on the baseline fuel. The oil and coolant heaters are switched on to reach steady state operating temperature more quickly. The fuel flow rate is set at ~ 23 cc/minute and speed to 2400 rpm.

4) When the oil and coolant temperatures reach steady state ~ 85 °C and the airflow is constant (~ 9.1 g/s), the fuel flow and injection timing are varied to obtain the

baseline condition. CO_2 is measured and the exhaust-dilution transfer tube is opened fully.

5) The dilution air valve is varied to give a dilution ratio of ~ 15 for filter measurements or ~ 50 for SMPS measurements.

6) At this point baseline NOx, filter (if required) and SMPS measurements are made.

7) These measurements are compared to previous baseline measurements. If there are no obvious operating or equipment problems indicated by this comparison, then the engine can be switched over to the test fuel.

8) This is accomplished by (See Figure 2.2)
   a) Switching valves A & B to dump the baseline diesel,
   b) Switching valve C to the test fuel,
   c) Dumping the mixture of fuels for ~ 15 seconds,
   d) Switching valve B to connect return to pump inlet.

9) Measurements are then performed for this test fuel. NOx, CO2, particulate and performance measurements are made at the test condition across a range of injection timings at steady state conditions.

10) If measurements are required for another test fuel, the system is switched back to baseline diesel, the test fuel bottles are switched and step (8) is repeated.

11) At the end of testing baseline diesel measurements are redone.

The test fuels used and the measurements made are listed in Table 2.5 and 2.6.

Table 2.5 Fuel Properties

Fuel Type [1]	Sample No(s).	H/C	O/C	% Cetane Improver	Density@ 25°C	LHV (MJ/kg)
Base Diesel	**QET Matrix Fuel [2]**	2.081	0	0.0	n/a	42.01
6% Water	QF 224-01	2.061	0.0108	0.0	n/a	39.42
9% Water	QF 223-01	2.048	0.0162	0.0	n/a	37.71
12% Water	QF 173-04	2.043	0.0219	0.0	n/a	36.16
Base Diesel	**MK-1 Fuel [3]**	2.2042	0	0.0	0.803	43.07
6% Water (NH_3) [4]	QF 239-02	2.2038	0.0134	0.1	0.813	39.66
6% Water (MEA) [5]	QF 236-02	2.1904	0.0177	0.1	0.820	39.34
9% Water (NH_3)	QF 237-04	2.2043	0.0196	0.1	0.823	37.61
Base Diesel	**GO-11 Fuel [6]**	1.8959	0	0.0	0.852	42.76
6% Water (NH_3)	QF 285-01	1.8784	0.0131	0.1	0.858	39.37
6% Water (MEA)	QF-240	1.8662	0.0173	0.0	0.861	39.06
9% Water (NH_3)	QF 251-02	1.8959	0.0192	0.1	0.862	37.34

[1] The notation used here is the one provided by QET.

[2] Diesel used by Massachusetts Bay Transit Authority Buses.

[3] Low sulfur diesel fuel provided by Statoil.

[4] NH_3 : Ammonia neutralized surfactant package.

[5] MEA: Monoethanolamine neutralized surfactant package.

[6] Conventional European diesel fuel provided by Statoil.

Table 2.6 Test Fuels

Fuel	% Water by mass	Test Period	Measurements			
			Performance	NOx	Filters	SMPS
QET Diesel (a)	0	Jan. – Feb.98	√	(b)		
BM1-4 (a)	12		√	(b)		
Matrix Diesel	0	April – May 98	√	√		
QF 224-01	6		√	√		
QF 223-01	9		√	√		
QF 173-04	12		√	√		
MK-1 Diesel	0	May – June 98	√	√		
QF 236-02	6		√	√		
QF 239-02	6		√	√		
QF 237-04	9		√	√		
GO-11 Diesel	0	July – Aug. 98	√	√	(c)	
QF 285-01	6		√	√	(c)	
QF 240	6		√	√	(c)	
QF 251-02	9		√	√	(c)	
GO-11 Diesel	0	Nov. – Dec. 98	√	√	√	Range 1 (d)
QF 285-01	6		√	√	√	Range 1
QF 240	6		√	√	√	Range 1
QF 251-02	9		√	√	√	Range 1
GO-11 Diesel	0	Jan. – Feb. 99	√	√		Range 2 (d)
QF 285-01	6		√	√		Range 2
QF 240	6		√	√		Range 2
QF 251-02	9		√	√		Range 2
GO-11 Diesel	0	March 99	√	√		Range 2
QF 251-02	9		√	√		Range 2

(a) No information on fuel properties
(b) Problems with NOx Analyzer (Section 2.5)
(c) Injector Nozzle Wear (Section 3.1.4)
(d) See Table 2.2

2.7 Heat Release Analysis

The heat release analysis used in this research was adapted by Shihadeh [27] for diesel combustion analysis, from SI code developed by Cheung [28]. The program utilizes a First Law single-zone treatment of the combustion chamber contents assuming perfect gas relations, given in the equation below:

$$\frac{dQ_{rel}}{d\theta} = \frac{\gamma}{\gamma-1} p \frac{dV}{d\theta} + \frac{1}{\gamma-1} V \frac{dp}{d\theta} + \frac{dQ_{ht}}{d\theta} \tag{2.2}$$

where Q_{rel} = the energy release by combustion

Q_{ht} = the heat transfer to the chamber walls

p = cylinder pressure

V = cylinder volume

γ = ratio of specific heats

Ignition delay is calculated in this program as the time elapsed from start of injection (SOI) to the time at which the instantaneous heat release rate reached a value of 5% of the peak release. For a more detailed explanation of this program, see Shihadeh [27].

A sample of normalized pressure, needle lift, instantaneous heat release and mass fraction burned is shown in Figure 2.5 for the GO-11 base diesel. The intense fluctuations in the "actual" heat release are due to pressure oscillations recorded by the pressure transducer. The frequency of the oscillations corresponds to the characteristic frequency of the cylinder chamber and they are inherent in the design according to the engine manufacturer. The heat release was "smoothed" using a polynomial fit to the fluctuations. Mass fraction burned is also the cumulative normalized heat release and is calculated from the heat release rate.

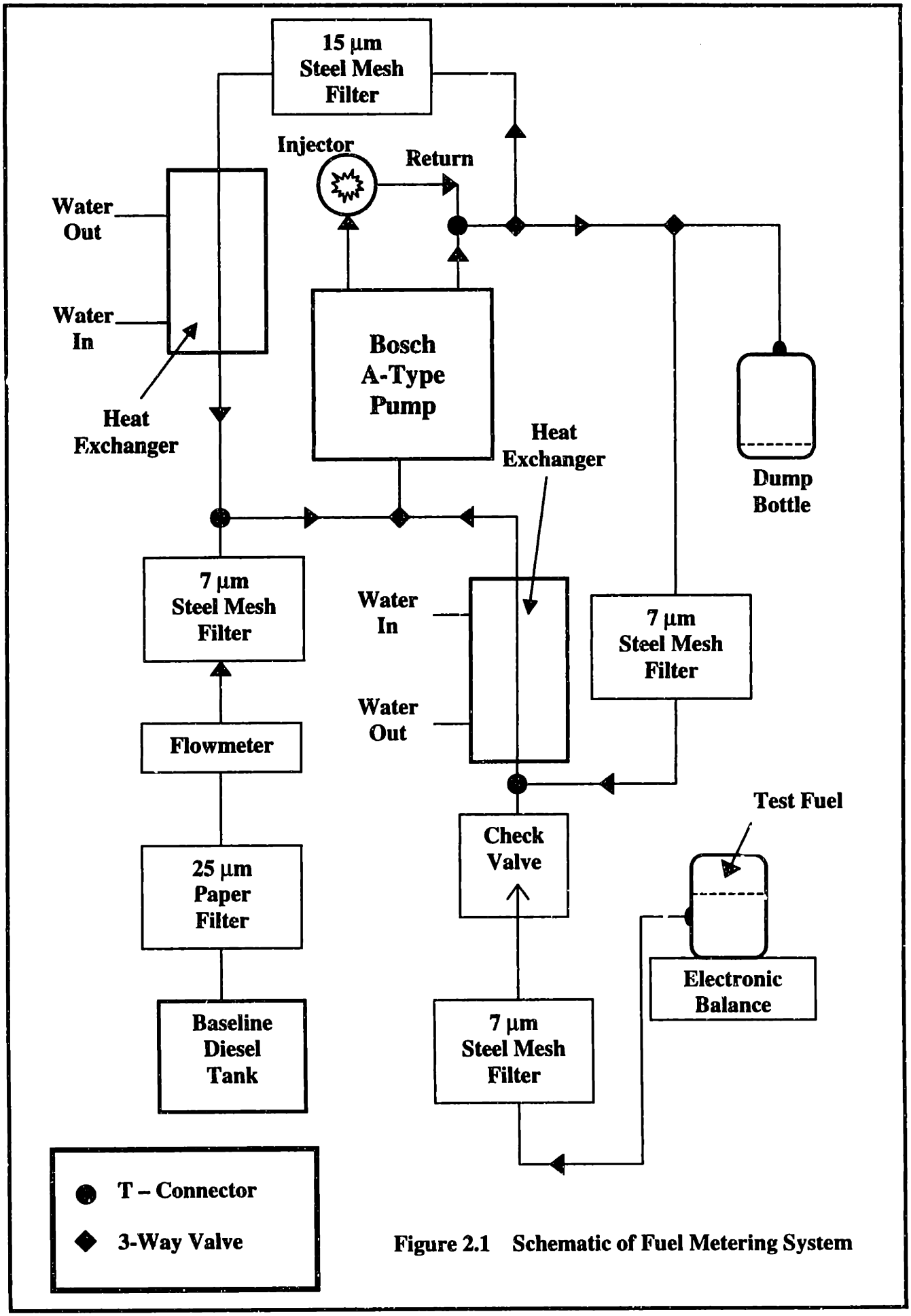

Figure 2.1 Schematic of Fuel Metering System

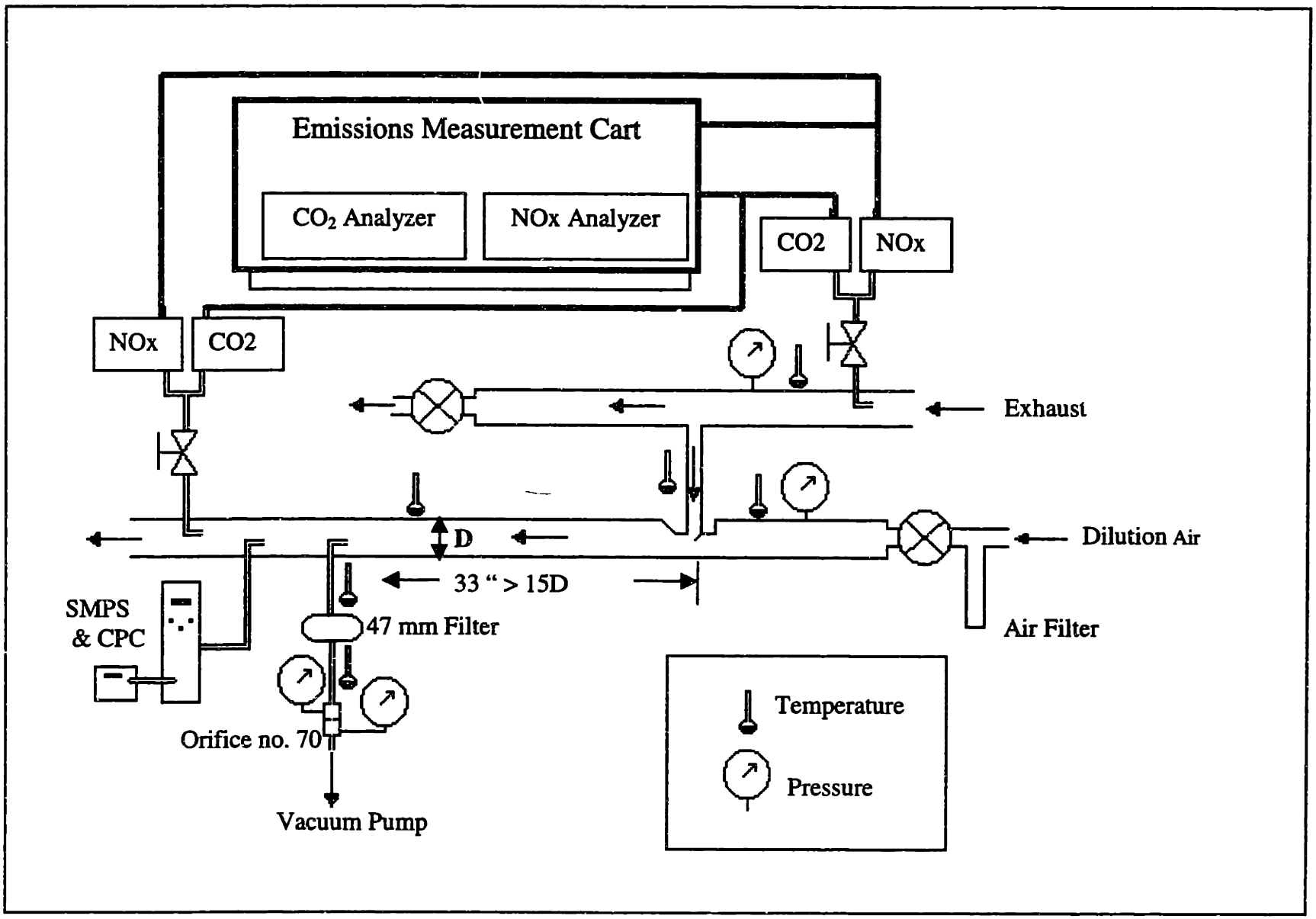

Figure 2.2 Dilution Tunnel Set-Up

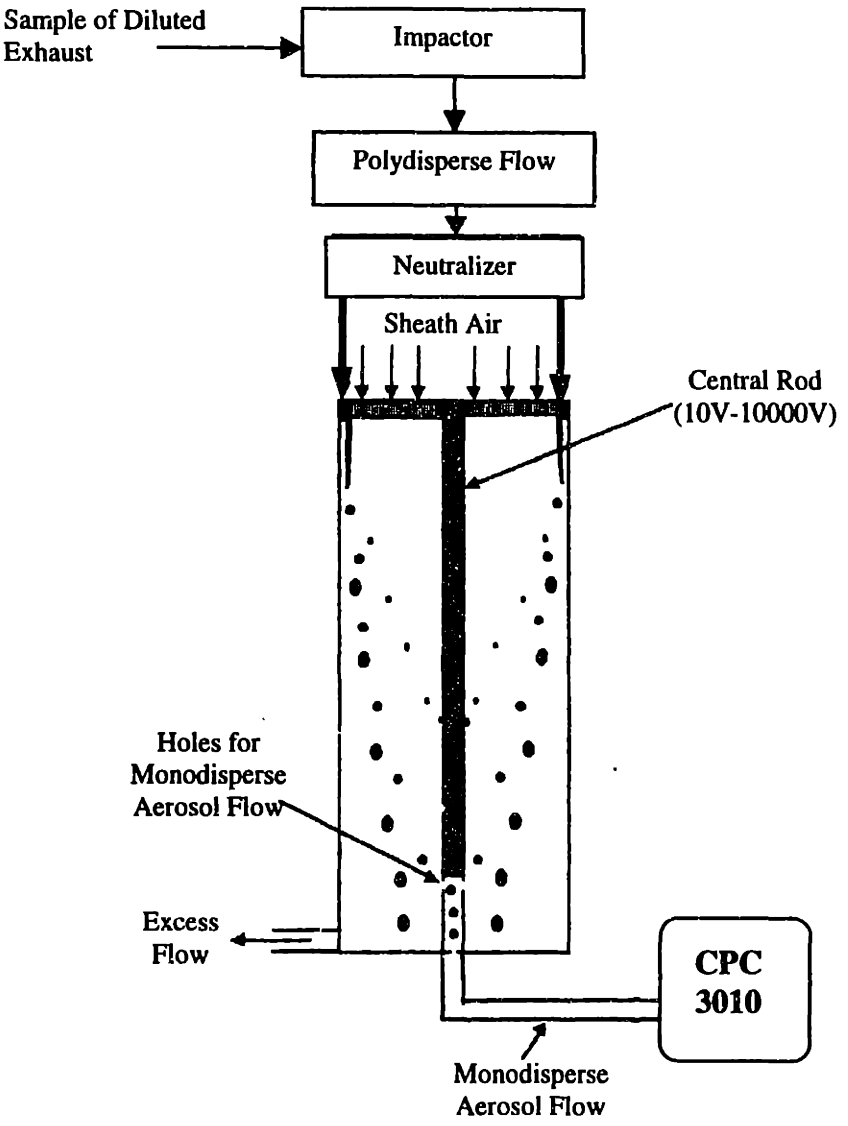

Figure 2.3 Schematic of the Scanning Mobility Particle Sizer (SMPS)

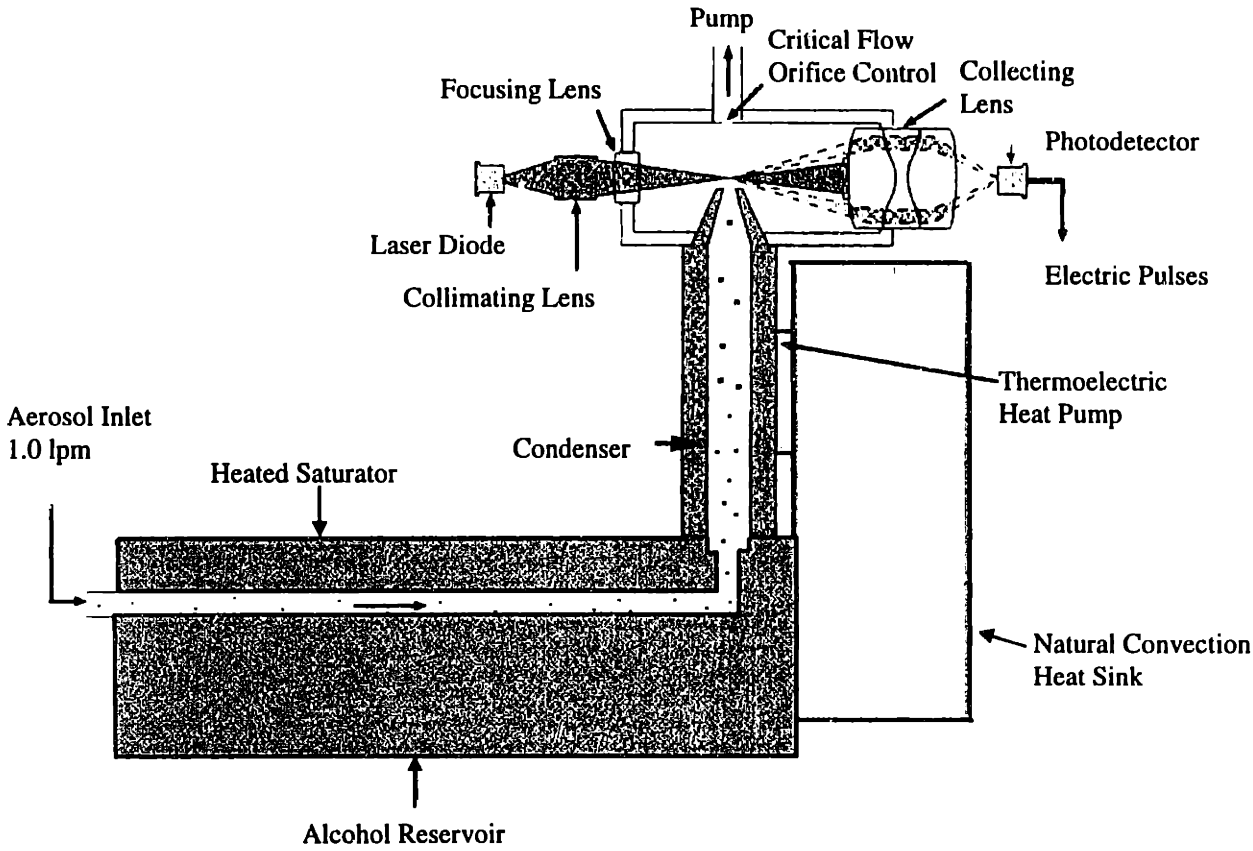

Figure 2.4 Schematic of the 3010 Condensation Particle Counter

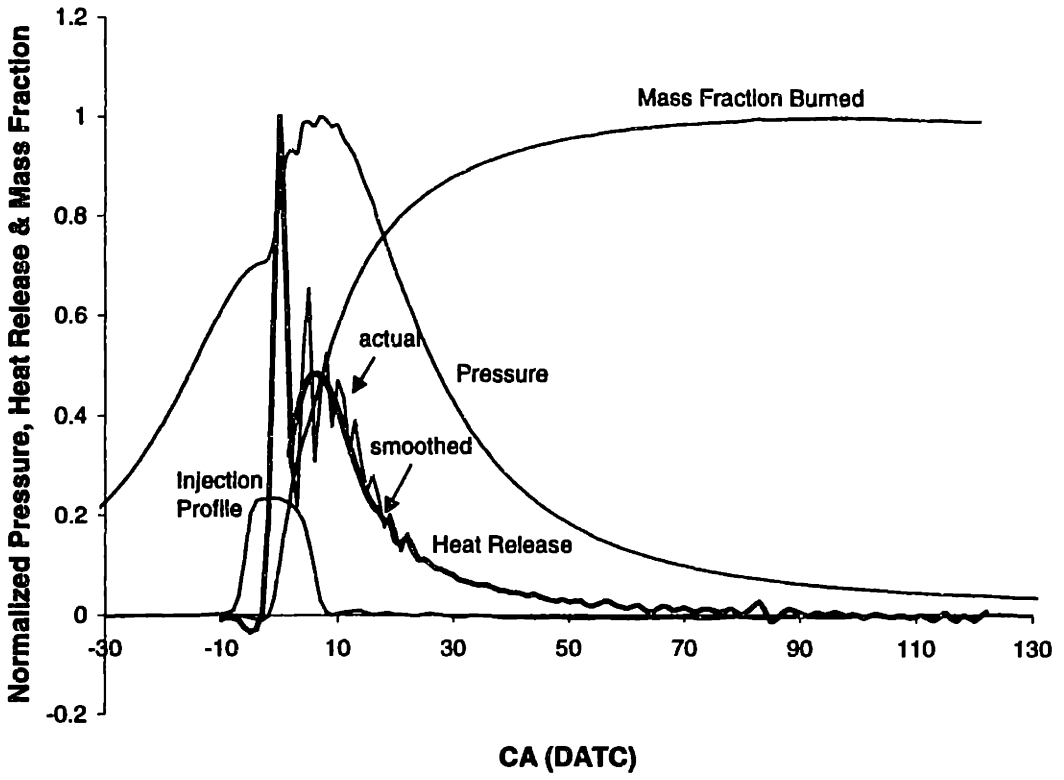

Figure 2.5 Sample of Results from Pressure Data Analysis for the GO-11 Fuel (SOI = 6.12 DBTC)

CHAPTER 3

RESULTS AND OBSERVATIONS

3.1 Experimental Observations

3.1.1 Unsteady Injection

During preliminary testing it proved very difficult to obtain a steady operating point for the emulsified fuels, unlike operation with the base fuels. It was not possible to maintain the imep in the range 5.4 – 5.6 bar. The needle lift indicated that the injection was unstable. Figure 3.1 shows the unstable needle lift profile for a QF 224-01 (6% water emulsion) compared to a normal one for the base diesel. Initially it was assumed that there was a problem with the injection pump, however when this was replaced the problem persisted. From discussion with QET and Boston Fuel Injection, it was postulated that the emulsion caused different pressure wave effects in the injection line due to higher density and/or different compressibility of the emulsified fuel. The sound speed in diesel is ca. 1300 m/s and it would be higher in a denser liquid (e.g. a fuel containing water).

The 1.7 mm diameter 450 mm long line was replaced with a 2.2 mm diameter 350 mm long line in order to try to change the pressure wave effect. After this change it was possible to obtain stable injection even at low loads.

3.1.2 Copper Corrosion

After 40-50 hours of testing, leakage started to occur around the copper sealing rings on the injection pump fittings and on the brass fittings in the test fuel line. The metal surfaces were free of tarnish and the fuel droplets had a greenish color. This indicated a corrosive attack of the metal surface due to an uptake of Cu (II) ions into the fuel. Copper is quite resistant to corrosion by water in general, however the presence of ammonia with the water will result in corrosion by the following mechanism [29]:

$$Cu + 4NH_3 \rightarrow Cu(NH_3)_4^{++} + 2e^-$$

$$2\ Cu(NH_3)_4^{++} + H_2O + 2e^- \rightarrow Cu_2O + 2NH_4^+ + 6\ NH_3$$

Since some of the emulsions contain ammonia this could be the mechanism for the observed copper corrosion.

The brass fittings were replaced with stainless steel ones where possible and the copper sealing rings were replaced periodically.

3.1.3 Stability at Higher Temperatures

When swapping over from emulsion back to baseline diesel, fuel was dumped into a clear Nalgene™ waste bottle. This was done with the engine at operating temperature. The fuel was at 45°C in the fuel pump and at an even higher temperature (estimated at 60°C) leaving from the injector into the return line. It was noted that the fuel was partially cloudy when it was dumped to the waste bottle. This cloudiness disappeared when the bottle was shaken. White jelly-like precipitate was also observed on some of the return line fittings. It is postulated that this precipitate was the neutralized salt of the surfactant fatty acid separating out of the emulsion at elevated temperatures. In later testing this phenomenon was observed less often. In practice, formation of deposited material in the fuel system can lead to filter and injector blocking and pump wear.

3.1.4 Injector Nozzle Wear

During testing of the MK-1 & GO-11 test fuel batches (June – August '98) it was noted that the fuel consumption for the baseline condition point had increased consistently over the test period. This indicated a problem with the injection pump or the injector. The injector was removed and connected to an injector test rig. At the opening pressure it was observed that although the injection profile was adequate there was some dribbling

of fuel at the tip. Also the opening pressure was at ~ 230 bar when it had originally been set at 250 bar when the injector nozzle had been replaced previously. The injector was disassembled and wear was noted on the injector holder, spacer plate and the needle of the injector nozzle. The needle appeared polished and the shoulder was smoothed (Figure 3.2). The injector pump was checked and wear was noted on the seat of the delivery valve. This wear may have been due to high temperature corrosion and/or the precipitate formed at elevated temperature.

The nozzle and spacer plate were replaced on the injector, as was the delivery valve in the pump. Also a corrosion inhibitor was added to later batches of the GO-11 fuels to prevent further corrosion. At the end of testing of the last batch of GO-11 the injector was checked again and there was no observable deterioration of the injection profile or wear on the needle body.

3.2 Experimental Results

3.2.1 Preliminary Testing

QET Diesel and BM1-4 Emulsion

The testing of the first batch of QET fuels produced invalid results because of problems with the NOx analyzer and keeping the fueling constant. The testing was useful in that it highlighted problems with other equipment i.e. the dilution tunnel setup, the dyno load cell calibration and the airflow calibration. These problems were corrected before the next batch was tested.

3.2.2 QET Matrix Base Diesel Batch

The indicated specific fuel consumption (isfc) and NOx emission results are shown in Figure 3.3 & 3.4. The optimum isfc injection timing for the Matrix Diesel is 6-7 degrees before top-center (DBTC) and for the three emulsions it was 7-8 DBTC. The isfc curves

are U-shaped because as injection is retarded from the optimum, combustion occurs too late and as it is advanced from the optimum, combustion occurs too early. There is overlap in the curves for the emulsions and the isfc values are lower than expected based on heating value. Since the lower heating value for the base diesel is 42 MJ/kg and 36 MJ/kg for the 12% water emulsion (QF 173-04), a decrease of 14%, it is reasonable to expect a similar increase in isfc. However, the difference is only 7-8 %.

For all the fuels NOx increases as the timing is advanced, since peak pressure and temperature increase as the peak combustion rate occurs closer to top center and the ignition delay increases. As with the isfc results the NOx curves for the various fuels overlap and there is no trend with increasing water content.

These results for isfc and NOx emissions were unexpected and did not agree with those previously reported by QET. On investigation of the fuel batch close to the end of testing, a milky liquid and white jelly-like substance was observed at the bottom of the five-gallon cans containing the emulsions. Some of the water and surfactant had separated from the emulsion and settled as a layer under the emulsified diesel because of the higher density of the separated phase. Two possible explanations for this are:

1) The fuels had been stored in an unheated outdoor fuel shed over the winter period and due to the below 0°C temperatures ice crystals formed and the emulsion became unstable, leading to separation, with the less dense fuel rising to the top, while the water settled at the bottom.

2) The incorrect amount of surfactant was used and the emulsion was unstable, resulting in separation after long storage. A similar error occurred in fuels sent by QET to Statoil for testing.

When mixed with a sample of the partially emulsified fuel and shaken, the milky liquid mixed completely and the emulsion was clear. This separation of the emulsions explains the lack of sensitivity to water in the results discussed above. Since the separation of the

emulsions was noticed late on in testing, there was an insufficient quantity of emulsified fuel remaining to repeat the tests.

3.2.2 MK-1 Base Diesel Batch

Isfc, Indicated Efficiency and NOx

Indicated specific fuel consumption, indicated fuel conversion efficiency and NOx results for the batch of MK-1 fuels are shown in Figures 3.5, 3.6 & 3.7. The isfc and NOx curves show the same trends with SOI as the previous batch, but they also exhibit clear trends with increasing water content. The optimum timing for the base diesel is 5 – 6 DBTC and 6 – 7 DBTC for the three emulsions. When comparing the fuels on a fuel energy conversion basis there is no improvement/deterioration in performance, the four fuels have an indicated efficiency of 37 – 38%. There is a significant decrease in specific NOx emissions with water content over the whole injection timing range. The results for SOI = 6.12 DBTC (optimum timing for the emulsions) are summarised in Table 3.1.

Table 3.1 Summary of MK-1 Results at fixed SOI = 6.12 DBTC

Fuel	ISFC (g/kWhr)	% Increase in ISFC (relative to base)	Indicated Specific NOx (g/kWhr)	% Decrease in NOx (relative to base)
MK-1 (Base Diesel)	223	0.0	6.6	0
236-02 (6% water)	241	8.1	5.8	12
239-02 (6% water)	243	9.0	5.8	12
237-04 (9% water)	255	12.5	5.3	20

Heat Release Results

Pressure and normalized instantaneous heat release curves for the MK-1 fuels at SOI ~ 6 DBTC are shown in Figures 3.8 & 3.9 (The 236-02 fuel is not included because the imep

values were higher ~ 5.7 bar than the other three and some pressure data files were corrupted). The imep was 5.5 ± 0.05 bar for the three cases shown. Table 3.2 summarizes a sample of the results for SOI = 4, 6, 8.

The peak pressure increases as the injection timing is advanced since peak heat release occurs closer to TDC. There is no significant difference in either the magnitudes of peak pressure or the locations of peak pressure for the fuels. The ignition delays are short and approximately the same over the range of fuels and timings due to the high temperatures prevailing in the high-compression ratio test engine. The ignition delay for the 6% water emulsion is slightly shorter than the base diesel probably due to the 0.1% cetane improver in it. The 9 % fuel has a longer ignition delay with the same amount of cetane improver, indicating that the presence of water increases the delay as found in other studies. From Figure 3.9 the peak heat release rate is highest for the 9% emulsion although it has the same ignition delay as the base fuel. The 6% emulsion is between the two although it has a shorter ignition delay than the base. For both cases this is due to better fuel-air mixing probably as a result of the microexplosion phenomenon.

Table 3.2 MK-1 Heat Release and Pressure Analysis Results

Fuel	SOI (DBTC)	Peak Pressure (bar)	Peak Pressure Location (DATC)	SOC (DBTC)	Ignition Delay (CAD)
MK-1	4.0	74.2	8	0.0	4.0
	6.0	79.5	7.5	2.0	4.0
	8.0	84.5	6	3.7	4.3
237-04 (9%)	4.0	73.7	8.5	0.0	4.0
	6.1	79.0	8	2.0	4.1
	8.1	84.0	6	3.8	4.3
239-02 (6%)	4.0	74.2	9	0.7	3.3
	6.1	79.6	8	2.3	3.8
	8.1	84.0	6	4.0	4.1

3.2.4 GO-11 Base Diesel Batch

The most extensive testing was done for the GO-11 batch of fuels. The initial batch tested in July – August '98 did not contain corrosion inhibitor. All batches tested after this had a corrosion inhibitor added to avoid the wear phenomenon observed in the first batch (Section 3.1.4). Filter measurements were made for the first batch and it was observed that the total particulate rate (TPR) increased with time for the baseline fuel (Ultra Low Sulfur Type 2 Diesel). This was due to increasing wear of the injector resulting in poorer atomization and therefore higher particulates. The first set of filter results is not reported.

Isfc and Indicated Efficiency

The isfc and indicated fuel efficiency results for December '98 testing are shown in Figure 3.10. Table 3.3 summarizes the results at optimum injection timing for all the test periods. For the base diesel and all three emulsions the optimum timing is ~ 6 DBTC. Isfc increases with increasing water content. The increases are fully accounted for by the differences in heating values for the fuels. For example 14% more of the 9% water emulsion (251-02) is consumed than GO-11 at the same load point and the difference in heating values = (42.16/37.34) – 1 = 14.5 %. This is similar for the other two 6% water fuels with QF-240 having a somewhat lower heating value and therefore a slightly higher isfc than 285-01.

The average maximum indicated fuel conversion efficiency occurs at SOI ~ 6 DBTC and is 37 – 38% for all fuels. The trends in the efficiency curves with SOI are the same for all the fuels over the range used. Therefore, there is no significant performance penalty or bonus associated with running the emulsion fuels at this load condition.

Table 3.3 Indicated Efficiency and NOx Decrease at Optimum Injection Timing

Fuel	**GO-11**	**285-01 (6%)**	**QF-240 (6%)**	**251-02 (9%)**
Indicated Efficiency (%)				
August '98	37.1	36.4	36.9	37.2
December '98	37.4	37.8	37.7	37.6
February '99	38.2	37.4	37.8	38.1
Average	37.6	37.2	37.5	37.6
NOx Decrease Relative to Base (%)				
August '98	-	5.2	6.7	13.1
December '98	-	6.2	9.0	12.9
February & March '99	-	6.3	6.3	12.0 & 12.5
Average	-	5.9	7.3	12.6

NOx Results

NOx results are shown in Figure 3.11 and 3.12. Since the baseline fuel (ultra-low sulfur Type 2) was always used to correct for the effect of humidity, the absolute values of specific indicated NOx are slightly different between the different test periods. As observed in the other batches NOx increases with advancing injection timing. From Table 3.3 the decrease in NOx for the monoethanolamine (MEA) neutralized QF-240 is greater than for the ammonia neutralized 285-01 emulsion although each has the same amount of water. For the 9% emulsion the average decrease in NOx is 12.6 % at the optimum timing.

Filter Results

The average filter total particulate rate (TPR) results for the December test period are shown in Figure 3.13. They are normalized relative to the actual average value for the GO-11 fuel at SOI = 6 DBTC (0.57 g/kWhr). Three filters were taken at each point and the TPR was calculated for each and then the average TPR was calculated. Only one complete set of filter data was taken due to insufficient fuel.

The trends with injection timing are interesting. Initially as timing is advanced for the emulsion fuels from 2 DBTC the TPR decreases until 6 DBTC which is the optimum isfc timing. After this point the TPR increases as timing is further advanced. However for the base diesel the lowest TPR occurs at 8 DBTC (being 8% lower than the value at 6 DBTC).

Scanning Mobility Particle Sizer (SMPS) Results

Initially particles in the 10 – 360 nm diameter range (range 1) were measured. This was the range used by Kayes [24] in previous compression ignition and spark ignition research. Although, this range is adequate to include most of the number concentration of the diluted exhaust (Figure 3.14), a large fraction (> 50%) of the volume is not included. Therefore tests were run at lower flowrates to obtain a wider range from 21 – 835 nm (range 2). The narrower range is useful for investigating whether the emulsions have a significant effect on the number concentration in the nanoparticle range.

Figure 3.15 and 3.16 show the number and volume concentration with SOI for Range 1. The normalized number and volume distribution at SOI = 6.12 DBTC for the four fuels are combined in Figure 3.14. They are normalized relative to the peak number and volume for the GO-11 fuel. The number and volume concentrations for optimum timing are summarized in Table 3.4

The number distributions shown in Figure 3.14 exhibit the characteristic lognormal distribution associated with diesel particulate emissions. Up to 50 nm the number concentration is approximately the same for all the fuels, indicating no reduction in the concentration of nanoparticles. As the diameter increases there is a significant decrease in number concentration, with the 9% emulsion showing the greatest decrease in number concentration. Overall, the number concentration for this emulsion is 6% lower than the base diesel. Since the decrease in number concentration occurs more for the larger diameter particles there is a more significant decrease in volume concentration, ~ 13% for 251-02. The number and volume concentration with SOI shows the same trends as Figure 3.13 for the filter results. The base diesel has its minimum number and volume concentrations at SOI = 8 DBTC compared to 6 DBTC for the three emulsions.

Table 3.4 Filter and SMPS Results at Optimum Injection Timing

Fuel	**285-01 (6%)**	**QF-240 (6%)**	**251-02 (9%)**
Filter Total Particulate Rate Decrease Relative to Base (%)			
December '98 (dil. ratio = 15)	9.2	7.1	15.4
SMPS Number Conc. Decrease Relative to Base (%)			
Range 1: 9.7 - 360 nm (Dec. 98)	2.0	2.4	6.2
Range 2: 21.3 - 850 nm (Feb. 99)	7.1	6.0	10.0
Range 2: 21.3 - 850 nm (Mar. 99)	-	-	10.3
SMPS Volume Conc. Decrease Relative to Base (%)			
Range 1: 9.7 - 360 nm (Dec. 98)	6.3	6.0	12.9
Range 2: 21.3 - 850 nm (Feb. 99)	12.3	10.5	20.1
Range 2: 21.3 - 850 nm (Mar. 99)	-	-	19.9

Figures 3.17 and 3.18 show the number and volume concentration with SOI for the wider range (Range 2) and Figure 3.19 shows the normalized number and volume distribution at optimum timing for the wider range. The differences between the fuels are more pronounced in this range since the decrease at higher diameters is more significant. The results are shown in Table 3.4. The 251-02 (9% water) emulsion has a 10% decrease in number concentration corresponding to a 20% decrease in volume concentration. The trends in the volume concentration (21 – 850 nm) are similar to those in the filter results for changing fuels; the 9% emulsion shows the biggest decrease and the ammonia neutralized emulsion shows a greater decrease than the MEA neutralized one in both cases. The reason the SMPS decreases are higher maybe due to method by which the SMPS calculates volume from mobility diameter (see reference [26]). In general the SMPS tends to over-estimate the volume at larger diameters since it takes the particles as being spherical whereas the larger particles are usually chain like agglomerates. Maricq et al [30], have found similar results in their research at Ford Motor Company.

Heat Release

As with the MK-1 results there is no significant difference in the magnitude of the peak pressure or the location of the peak pressure for fuels in this batch (see Table 3.5). The ignition delay is longest for the 9% emulsion over the range of injection timings. QF-240 has a shorter ignition delay than 285-01 even though it does not have an ignition improver. According to QET this is possibly due to monoethanolamine (MEA) acting as a Cetane Number enhancer.

The heat release comparisons for SOIs of 6.12 and 8.16 are shown in Figures 3.20 and 3.21*. The peak heat release rates for the emulsions are higher than the base diesel for both timings and the 9% emulsion has the highest rate of heat release. Both 6% emulsions have similar peak rates with the QF-240 rate lower probably due to the shorter

* The heat release curves in Figure 3.21 are not smoothed because the only area of interest is from SOI to the peak heat release rate (-9.0 – 2.0 DATC).

ignition delay. For the more advanced timing of 8.16 DBTC the peak release rates for the fuels are higher than for the same fuels at 6.12 DBTC.

Table 3.5 GO-11 Heat Release and Pressure Analysis Results

Fuel	SOI (DBTC)	Peak Pressure (bar)	Peak Pressure Location (DATC)	SOC (DBTC)	Ignition Delay (CAD)
GO-11	4.1	74	8	0.7	3.4
	6.1	77	8	2.5	3.6
	8.2	83	6	4.5	3.7
QF-240 (6%)	4.0	74	7	0.0	4.0
	6.1	78	8	2.0	4.1
	8.1	85	6	4.0	4.1
285-01 (6%)	4.0	74	7	0.0	4.0
	6.1	78	8	1.6	4.5
	8.0	84	7	3.1	4.9
251-02 (9%)	4.0	74	8	-0.6	4.6
	6.1	80	9	1.4	4.7
	8.1	85	7	3.0	5.1

3.3 Discussion of Results

3.3.1 Indicated Fuel Efficiency

For both the MK-1 and GO-11 fuels there is no significant change in fuel efficiency. Since the presence of water increases the heat capacity of the charge and increases the injection duration, a decrease in efficiency would be expected. However, this is countered by the following:

- Better atomization and therefore better mixing due to the microexplosion effect.
- Decreasing cooling loss due to lower combustion temperature and a less luminous flame.
- Increased air-entrainment in the spray due to increased spray momentum.
- A larger premixed combustion due to better mixing and a longer ignition lag for some fuels.

Both Sheng et al, and Crookes [13], [8] found similar results for fuel efficiency at high loads and high speeds.

3.3.2 NOx Emissions

The emulsified fuels from both the MK-1 and GO-11 base diesel batches show significant reductions in NOx emissions, with the reduction increasing with increasing water content. The reasons for the reduction in NOx emissions are discussed in detail in Section 1.4. In brief, the NOx is reduced due to decreases in the local gas temperatures of the burning and burnt zones, due to the effect of vaporizing water and increased heat capacity of the in-cylinder charge.

For both batches there are two 6% water emulsions, one neutralized with ammonia and one neutralized with monoethanolamine. For the MK-1 batch both 6% emulsions exhibit the same reduction in specific NOx emissions (i.e. around 12%). For the GO-11 batch the ammonia-neutralized 285-01 exhibits less of a reduction in specific NOx emissions than

the MEA-neutralized QF-240 (i.e. 6% vs. 7.3%). These results suggest that there is no significant "denoxing" effect due to the presence of ammonia in the emulsion, or, conversely, there is an increase in NOx due to oxidation of the nitrogenated compounds in the emulsion.

The reduction for the MK-1 batch is greater than that for the GO-11, e.g. 20% vs. 13% for the 9% water emulsion case. It is unclear why this is the case. The reduction in NOx due to the thermal effects of water is countered by the microexplosion effect. This effect causes better atomization and better fuel-air mixing leading to a higher peak heat release rate and higher temperatures than would be the case without microexplosions. From Figure 3.9, the peak heat release for the 9% emulsion for the MK-1 batch (237-04) is 10% greater than the peak for the MK-1 base diesel. For the GO-11 batch in Figure 3.20, the 9% emulsion (251-02) has a peak 16% higher than the GO-11 base diesel. This small difference indicates that the emulsions formed from the two base fuels behave differently during combustion, either through better microexplosions or atomization of the faster burning emulsion (251-02 in Figure 3.20). In addition the MK-1 diesel produces higher specific NOx emissions than the GO-11 diesel at the same operating condition, 6.6 g/kWhr vs. 6.1 g/kWhr. So it is possible that the water has a greater effect on diesels that are higher NOx producers.

In previous studies [8, 10, 11] NOx reductions in the range 12 – 40% have been reported for emulsions with 10% water. The NOx reductions for 9% water emulsions found in this research fall into that range. There is no indication that nanostructured emulsions have any advantage over normal microemulsions in reducing NOx emissions.

3.3.3 Particulate Matter Emissions

Net reductions in specific particulate matter emissions were observed with operation on water emulsions. The reductions in particulate matter increase with increasing water

content, from around 8% for the 6% water emulsions to 15% for the 9% water emulsion based on filter measurements and from around 11% to 20 %, respectively, based on SMPS volume concentration. There is much about the effect of water on the soot formation process that is poorly understood. However, the observed results can be explained by the following mechanisms;

- The proposed microexplosion effect (Section 1.4) results in better atomization of the spray droplets, greatly expanding the spray head and increasing the spray angle. This leads to improved air-fuel mixing and thus better oxidation.
- Increased air entrainment into the spray due to greater fuel jet momentum results in better mixing.
- Soot oxidation maybe improved by the presence of OH radicals resulting from the dissociation of water.
- The lower temperatures at peak combustion times may lead to lower soot formation rates.

The first two mechanisms account for the higher peak heat release rates observed for the emulsions compared to their base diesels (figures 3.9 and 3.20). The greater proportion of premixed combustion results in a corresponding lower proportion of diffusion flame burning. Soot is formed mainly in the diffusion flame burning period [31].

The PM reductions are not significantly higher than those reported in literature for normal microemulsions. In fact, Andrews et al. [10], reported a much larger reduction than found in this research, namely a 40% reduction in PM on a mass basis for a 5% water microemulsion and a 70% reduction for a 10% microemulsion. Therefore these results do not support the theory that the water nanoclusters further reduce PM by producing catalytic effects.

3.3.4 Comparison to Statoil Results

As mentioned in the Section 1.7, Statoil performed tests on fuels similar to those tested in this research. The Statoil tests were performed on a Ricardo Hydra Indirect Injection Engine and the standard European 13-mode test cycle (steady state test type) was used. Similar reductions in PM were found by Statoil, namely ca. 20% reduction for the 9% water emulsion (251-02) using an AVL infrared analyzer. However no directionally consistent effect on NOx emissions was observed for the Statoil tests. This finding does not agree with previous studies or the results discussed in Section 3.3.1 – 3.3.3. It is invalid to directly compare the Statoil results to the results discussed above (Section 3.3.1 – 3.3.3) since a different engine and test cycle were used and also no information on injection timing was reported by Statoil.

Figure 3.1 Unsteady Needle Lift Profile

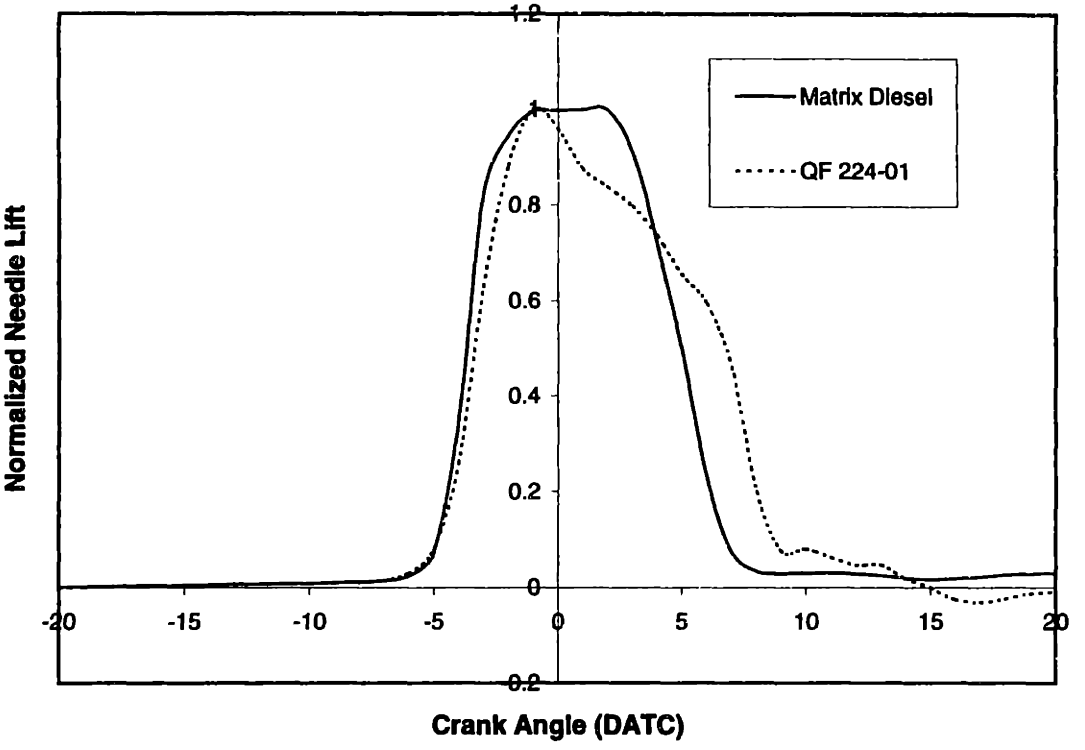

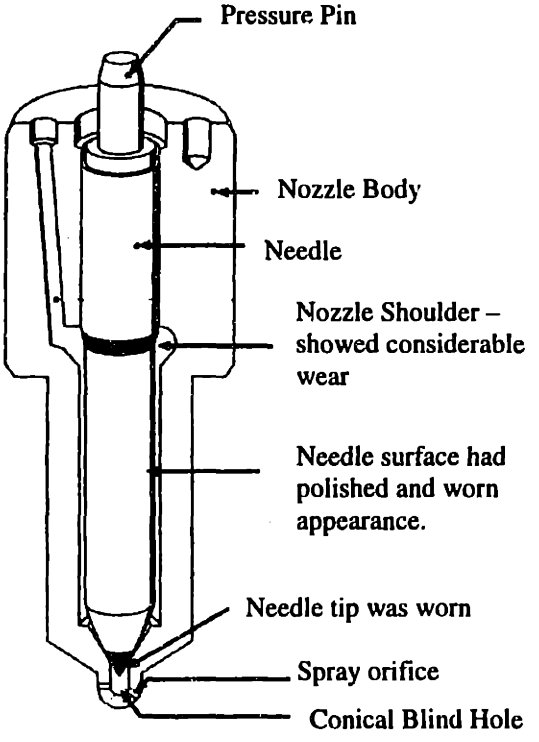

Figure 3.2 Cutout View of Injector Nozzle and Needle

Figure 3.3 Indicated Specific Fuel Consumption v SOI (Matrix)

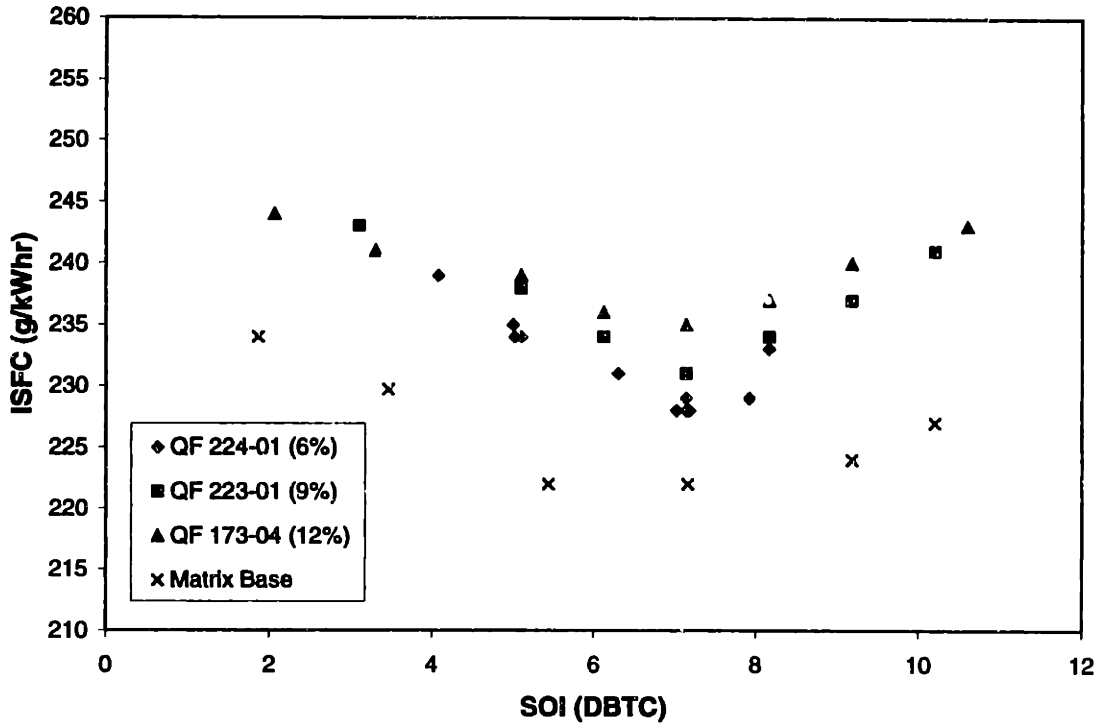

Figure 3.4 Indicated Specific NOx v SOI (Matrix)

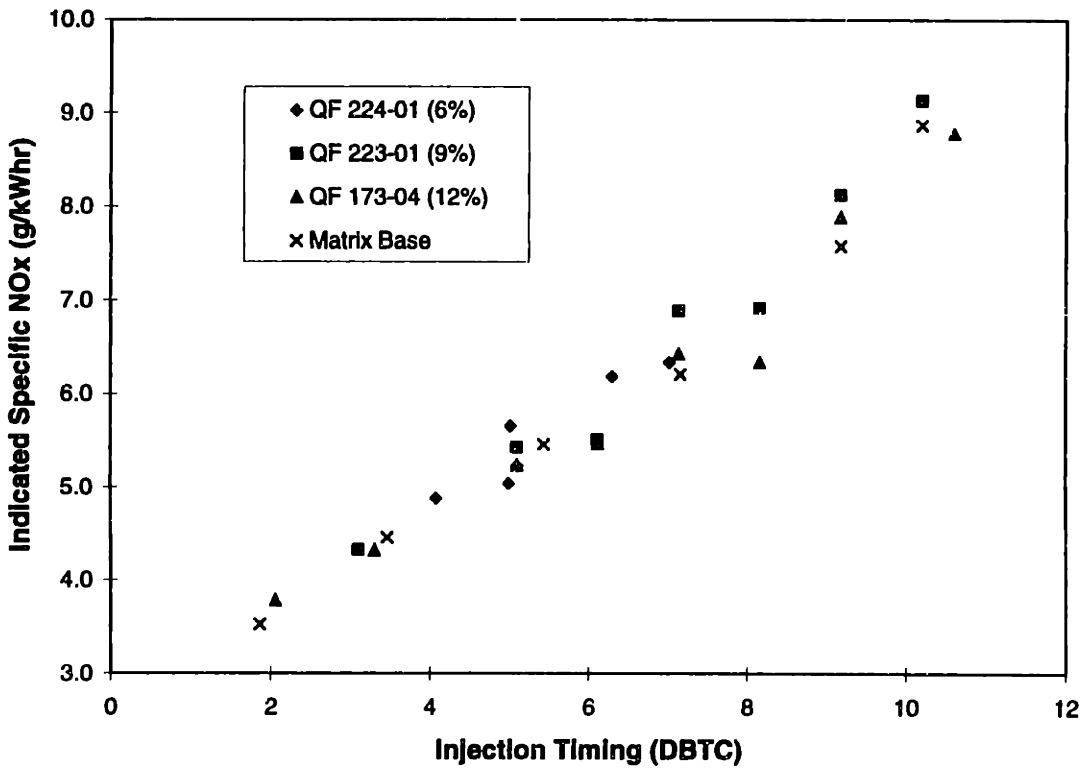

Figure 3.5 Indicated Specific Fuel Consumption v SOI (MK-1)

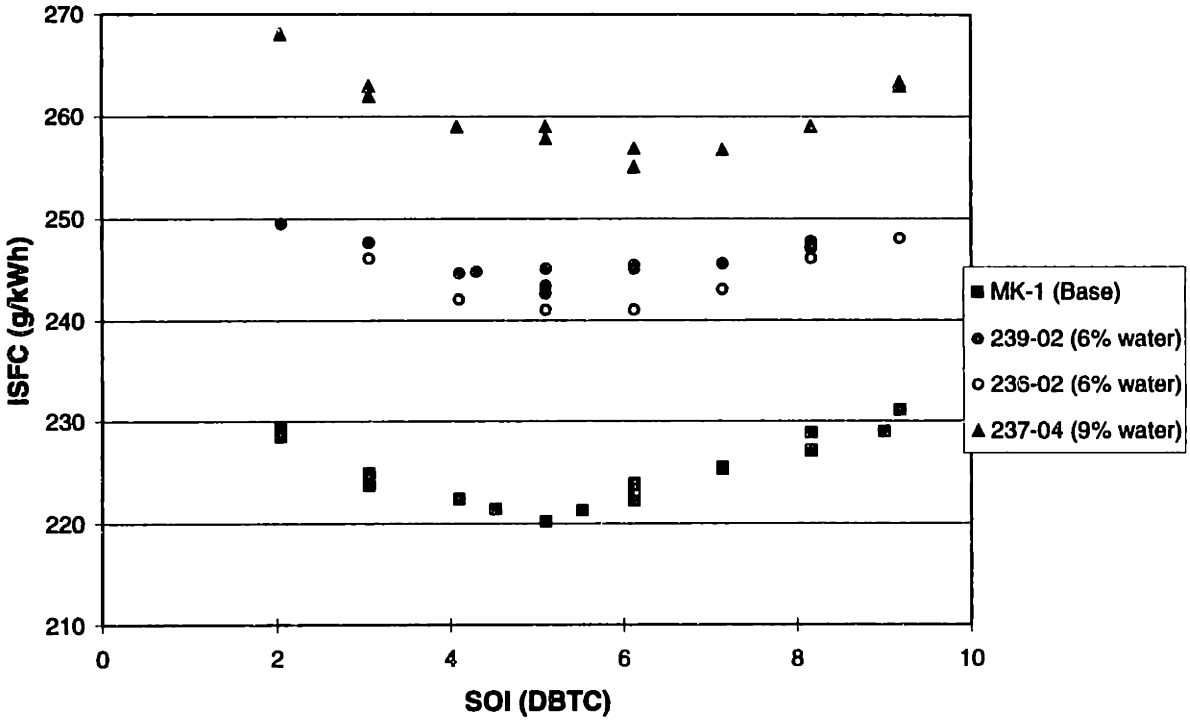

Figure 3.6 Indicated Fuel Conversion Efficency v SOI (MK-1)

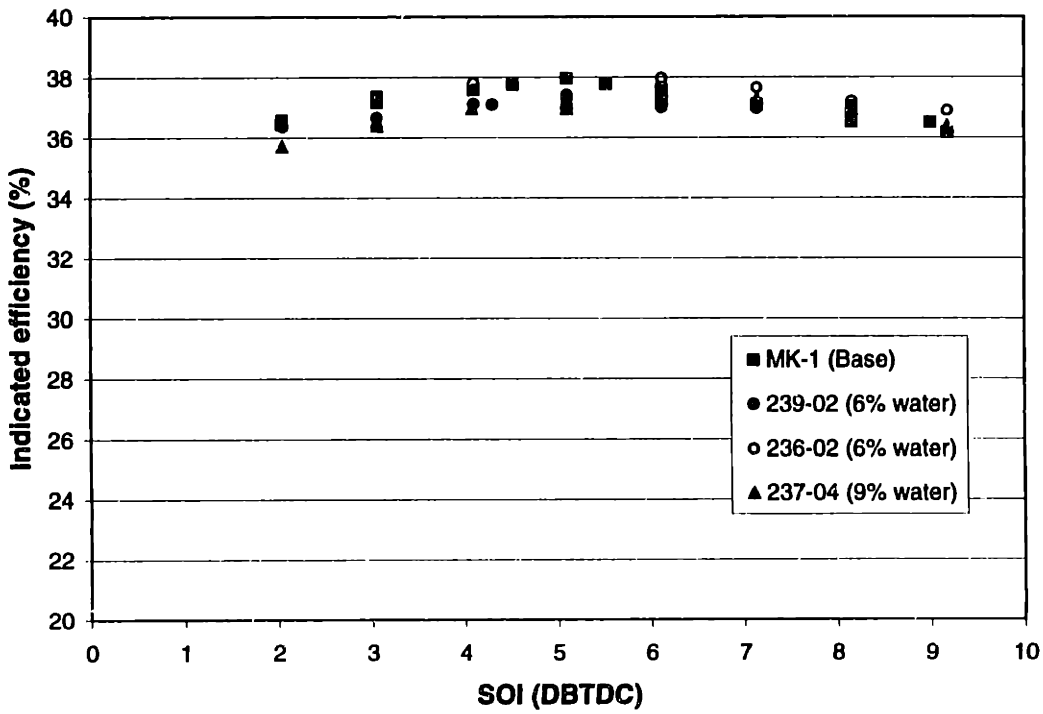

Figure 3.7 Indicated Specific NOx v SOI (MK-1)

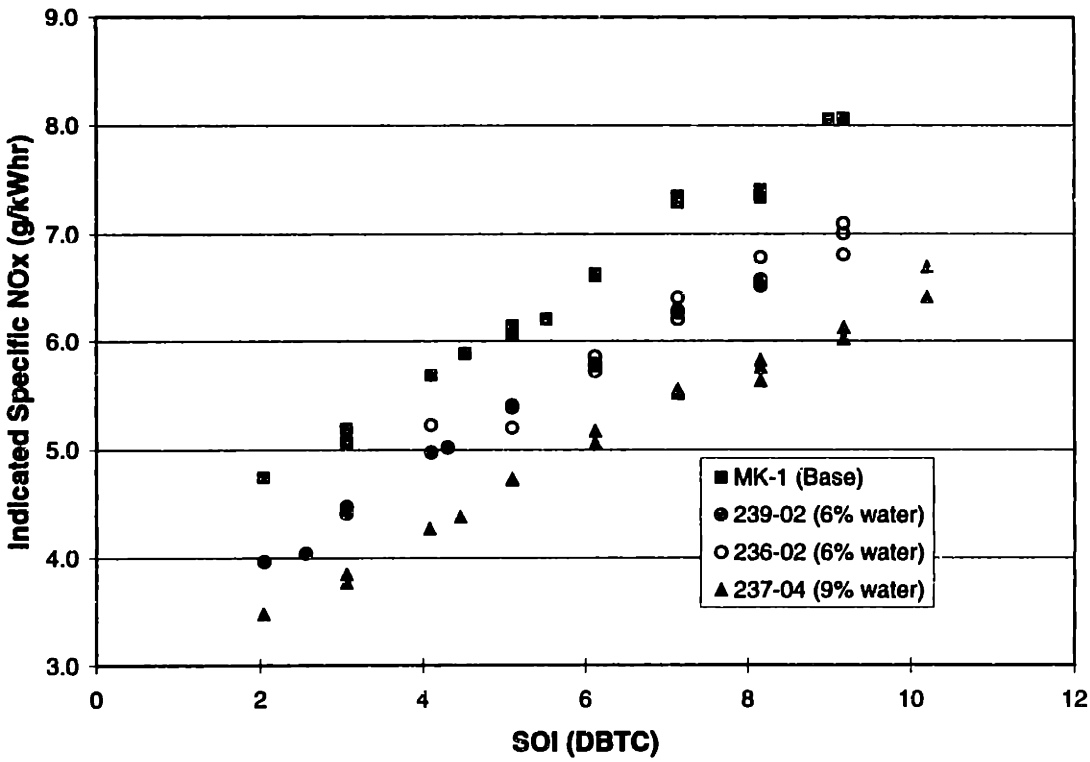

Figure 3.8 Presssure Comparison for MK-1 Batch

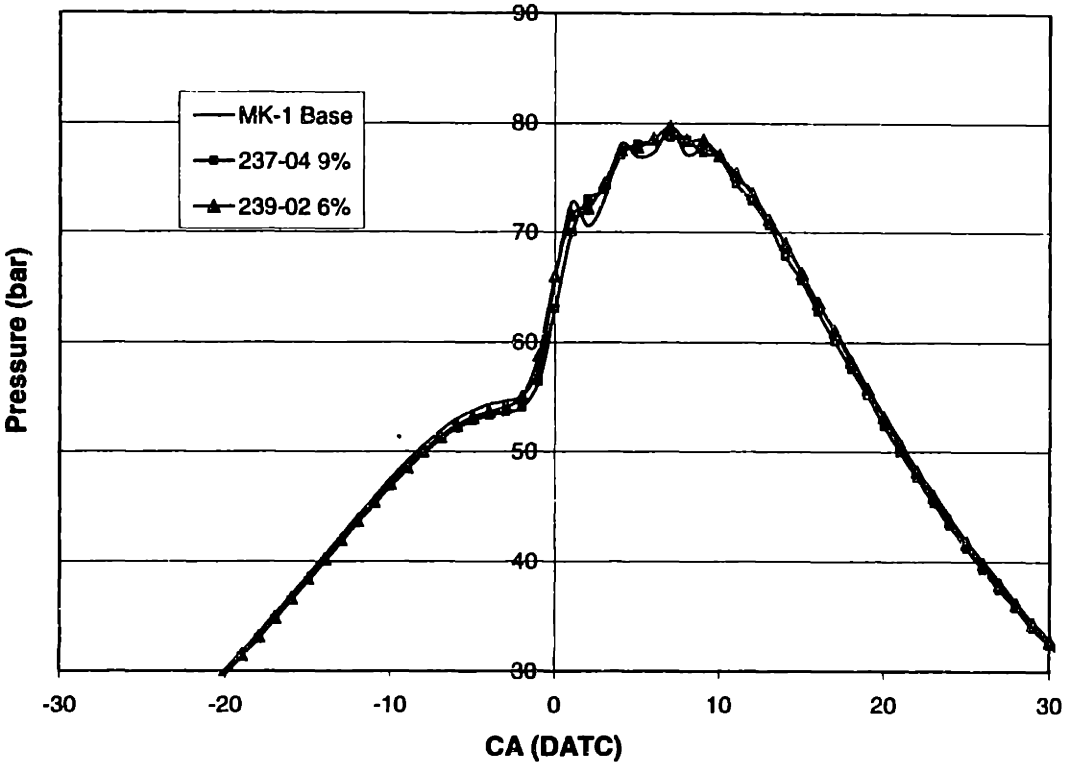

Figure 3.9 Heat Release Comparison for MK-1 Batch

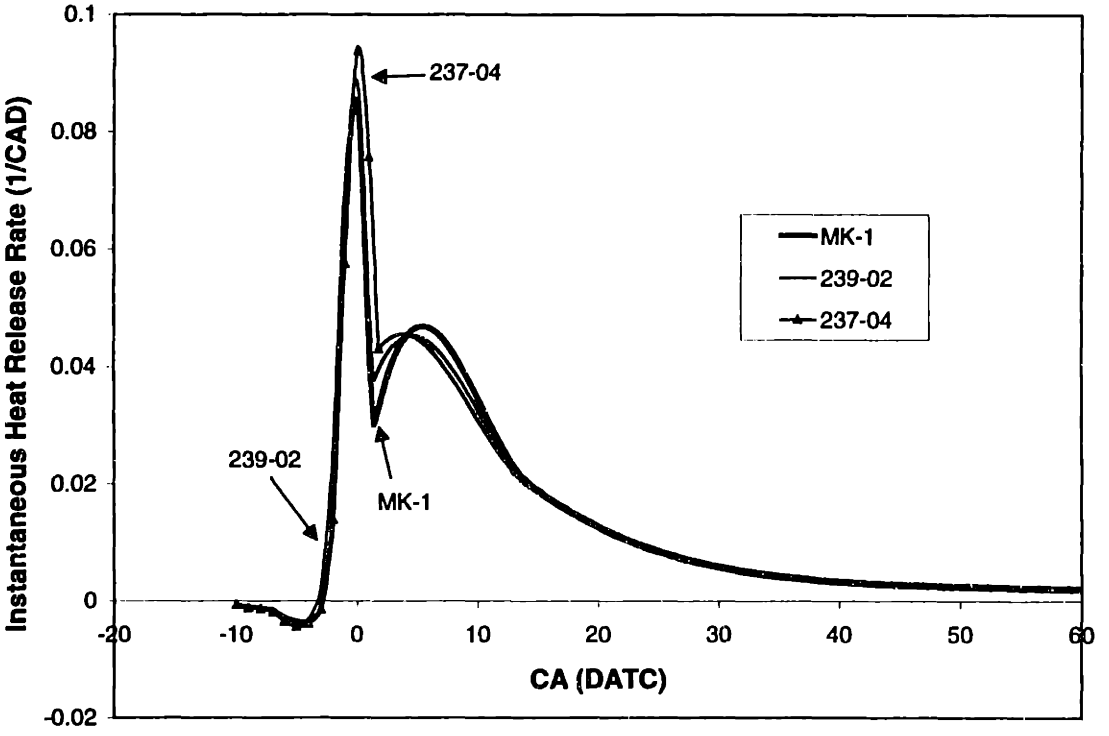

Figure 3.10 Indicated Specific Fuel Consumption & Efficiency v SOI (GO-11 Dec.)

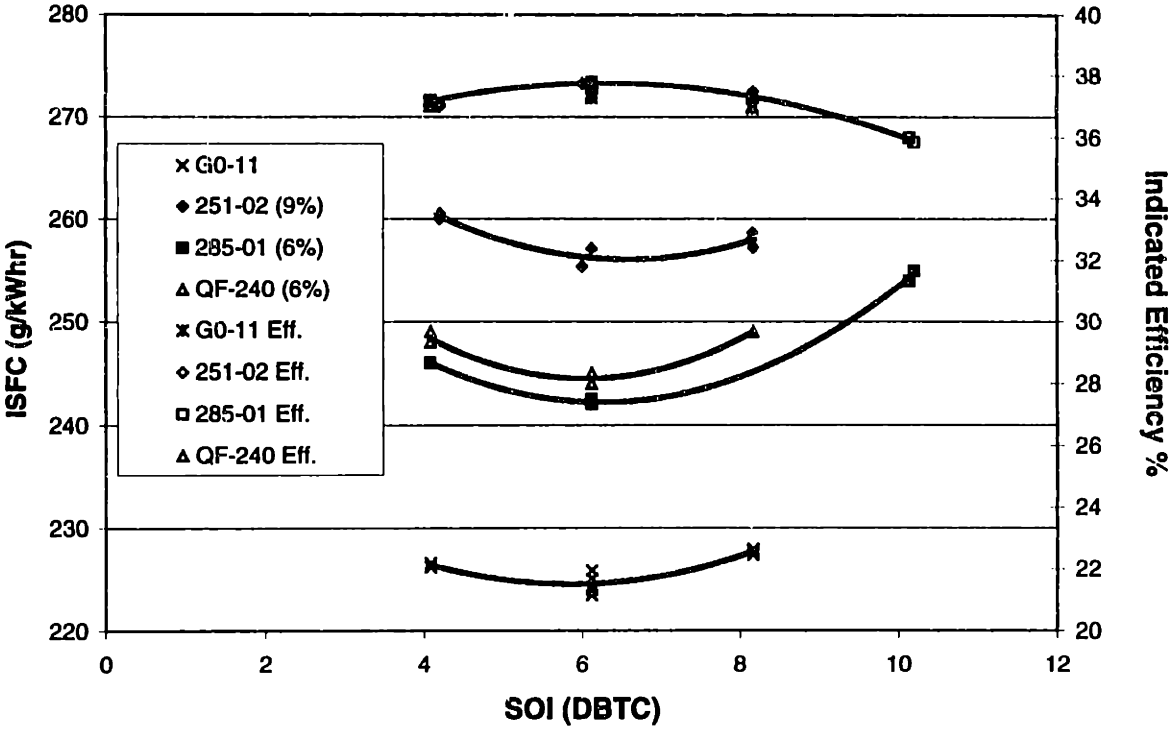

Figure 3.11 Indicated Specific NOx v SOI (GO-11 Aug.)

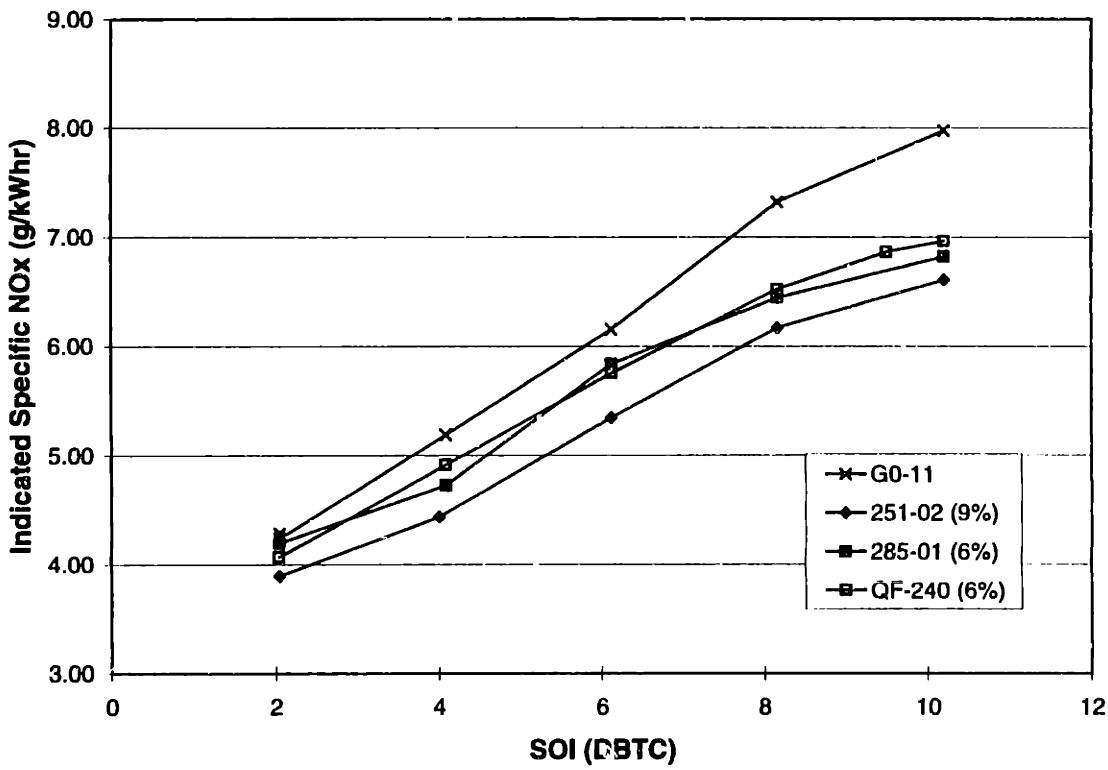

Figure 3.12 Indicated Specific NOx v SOI (GO-11 Dec.)

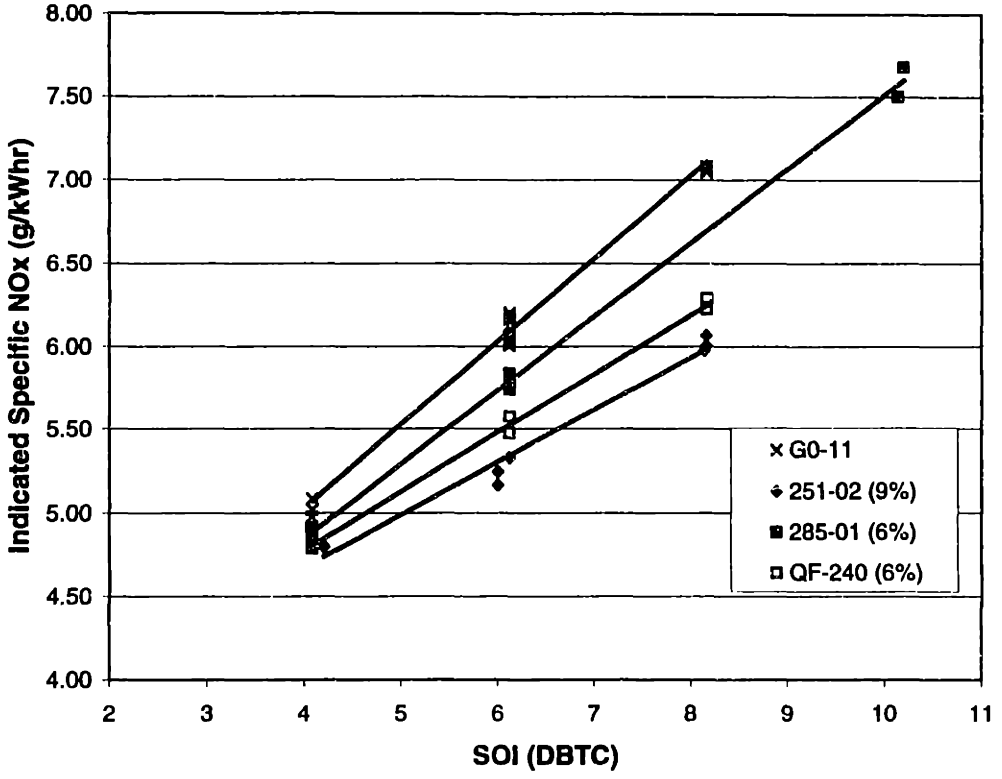

Figure 3.13 Average Normalized Total Particulate Rate v SOI (GO-11)

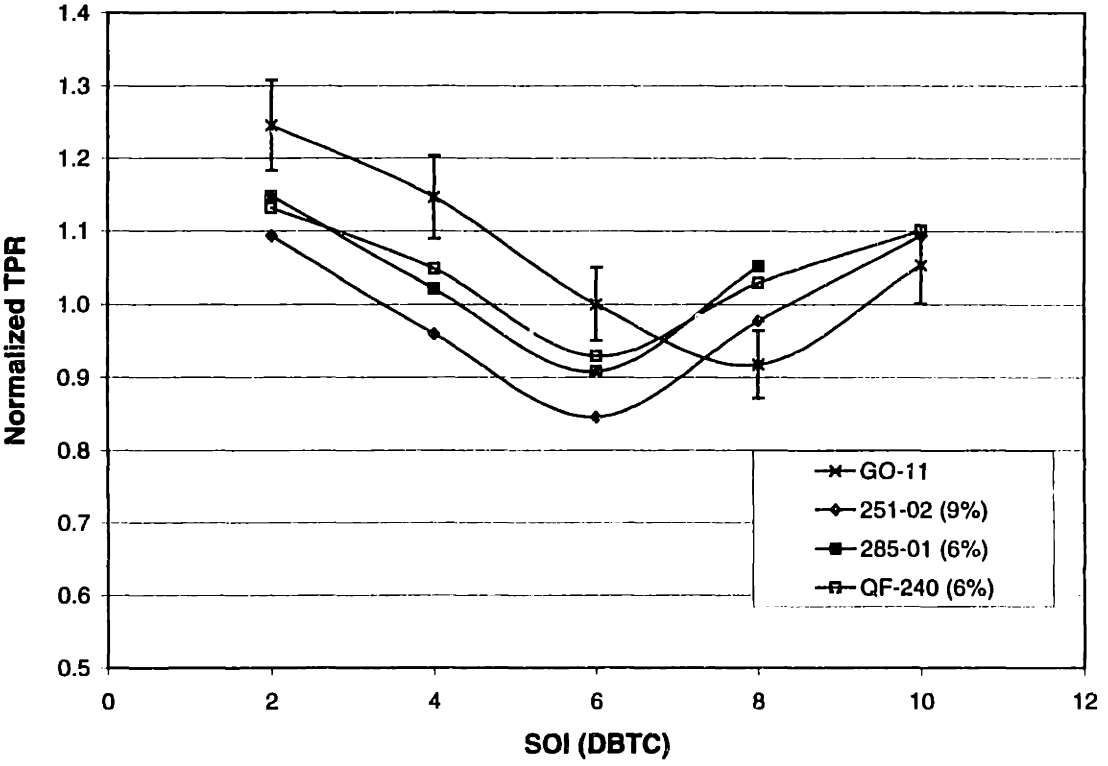

Figure 3.14 Normalized Number & Volume Concentration Distribution for GO-11 Fuel Batch (Range 1: 9 - 360 nm)

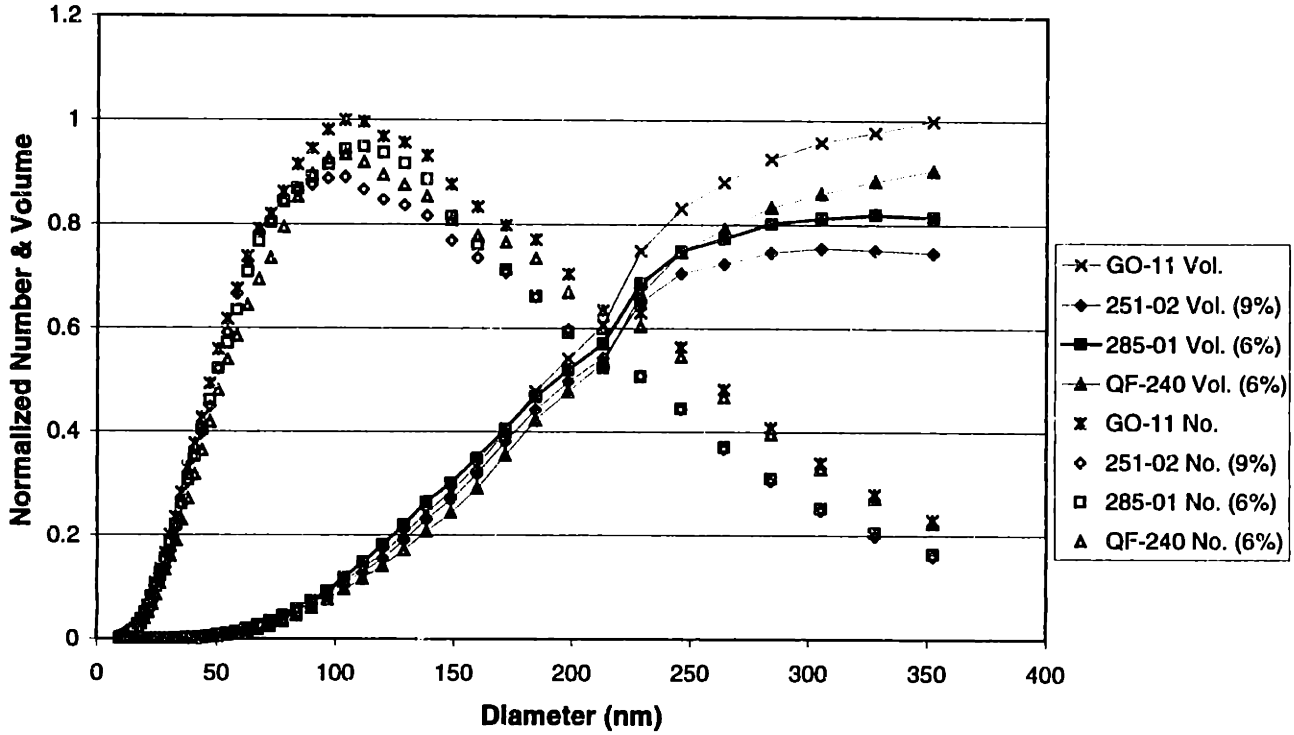

Figure 3.15 SMPS Number Concentration v SOI (Range 1)

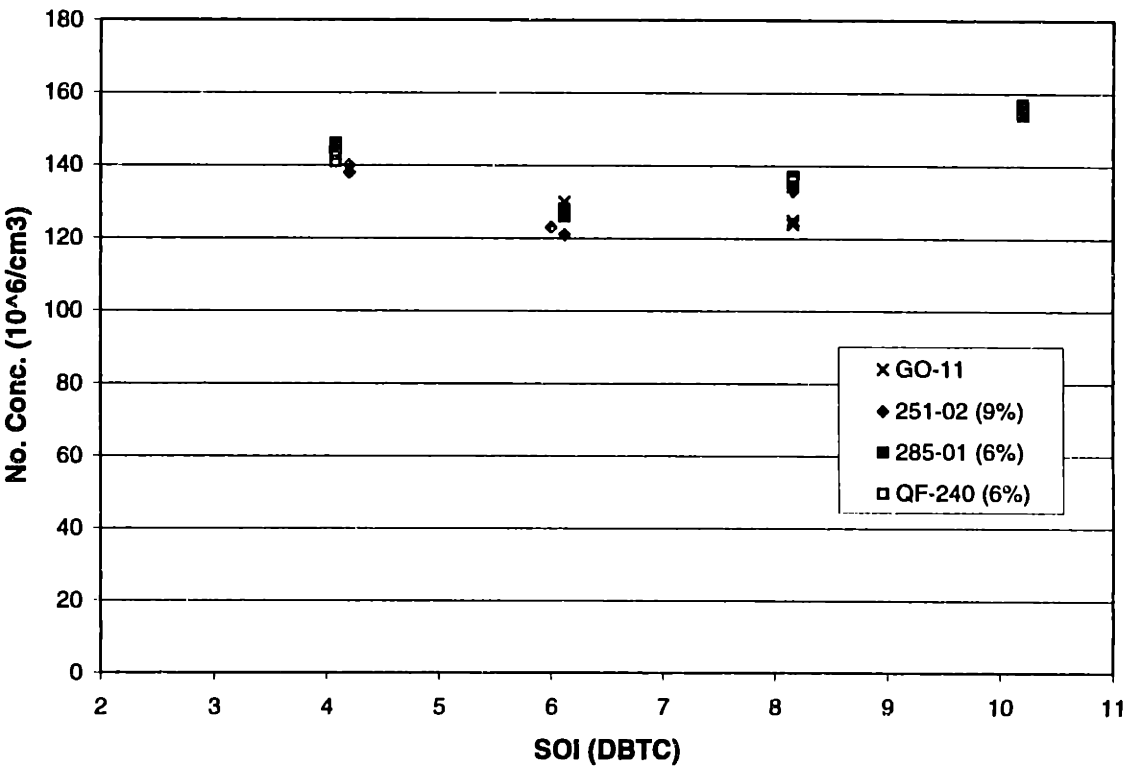

Figure 3.16 SMPS Volume Conc. v SOI (Range 1)

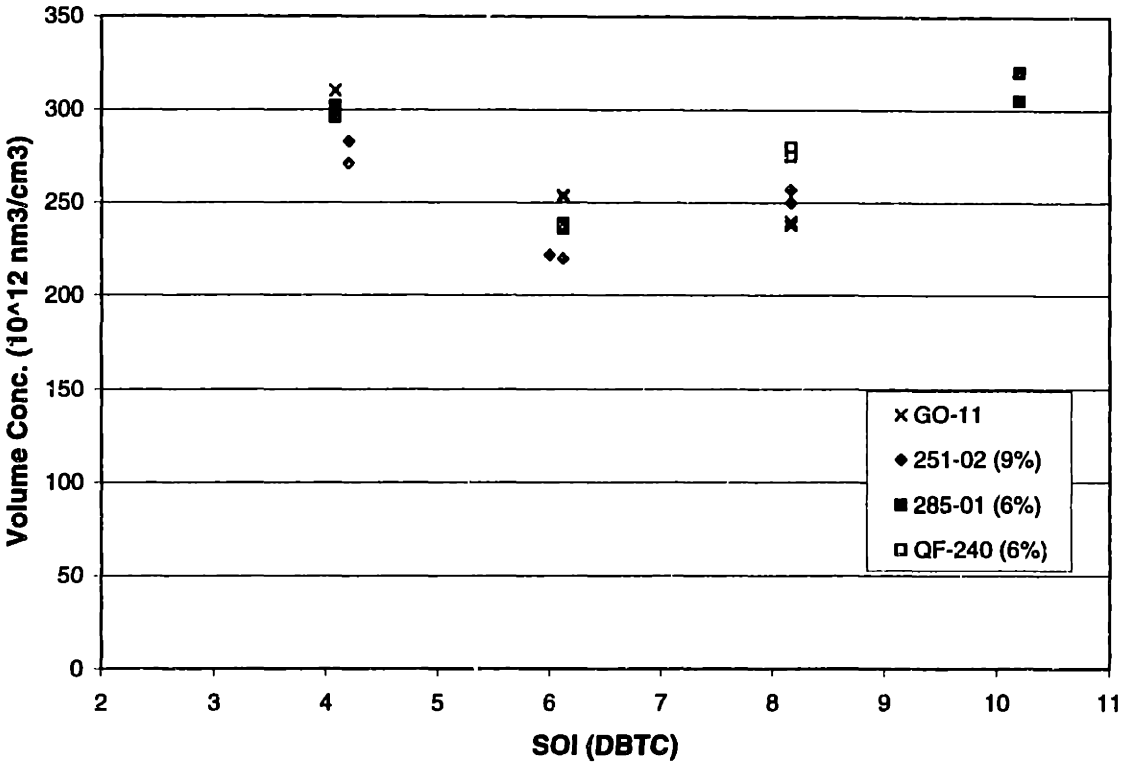

Figure 3.17 SMPS Number Concentration v SOI (Range 2)

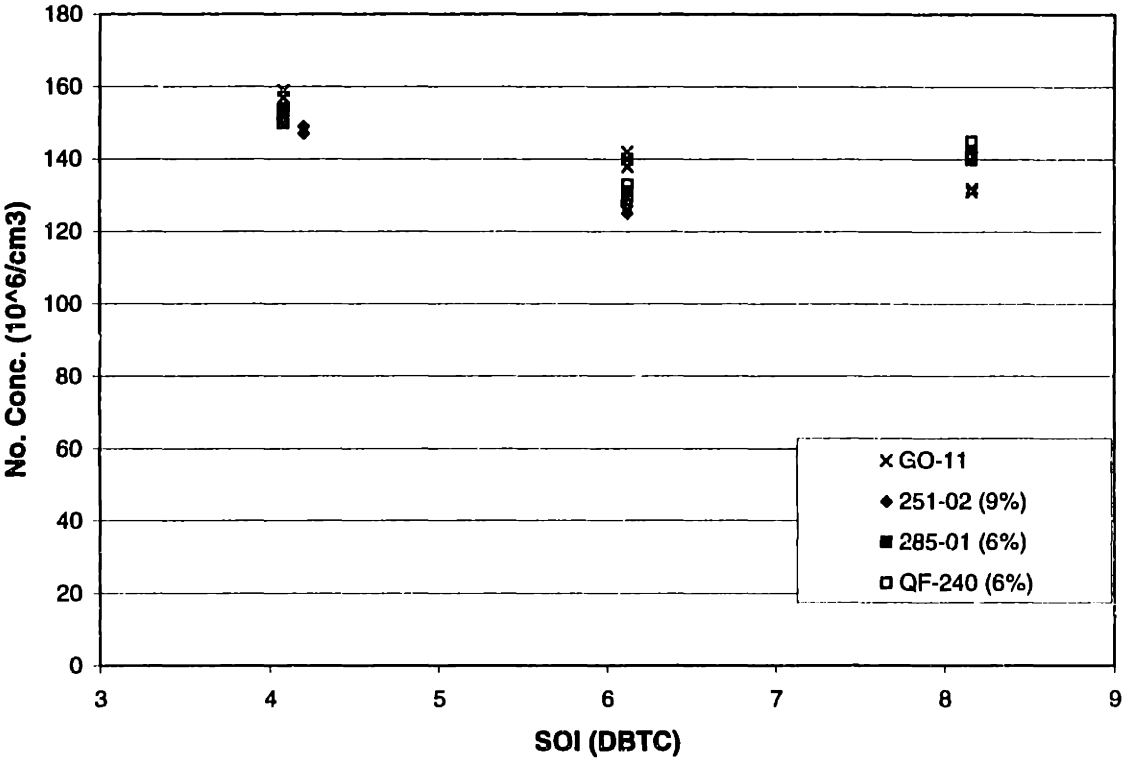

Figure 3.18 SMPS Volume Conc. v SOI (Range 2)

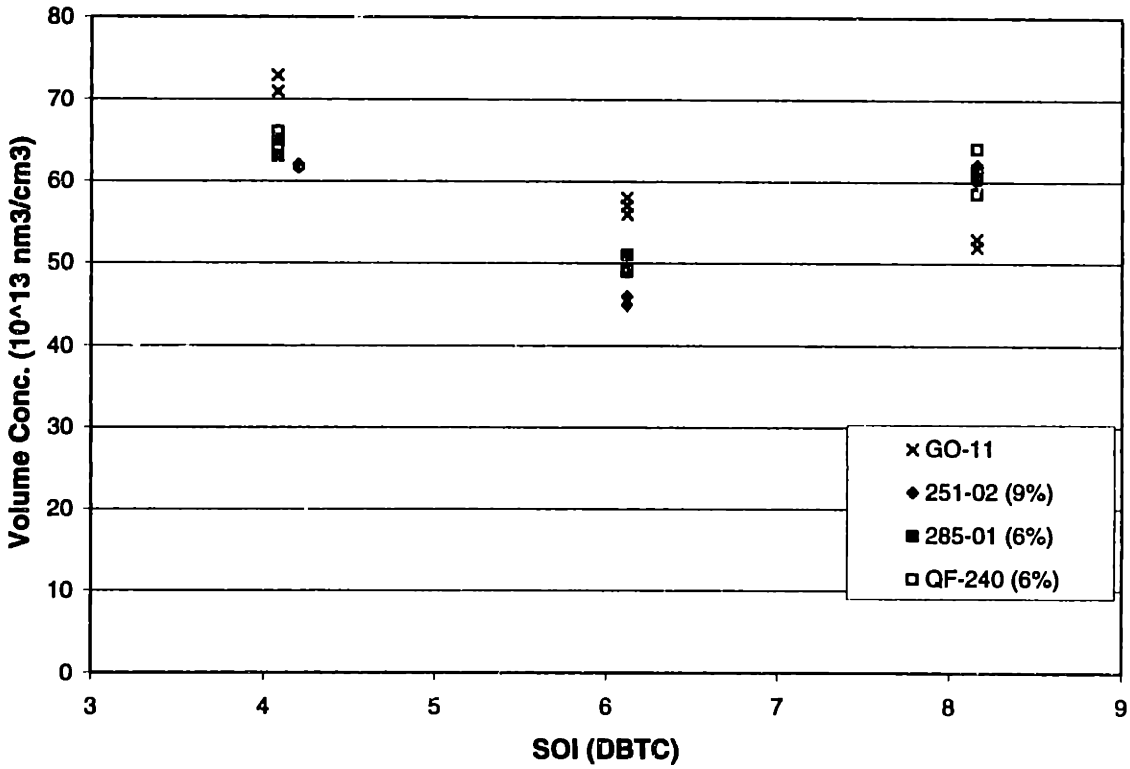

Figure 3.19 Normalized Number & Volume Concentration Distribution for GO-11 Fuel Batch (Range 2: 22 - 850 nm)

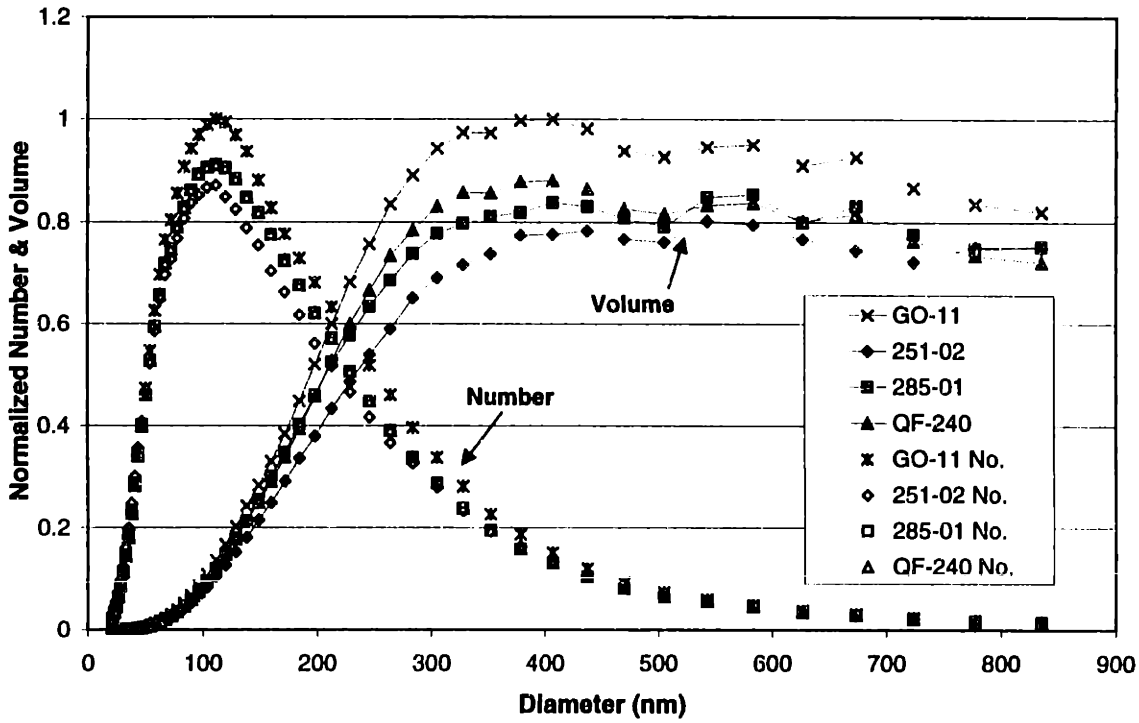

Figure 3.20 Heat Release Comparison for GO-11 Batch (SOI = 6.12)

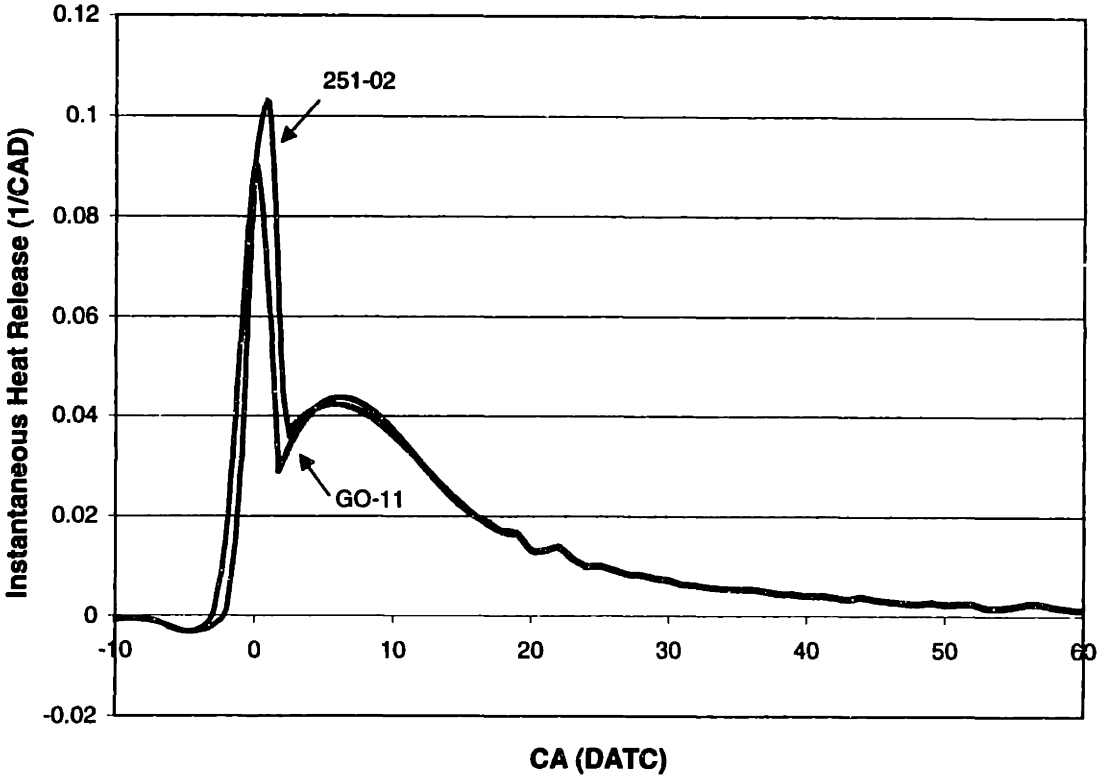

Figure 3.21 Heat Release Comparison for GO-11 Batch (SOI = 8.16)

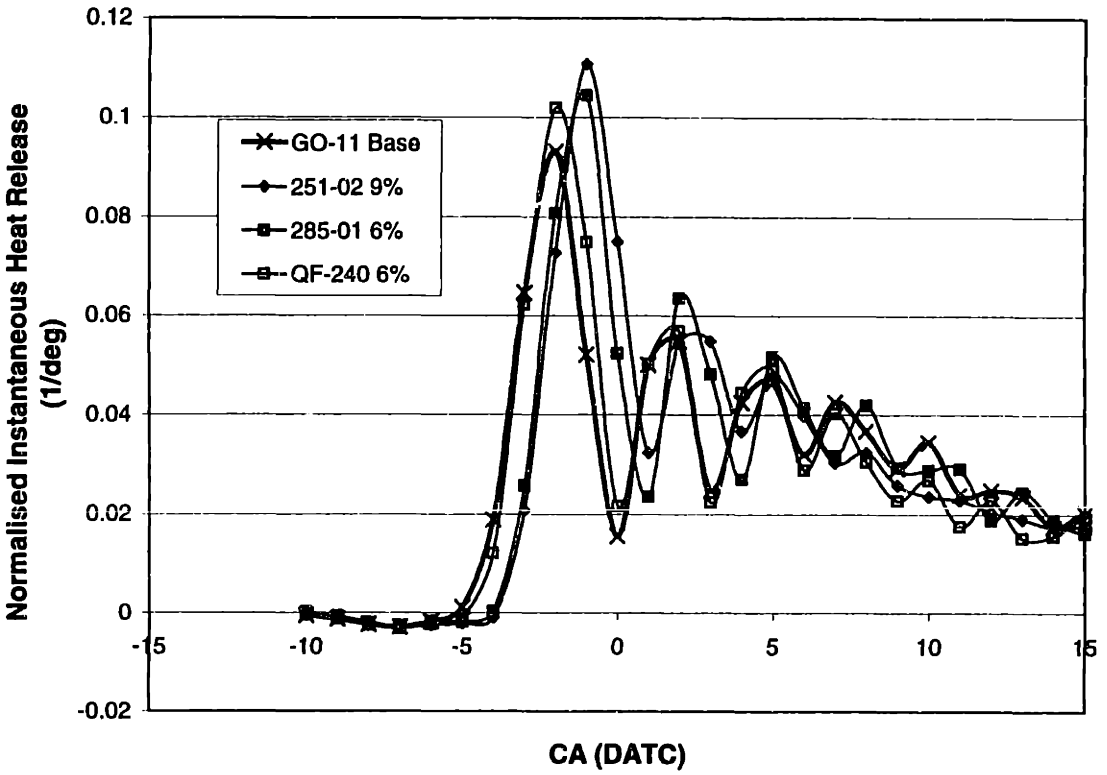

CHAPTER 4

MODELING

4.1 Background

In order to separate the various potential effects of a nanostructured emulsion on the diesel combustion process and NOx emissions, there was a need to quantify the impact of water on ignition, vaporization (via latent heat) and flame temperature. Therefore a phenomenological spray combustion model was utilized. This model was adapted and verified for the single cylinder Ricardo by Shihadeh [27] using GT-Power Version 4.3 engine simulation software developed by Gamma Technologies Inc. The model accounts for the in-cylinder processes of fuel-jet formation, the breakup of the jet into droplets, entrainment of air, evaporation of fuel droplets, mixing of air with fuel vapor, ignition, combustion, and NOx formation.

4.1.1 Model Description

The core of the modeling approach is the division of the jet plume into hundreds of subzones, tracking in time the evolution of small packets of fuel issuing from the injector. Each subzone grows as fuel is injected into it and then it entrains air as it travels into the cylinder. Evaporation occurs with entrainment and the vapor mixes with the air. When the fuel-air mixture in the packet is within the combustion limits, the fuel-air charge burns after the ignition delay period which, is calculated using an Arrhenius rate expression. The burn rate is dependent on local temperature and fuel equivalence ratio. The energy conservation equation is solved at each time step for the individual subzones and the cylinder as a whole. The cylinder temperature and pressure are updated every time step to account for the heat release from each package. A detailed description of the model including the verification method and a comparison to experimental work by Dec [5] is presented in Shihadeh [27]. For this study the NOx submodel was added.

4.1.2 NOx Emissions Model

The formation of NO is represented by the generally accepted Extended Zeldovich mechanism:

$$N + NO \leftrightarrow N_2 + O$$
$$N + O_2 \leftrightarrow NO + O$$
$$N + OH \leftrightarrow NO + H$$

where the rate constants (in units of m^3/kmole) are:

$$k_{-1} = 7.60 \times 10^{10} \exp(-38000/T_b)$$
$$k_2 = 6.40 \times 10^6 T_b \exp(-3150/T_b)$$
$$k_3 = 4.10 \times 10^{10}$$

where T_b is the temperature of a burned subzone. The k_{-1}, k_2 and k_3 values are those recommended by Heywood [31] from a review of published studies.

Because the kinetics of O, OH, H are much faster than the kinetics of NO and assuming that N is consumed as fast as it is produced, the three kinetic rate equations can be reduced to a single equation:

$$d[NO]/dt = 2R_1(1-b^2)/(bR_1/(R_2 + R_3) + 1) \quad (4.1)$$

where

$$b = [NO]/[NO]_{eq}$$
$$R_1 = k_{-1}\,[N_2]_{eq}\,[O]_{eq}$$
$$R_2 = k_2\,[O_2]_{eq}\,[N]_{eq}$$
$$R_3 = k_3\,[OH]_{eq}\,[N]_{eq}$$

where "eq" denotes values obtained from the full equilibrium calculations. Since [NO] is the concentration in kmole/m^3, for any given burned subzone the above equation can be integrated to give the mass of NO in that subzone as a function of time as:

$$d\,m_{NO} / dt = V.\,MW_{NO}\,.\,d[NO]/dt \qquad (4.2)$$

where V is the volume of the subzone (m^3)

W_{NO} is molecular weight (kg/kmole)

The kinetics of this model is very sensitive to temperature, producing rapidly increasing amounts of NO with increasing temperature.

4.1.3 Model Inputs

A table of the most important inputs is shown below. See Appendix D for complete input file (215g11.dat).

Table 4.1 Model Inputs

Engine Data	**Fuel Injection**	**Fuel Properties**	**Multipliers**
Compression ratio	Mass of fuel injected per cycle	LHV	Ignition
Bore	Injection pressure profile	Heat of vaporization	Evaporation
Stroke	Injection timing	C/H/O content	Combustion Rate
Connecting rod length	Injection duration	Liquid density	
Piston cup diameter and depth	Number and diameter of nozzle holes	10, 50, 75 % volume distillation temperature	
Wall temperature	Fuel temperature at injection	Ignition activation energy	
Speed			
Valve timing			
Swirl			

4.1.4 User Input Multipliers

In order to match modeling results to experimental data user input multipliers are used to adjust rates of evaporation, ignition and combustion. It is important to explain how the evaporation, ignition and combustion multipliers relate to their respective governing equations. Again, this is treated in more detail by Shihadeh.

Ignition Multiplier

The ignition delay (τ) is calculated with an Arrhenius type expression which includes the local air fuel equivalence ratio, the local temperature and pressure, the fuel activation energy and an ignition multiplier M_i.

$$\tau = M_i A_i / ([\phi(3-\phi)^2]\, p^{Bi} \exp(-C_i/T)) \qquad (4.3)$$

where Ai, Bi and Ci are values based on previous correlations with published data, ϕ is the local vapor phase fuel equivalence ratio, and T and p are the local temperature and pressure.

Evaporation Multiplier

The evaporation rate per droplet is approximated by:

$$dm_v/dt = M_v G \pi D_d^2 \qquad (4.4)$$

where M_v is the evaporation multiplier and D_d is the instantaneous droplet diameter. In the case of diffusion-limited evaporation, G, the mass flux is a function of droplet density, the mass diffusion coefficient, the Sherwood number and D_d. In the case of boiling limited evaporation:

$$G = Q / h_{fg}$$

where Q is the heat flux to the droplet and h_{fg} is the latent heat of vaporization.

Combustion Rate Multiplier

Normally, combustion kinetics in CI engines is not the limiting rate on combustion. The rate is determined by the amount of fuel vapor and air mixed to within combustible proportions.

The chemical kinetics can become the rate limiting step at low local temperatures e.g. around start of combustion. The rate of combustion for this case is given by:

$$dm_k/dt = M_c A_c \phi(3-\phi)^2 \; p^{Bc} \exp(-Cc/T) \qquad (4.5)$$

where m_k is the mass of fuel, M_c is the combustion rate multiplier, and Bc and Cc are equal to 2.5 and 400 K, respectively.

Matching Methodology

The matching methodology is an iterative method using the three input multipliers. First, the correct ignition delay is obtained using the ignition multiplier. Then the combustion multiplier is adjusted so that the peak heat release rate occurs at the correct timing. Finally the evaporation multiplier is adjusted to match the peak pressure. The evaporation multiplier affects the ignition delay, therefore iteration is usually required. The method converges to a unique solution because only the combustion multiplier can significantly affect the location of the peak heat release relative to start of combustion.

4.2 Matching Model to Experimental Results

The objective behind using the model was to match it to a selected set of base diesel experimental results and then change the fuel properties to account for the presence of water in the emulsion, match the model again, and compare the difference in NOx for the experimental and modeled cases. This was to see if there were any effects on the NOx emissions other than those due to the presence of water e.g. "denoxing" due to NH_3 or some catalytic effect due to nanoclusters.

Since the GO-11 batch of fuels was the most extensively tested, GO-11 was chosen as the base fuel for the model. 251-02 (9% water) emulsion was chosen because it had the highest water content of the GO-11 fuels. The two runs in Table 4.2 are samples of the experimental runs compared.

Table 4.2 Samples of Experimental Data for Runs Used in Modeling

Fuel	File	SOI (DBTC)	Imep (bar)	Equivalence Ratio	NOx (ppm)
GO-11	215G11.dat	6.12	5.63	0.49	990
251-02	221B3.dat	6.12	5.62	0.50	880

4.2.1 Modeling GO-11 Base Diesel

The GO-11 properties (supplied by Statoil) were input into the diesel properties file. Information about the latent heat was not available therefore a value of 250 kJ/kg [31] was used. Since Shihadeh had used a different base diesel small adjustments to the diesel case multipliers were necessary to match the model pressure trace to the experimental pressure trace. While the pressure trace and ignition delay matched closely with experimental data, it was not possible to match the heat release rates as closely. The initial heat release rate calculated from the pressure data is too high due to the pressure oscillations in the cylinder. Therefore, instead of comparing the heat release rates, the cumulative heat releases were compared. The cumulative heat release has an exponential decay profile, so the time from SOI to the point at which the normalized heat release reached a value of $(1-e^{-1}) = 0.632$ was used as a basis for comparison.

The GO-11 modeling - experimental comparison results are shown in Figure 4.1. The engine out modeled NOx concentration was 1400 ppm compared to 990 ppm for the experimental case. The difference is due to the sensitivity of NOx emissions to temperature and the inaccuracy in the rate constants [31].

4.2.2 Modeling 251-02 Emulsion

It is not possible to input a two-phase fuel into the model. Therefore to account for the water, the C/H and C/O ratios of the fuel were changed and the fuel was treated as a mixture of water and GO-11 diesel with a correspondingly mass-averaged latent heat of vaporization. The latent heat of the surfactant was assumed to be the same as the fuel. The LHV and density of the emulsion provided by QET was used in the model. There was no accurate distillation curve information for the emulsion, (Statoil found that it was difficult to maintain the required distillation flowrate due to vigorous distillation during the initial stages), the GO-11 curve was used instead with the expectation that the difference could be corrected with the evaporation multiplier. Likewise, the activation energy was not changed. The nitrogen in the fuel was not taken into account.

The model was matched by varying the three input multipliers. Firstly the ignition delay was corrected. The combustion multiplier was adjusted so that the heat release peak occurred at the proper timing. Then the evaporation multiplier was adjusted so that the pressure curves matched. Iteration was required since varying the combustion and vaporization multipliers affects the ignition delay. The ratio of the emulsion multipliers to the diesel ones was:

ignition (M_i)	= 0.86
combustion (M_c)	= 0.90
evaporation (M_v)	= 2.00

The modeling and experimental comparisons are shown in Figure 4.2. Again it was possible to match the pressure and cumulative heat release closely. The ignition multiplier is lower because the model does not account for the cetane improver in the emulsion and possibly the microexplosion effect. The combustion multiplier is lower reflecting the slower chemical kinetics probably due to lower flame temperature. This lower flame temperature could be due to the latent heat of the surfactant package, which was not included in the modified fuel properties. The evaporation multiplier is higher.

This is explained by the microexplosion effect significantly increasing the rate of evaporation and the difference in the distillation curves which was not taken into account.

4.2.3 Comparison of Modeled NOx Emissions

The in-cylinder NOx emissions are shown in Figure 4.3 for the two fuels. They are normalized relative to the exhaust NOx concentration for the GO-11 fuel. It is interesting to note that there is a smaller than expected amount of NOx decomposition in the cylinder after the occurrence of peak NOx compared to experimental studies [31]. Therefore the model could be over-predicting the exhaust NOx emissions. However this is the case for both fuels so it should not affect the comparison of the fuels. The actual exhaust concentration for the GO-11 model was 1400ppm (wet) compared to 990ppm (dry) for the experimental results. Taking into account the sensitivity of the NOx formation rate to temperature and the inaccuracy of the rate constants this is not unexpected.

The difference in NOx for the modeled results is 16% compared to 11% for the experimental results. It is difficult to say that this is a significant difference given the accuracy of the model, however this would suggest that the ammonia does not have a significant denoxing effect compared to the reduction due to the water, otherwise the experimental decrease should be higher. Also it implies there is not some other NOx reducing catalytic affect due to the nanoclusters. The fact that it is higher could be explained by the presence of nitrogen in the fuel (not included in the model) and possibly higher flame temperatures during the mixing-controlled phase of combustion for the emulsion due to better droplet atomization.

Figure 4.1 GO-11 Cylinder Pressure & Heat Release

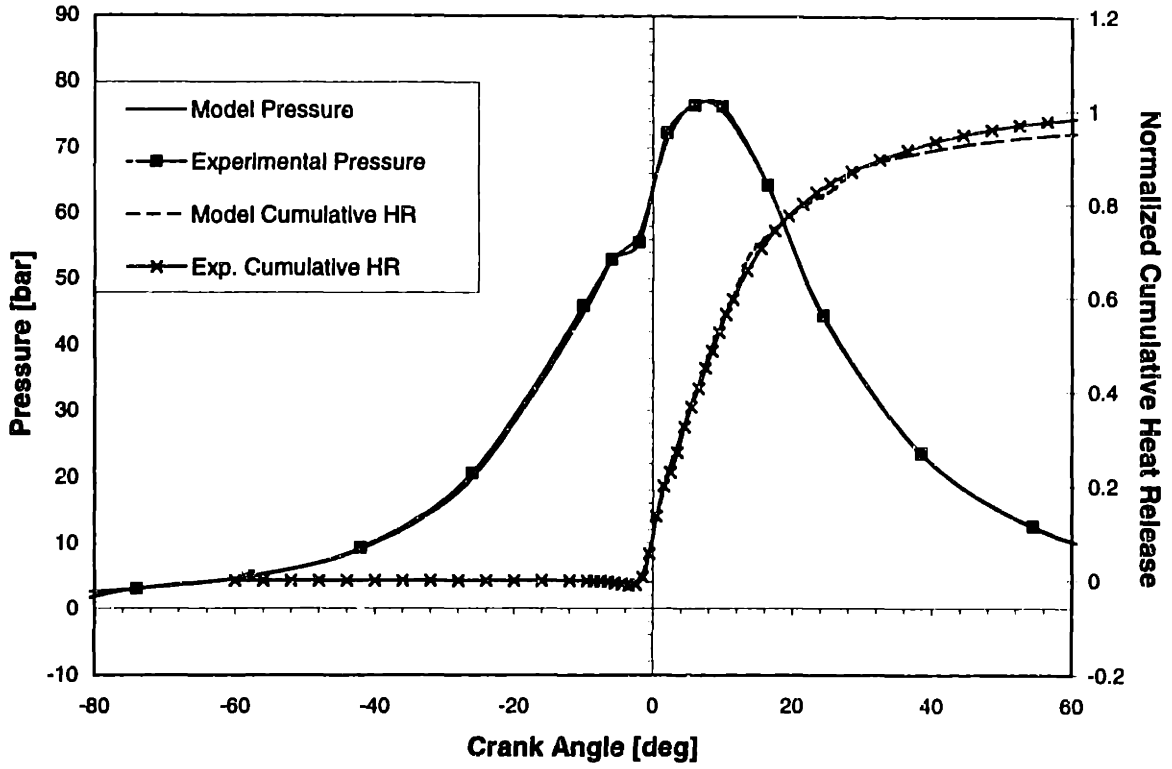

Figure 4.2 251-02 Cylinder Pressure & Heat Release

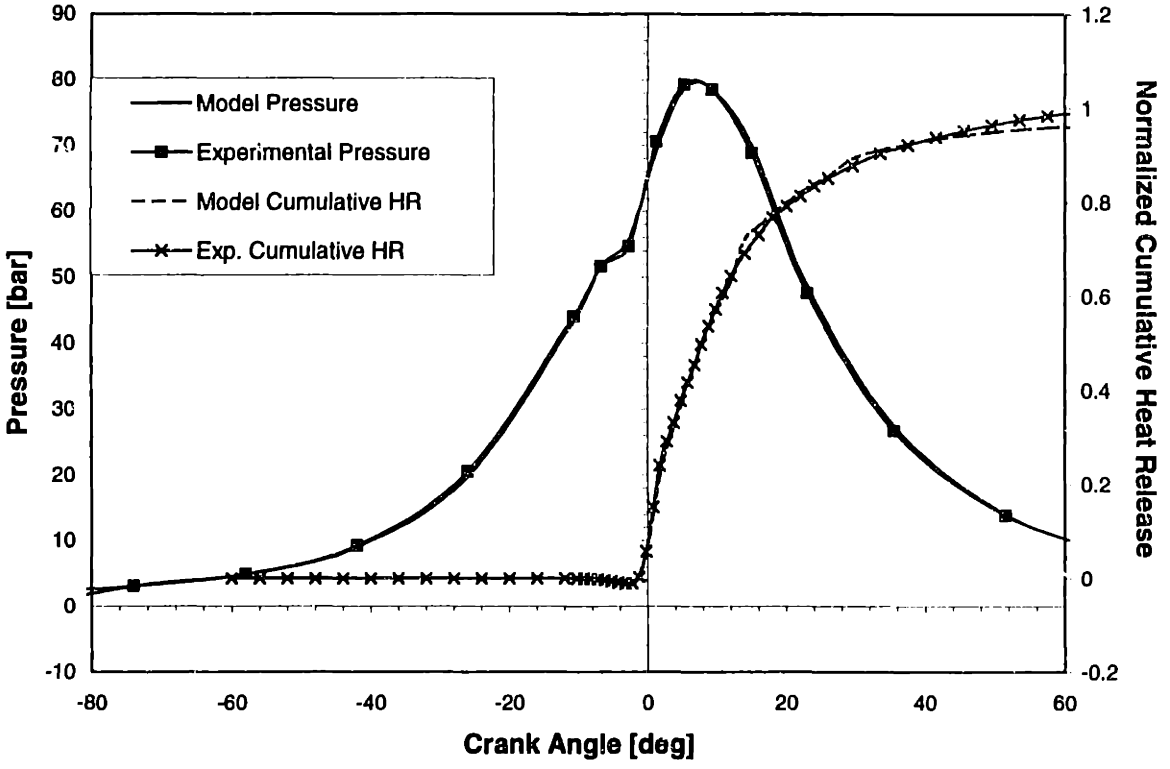

Figure 4.3 Modeled Normalized In-Cylinder NOx Concentration

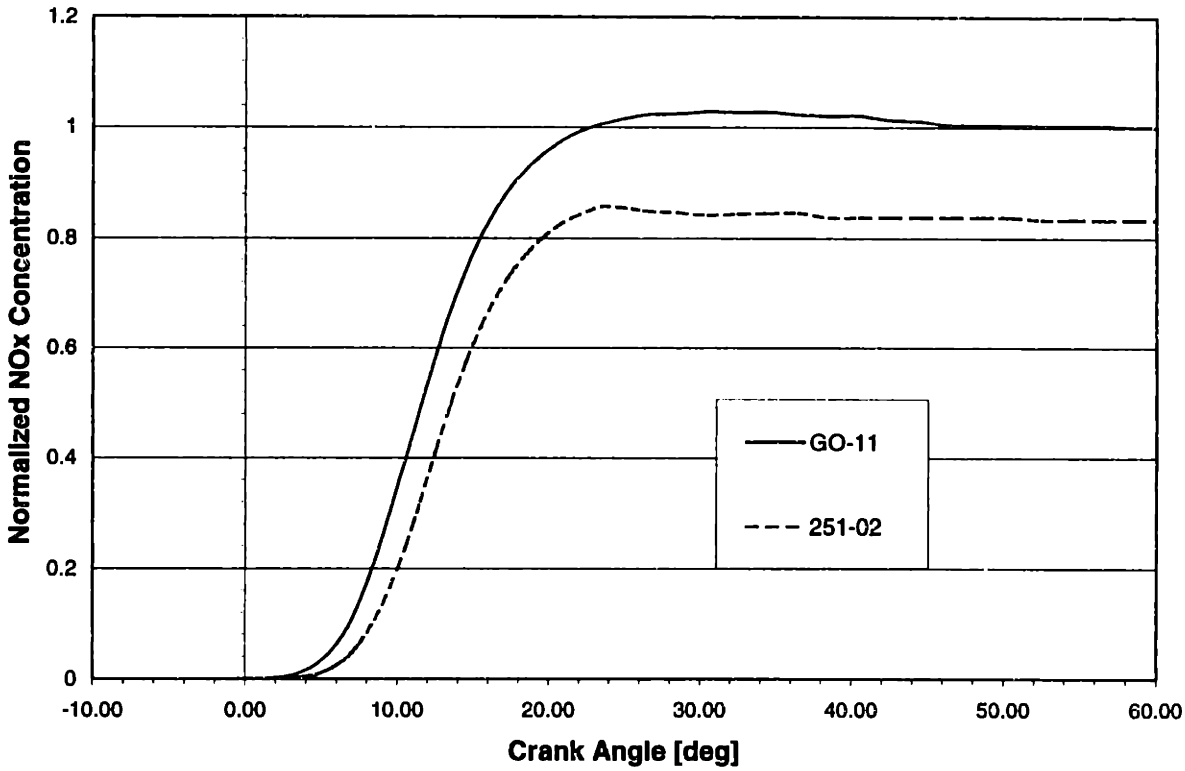

CHAPTER 5

CONCLUSIONS AND RECOMMENDATIONS

5.1 Summary

The purpose of this research was to investigate the effect of nanoemulsions supplied by Quantum Energy Technologies Corporation (QET) on NOx and particulate matter emissions and engine performance for a direct injection compression ignition engine. This objective was pursued by running tests on a single cylinder Ricardo Hydra test engine and modeling the effect of water addition to the base diesel fuel using a previously verified model of the test engine.

After some initial problems with the test equipment and the test fuels, tests were performed on two batches of emulsions based on different base diesels, namely MK-1 and GO-11 diesel. The model was matched to experimental results for a 9% water emulsion (251-02) and its base diesel (GO-11). A comparison of the modeling results was made.

5.2 Conclusions

The experimental and modeling results showed:

- There is no improvement or deterioration in indicated fuel conversion efficiency when operating with the nanoemulsions compared to their base diesel fuels.

- There is a significant reduction in specific NOx emissions when running with nanoemulsions, of the order of 13 to 20% for 9% water in the emulsion. This reduction increases with increasing water content.

- Nanoemulsions exhibit lower particulate matter emissions on both a number and volume/mass basis than their base diesels. Mass reductions are ca. 15% for a 9% water emulsion.

- The presence of ammonia as a neutralizer in the surfactant package of the emulsions does not appear to have a significant effect on NOx emissions.

- Nanoemulsions do not exhibit greater reductions in particulate matter than reductions reported in literature for microemulsions, indicating there is no "catalytic" effect due to the nanoclusters.

5.3 Recommendations

Further research is required into nanoemulsified fuels. All the tests in this work were performed at the same operating condition. Different operating conditions should be tested to investigate whether nanoemulsions produce the same benefits at other loads and speeds. The originally proposed test matrix should be completed to further elucidate the effects of the various components of the emulsion package on the observed results. Tests on a modern high-speed direct injection (HSDI) diesel engine would be more relevant as regards current and future diesel use in automotive applications.

In sum, nanoemulsified fuels have some promise for reducing NOx and PM emissions, however they do not exhibit any significant improvement over normal microemulsions. However, nanoemulsions have the advantage of providing stable mixtures for longer periods and over wider temperature ranges than microemulsions.

The final analysis of the economic viability of nanoemulsions for large scale use in compression-ignition engines will depend on the cost of overcoming technical barriers associated with long term emulsion stability and corrosion effects, in addition to the cost of producing the nanoemulsions, as compared to the unit cost of reducing NOx and PM by other means.

REFERENCES

[1] "Air Quality Criteria for Particulate Matter", EPA Vol. 1 1996

[2] Abdul-Khalek I. S., Kittelson, D. B.,
"Diesel Exhaust Particle Size: Measurement Issues and Trends." SAE Paper No. 980525, 1998.

[3] Bagley, S. T., Baumgard, K. J., Gratz, L. D., Johnson, J. H., and Leddy, D. G.
"Characterization of Fuel and Aftertreatment Device Effects on Diesel Emissions," Health Effect Institute, Research Report Number 76, September 1996.

[4] Flynn, P. F., Durrett R. P., Hunter G. L., zur Loye, A. O., Akinyemi, O. C., Dec, J. E., Westbrook, C. K.,
"Diesel Combustion: An Integrated View Combining Laser Diagnostics, Chemical Kinetics, and empirical Validation." SAE Paper No. 1999-01-0509, 1999.

[5] Dec, J.,
"A Conceptual Model of DI Diesel Combustion Based on Laser-Sheet Imaging," SAE Paper No. 970873, 1997.

[6] Tsukahara, M., Yoshimoto, Y., Murayama, T.,
"W/O Emulsion Realizes Low Smoke and Efficient Operation of DI Engine without High Pressure Injection." SAE Paper No. 890449, 1989.

[7] Yoshimoto, Y., Tsukahara, M.,
"NOx Reduction with EGR in a Diesel Engine Using Emulsified Fuel."
SAE Paper No. 982490, 1998.

[8] Crookes, R. J., Nazha, M. A. A., Kiannejad, F.,
"Single and Multi Cylinder Diesel Engine Tests with Vegetable Oil Emulsions"
SAE Paper No. 922230, 1992.

[9] Crookes, R. J., Nazha, M. A. A., Kiannejad, F.,
" Performance and Emissions of a 2.5 Litre Multi-Cylinder Direct Injection Automotive Diesel Engine with Alternative Diesel Fuels and Emulsions."
Proc. IMechE Seminar on Fuels for Automotive and Industrial Diesel Engines 1993.

[10] Andrews, G. E., Bartle, K. D., Pang, S. W., Nurein, A. M., Williams, P. T.,
"The Reduction in Diesel Particulate Emissions Using Emulsified Fuels"
SAE Paper No. 880348, 1988.

[11] Donnelly, J. J., White, H. M.,
"Water and Alcohol Use in Automotive Diesel Engines"
U.S. Department of Energy – September 1989.

[12] Dryer F. L.,
"Water Addition to Practical Combustion Systems – Concepts and Applications"
Sixteenth Symposium on Combustion, pp 279-295, The Combustion Institute 1976.

[13] Sheng, H., Chen, L., Wu, C.,
"The Droplet Group Micro-Explosions in W/O Diesel Fuel Emulsion Sprays"
SAE Paper No. 950855, 1995.

[14] Sekar, R. R., Schaus, J. E., Cole, R. L.,
"Cylinder Pressure Analysis of a Diesel Engine Using Oxygen-Enriched Air and Emulsified Fuels." SAE Paper No. 901565, 1990.

[15] Wirbeleit, F., Enderle, C., Lehner, W., Raab, A., Binder, K.,
"Stratified Diesel Fuel-Water-Diesel Fuel Injection Combined with EGR – The Most Efficient In-Cylinder NOx and PM Reduction Technology." SAE Paper No. 972962, 1997.

[16] Kohetsu, S., Mori, K., and Sakai, K.,
"Reduction of Exhaust Emissions with Water Injection System in a Diesel Engine." SAE Paper No. 960033 1996.

[17] "Acquisition and Analysis of Cylinder Pressure Data – Recommended Procedures," Ford Motor Company Standard 1992

[18] Miller, T. C.,
"Characterization of Lube Oil Derived Diesel Engine Particulate Emission Rate vs. Lube Oil Consumption" S.M. Thesis, M.I.T., May 1996.

[19] Hirakouchi, N., Fukano, I., Shoji, T.,
"Measurement of Diesel Exhaust Emissions with Mini-Dilution Tunnel"
SAE Paper No. 890181, 1989.

[20] "Diesel Particulate Filter Handling and Weighing,"
Test Procedure TP 714C, EPA 1994.

[21] "Explorer Balances" Instruction Manual, Ohaus Corporation, 1994.

[22] Amann, C. A., Stivender, D. L., Plee, S. L., MacDonald, J. S.,
"Some Rudiments of Diesel Particulate Emissions." SAE Paper 800251, 1980.

[23] MacDonald, S. J., Gross, G. P., Johnson J. H.,
"Status of Diesel Particulates Measurement Methods"
SAE Paper No. 840345, 1984.

[24] Kayes, D., Hochgreb, S.,
"Investigation of the Dilution Process for Measurement of Particulate Matter from Spark-Ignition Engines." SAE Paper No. 982601, 1998.

[25] Phone Conversation with Kathy Erickson, Sr. Application Engineer,
Particle Instrument Division, TSI Incorporated. August 1998.

[26] "Model 3071A Electrostatic Classifier" Instruction Manual,
TSI Incorporated 1997.

[27] Shihadeh, A. L.,
"Rural Electrification from Local Resources: Biomass Pyrolysis Oil Combustion in a Direct Injection Diesel Engine"
Ph.D. Thesis, M.I.T., September 1998.

[28] Cheung, H. M.,
"A Practical Burn Rate Analysis for Use in Engine Development and Design."
S.M. Thesis, M.I.T., 1993.

[29] Peyton, K. B.,
Fuel Field Manual – Sources and Solutions to Performance Problems,
McGraw-Hill Book Company, 1997.

[30] Maricq, M. M., Chase, R. E., Podsiadilk, D. H., Siegl, W. O., Kaiser, E. W.,
"The Effect of Dimethoxy Methane Additive on Diesel Vehicle Particulate Emissions," SAE Paper No. 982572, 1998.

[31] Heywood, J. B.,
Internal Combustion Engine Fundamentals, McGraw-Hill Book Company, 1988.

APPENDIX A

Calculations

Calculation of Indicated Specific Total Particulate Rate (TPR)

TPR (g/kWhr) is a measure of the amount of PM produced by the engine per kilowatt-hour of work done. In order to calculate TPR the rate of total mass of PM production must be calculated.

The mass deposited on the filter is simply the difference between initial and final filter mass.

$$m_{dep} = m_{final} - m_{initial}$$

where:

m_{dep} = Total Deposited Mass [grams]

$m_{initial}$ = Initial Filter Mass [grams]

m_{final} = Final Filter Mass [grams]

The mass of sampled diluted exhaust (m_{sample})

$$m_{sample} = \frac{P_{avg}.Q_{crit}}{R.(273+T_s)} * sampling\ time$$

where:

P_{avg} is the time averaged pressure upstream of the orifice estimated using integration of a 2nd order polynomial fit to the pressure data, [Pa]

Q_{crit} is the choked volume flowrate for the flow orifice, [m^3/s]

T_s is the temperature after the filter. [°C]

Mass deposited per mass of diluted exhaust sampled (m_{ds})

$$k_{ds} = m_{dep} / m_{sample}$$

The volumetric dilution ratio of diluted air to raw exhaust (r_d) is

$$r_d + 1 = \frac{[CO_2]_{exh} - [CO_2]_{bg}}{[CO_2]_{dil} - [CO_2]_{bg}}$$

The mass ratio of dilution air to exhaust gas (k_d) is

$$k_d = r_d * \frac{MWair}{MWexh}$$

The molecular weight of the exhaust (MWexh) is calculated at end of this section.
Therefore mass deposited per mass of raw exhaust sampled (k_{des})

$$k_{des} = k_{ds} * (k_d + 1)$$

Therefore rate of production of particulate matter (PM) [g/s]

$$PM = k_{des} * m_{exh}$$

where m_{exh} is the exhaust mass flowrate [g/s] = airflow [g/s] + fuel flow [g/s].

Indicated specific total particulate rate (TPR) [g/kWhr]

$$TPR = PM\ (g/s) * 3600 / (Indicated\ Power\ (kW))$$

Calculation of Molecular Weight of Exhaust

The calculation of the molecular weight of the exhaust requires use of information that is readily available from experimentation and from fuel specifics. The primary piece of data is the actual air to fuel ratio, λ. It can be calculated using the relationship given by

$$\lambda = \frac{\left(\frac{A}{F}\right)_{actual}}{\left(\frac{A}{F}\right)_{stoichiometric}}$$

Stoichiometric air to fuel ratio depends only on the hydrogen to carbon ratio, y, of the fuel. Heywood [31] lists this equation for calculation of the stoichiometric air to fuel ratio.

$$\frac{A_{st}}{F_{st}} = \frac{34.56(4 + y)}{12.011 + 1.008y}$$

Therefore, λ can be directly calculated using equation

$$\lambda = \frac{(12.011 + 1.008y)\cdot Q_{air}}{(138.24 + 34.56y)\cdot Q_{fuel}}$$

where:

λ	= Actual Air to Fuel Ratio
Q_{fuel}	= Mass Flow Rate of the Fuel [kg/sec]

The equation for the $MW_{exhaust}$ is then derived using the formula for stoichiometric combustion found as equation 3.5 in Heywood [31].

$$CaHb + \left(a + \frac{b}{4}\right)\cdot(O_2 + 3.773N_2) = a\cdot CO_2 + \frac{b}{2}\cdot H2O + 3.773\left(a + \frac{b}{4}\right)\cdot N_2$$

Miller [18] used the following formula to calculate the molecular weight of the exhaust.

$$MW_{exhaust} = \frac{32 \cdot \frac{2 \cdot \lambda \cdot \left(a + \frac{b}{4}\right) - 2 \cdot \left(a + \frac{b}{4}\right)}{2} + 32 \cdot a + 12.011 \cdot a + 2 \cdot \left(\frac{b}{2}\right) + 16 \cdot \left(\frac{b}{2}\right) + 3.773 \cdot (28.16) \cdot \left(a + \frac{b}{4}\right) \cdot \lambda}{a + \frac{b}{2} + \frac{\left[2 \cdot \lambda \cdot \left(a + \frac{b}{4}\right) - 2 \cdot \left(a + \frac{b}{4}\right)\right]}{2} + 3.773 \lambda \cdot \left(a + \frac{b}{4}\right)}$$

where:

$MW_{exhaust}$	= Molecular Weight of the Exhaust [kg/kmole]
a	= Number of Carbon Atoms / Fuel Molecule
b	= Number of Hydrogen Atoms / Fuel Molecule
λ	= Actual Air to Fuel Ratio
N_2	= 28.16 kg/kmole
O_2	= 32 kg/kmole
C	= 12.011 kg/kmole
H_2	= 2.016 kg/kmole

A simplified form of this formula is shown below as equation

$$MW_{exhaust} = \frac{a \cdot (138.25\lambda + 12.011) + b \cdot (34.562\lambda + 1)}{a \cdot (4.773\lambda) + b \cdot (1.19325\lambda + 0.25)}$$

This equation was used for calculating molecular weight of the exhaust for input into the mass dilution ratio equation.

APPENDIX B

FUEL PROPERTIES

Matrix Diesel						
Fuel Type	**Sample No(s).**	**H/C**	**O/C**	**% Cetane Improver**	**Density@25C**	**LHV (MJ/kg)**
Base Diesel	Matrix	2.081				42.01
6% Water	QF 224-01	2.061	0.0108	0.0		39.42
9% Water	QF 223-01	2.048	0.0162	0.0		37.71
12% Water	QF 173-04	2.043	0.0219	0.0		36.16

MK-1 Diesel						
Fuel Type	**Sample No(s).**	**H/C**	**O/C**	**% Cetane Improver**	**Density@25C**	**LHV (MJ/kg)**
Base Diesel	MK-1	2.204			0.803	43.07
6% Water (NH3)*	QF 239-02, QF 235	2.203	0.0134	0.1	0.813	39.66
6% Water (MEA)**	QF 236-02, BM 1-4	2.190	0.0177	0.1	0.820	39.34
9% Water	QF 237-04, QF 181	2.204	0.0196	0.1	0.823	37.61

GO-11 Diesel						
Fuel Type	**Sample No(s).**	**H/C**	**O/C**	**% Cetane Improver**	**Density@25C**	**LHV (MJ/kg)**
Base Diesel	GO-11	1.896			0.852	42.76
6% Water (NH3)	QF 285-01	1.878	0.0131	0.1	0.858	39.37
6% Water (MEA)	QF-240	1.866	0.0173	0.0	0.861	39.06
9% Water	QF 251-02	1.896	0.0192	0.1	0.862	37.34

NH_3 : Ammonia neutralized surfactant package
MEA: Monoethanolamine neutralized surfactant package

Certificate of Analysis

PHILLIPS CHEMICAL COMPANY
A DIVISION OF PHILLIPS PETROLEUM COMPANY

SPECIALTY CHEMICALS
P.O. BOX 968
BORGER, TX 79008-0968

DATE OF SHIPMENT

CUSTOMER ORDER NO.

INV./REQN. NO.

CONTAINER NO.

ULTRA-LOW SULFUR DIESEL FUEL
LOT W-541

TEST	RESULTS	SPECIFICATIONS	METHOD
Specific Gravity, 60/60	0.8333	Report	ASTM D-4052
API Gravity	38.3	40 Max.	ASTM D-1298
Flash Point-PM, °F	170	Report.	ASTM D-93
Pour Point, °F	+5	Report	ASTM D-2500
Cloud Point °F	+14	Report	ASTM D-2500
Viscosity, cs 40C	3.59	Report	ASTM D-445
Sulfur, ppm	0.1	0.5 Max.	ASTM D-4294
Net Heat of Combustion	18553	Report	ASTM D-3338
Particulate Matter (mg/l)	2.9	15 Max.	ASTM D-2276
Cetane Index	55.4	Report	ASTM D-976
Cetane Number	46.3	40 Min.	ASTM D-613
Carbon, wt%	86.5	Report	
Hydrogen, wt%	13.5	Report	
DISTILLATION, °F			ASTM D-86
IBP	376		
5%	426		
10	453		
15	474		
20	492		
30	515		
40	527		
50	536		
60	546		
70	558		
80	575		
90	604		
95	648		
EP	657		
Loss	1.0		
Residue	1.2		
HYDROCARBON TYPE VOL. %			ASTM D-1319
Aromatics	28.0	Report	
Olefins	5.7		
Saturates	66.3		

EAA:jam
11/10/1998
RF4000

APPENDIX C

RESULTS

1) **Matrix Diesel Batch**

QF 224-01

QF 223-01

QF 173-01

Matrix Diesel

2) **MK-1 Diesel Batch**

MK-1 Diesel

QF 237-04

QF 239-02

QF 236-02

Heat Release

3) **GO-11 Diesel Batch (December 1998)**

GO-11

QF 251-02

QF 240

QF 285-01

Sample Filter Results

SMPS Results (February 1999)

4) **Sample SMPS Output:**

Filename 221c8.000

QF 285-01 at SOI = 4.08, Dilution Ratio = 52

	DATE	18-Apr-98		TEST	QF224-01	6% Water						
TEST NO.	SOI (DBTDC)	IMEP (bar)	Indicated Power (kW)	Air Flow (g/s)	Fuel Flow (g/s)	ISFC (g/kWhr)	NOX (ppm dry)	NO (ppm dry)	AFR	NOx (g/hr)	NOx (g/kg fuel)	NOx (g/kW-h)
4189	8.16	4.49	4.04	9.42	0.262	233	750	690	35.95	27.94	29.63	6.92
41810	8.16	4.47	4.02	9.42	0.261	234	740	670	36.09	27.73	29.51	6.90
41811	6.3	4.49	4.04	9.42	0.259	231	670	610	36.37	25.05	26.86	6.20
41812	7.02	4.36	3.92	9.42	0.248	228	670	620	37.98	24.88	27.86	6.34
41813	5.02	4.46	4.01	9.42	0.261	234	610	560	36.09	22.74	24.21	5.67
41815	5	4.50	4.05	9.43	0.265	236	550	510	35.58	20.46	21.45	5.05
41816	5.1	4.45	4.00	9.43	0.26	234	560	510	36.27	20.96	22.39	5.24
41817	4.08	4.41	3.97	9.43	0.263	239	520	480	35.86	19.37	20.46	4.88
41819	9.18	4.43	3.99	9.42	0.261	236	810	740	36.09	30.25	32.20	7.59
4202	8.16	4.25	3.82	9.44	0.252	237	710	640	37.46	26.67	29.40	6.98
4204	7.92	4.21	3.79	9.44	0.24	228	710	640	39.33	26.64	30.83	7.03
4205	7.18	4.27	3.84	9.41	0.243	228	670	610	38.72	24.98	28.56	6.51
(a) LHV (MJ/kg)	39.4											

	DATE	5-May-98		TEST	QF 223-01	9% Water							
TEST NO.	SOI (DBTDC)	IMEP (bar)	Indicated Power (kW)	Air Flow (g/s)	Fuel Flow (g/s)	ISFC (g/kWhr)	NOX (ppm dry)	NO (ppm dry)	AFR	Exhaust Flow (g/sec)	NOx (g/hr)	NOx (g/kg fuel)	NOx (g/kW-h)
5051	10.2	4.1	3.69	9.49	0.247	241.1	900	830	38.42	9.74	33.70	37.89	9.14
5053	9.18	4.14	3.72	9.49	0.245	236.8	810	750	38.73	9.74	30.28	34.33	8.13
5055	7.14	4.38	3.94	9.48	0.253	231.2	720	650	37.47	9.73	27.15	29.81	6.89
5057	5.1	4.65	4.18	9.5	0.277	238.4	600	540	34.30	9.78	22.75	22.81	5.44
5059	3.1	4.82	4.34	9.48	0.291	241.6	500	460	32.58	9.77	18.80	17.95	4.34
50512	6.12	4.712	4.24	9.47	0.276	234.4	620	560	34.31	9.75	23.40	23.56	5.52
50512a	8.16	4.38	3.94	9.45	0.256	233.9	730	670	36.91	9.71	27.29	29.61	6.93
LHV (MJ/kg)	37.76												

	DATE	05-May-98		TEST	QF 173-04	12% water							
TEST NO.	SOI (DBTDC)	IMEP (bar)	Indicated Power (kW)	Air Flow (g/s)	Fuel Flow (g/s)	ISFC (g/kWhr)	NOX (ppm dry)	NO (ppm dry)	AFR	Exhaust Flow (g/sec)	NOx (g/hr)	NOx (g/kg fuel)	NOx (g/kW-h)
50514	10.6	4.44	3.99	9.53	0.27	243.4	920	820	35.30	9.80	35.08	36.09	8.79
50516	9.18	4.49	4.03	9.48	0.269	240.0	840	750	35.24	9.75	31.85	32.89	7.89
50518	7.14	4.64	4.17	9.49	0.273	235.4	710	640	34.76	9.76	26.67	27.34	6.44
50522	5.1	4.89	4.40	9.48	0.289	238.5	610	550	32.80	9.77	23.10	22.20	5.25
50524	3 3	4.96	4.46	9.47	0.299	241.4	510	460	31.67	9.77	19.31	17.94	4.33
50525	2.06	5.03	4.52	9.45	0.307	244.2	460	430	30.78	9.76	17.17	15.54	3.80
50527	8.16	4.75	4.28	9.46	0.281	236.6	720	650	33.67	9.74	27.17	26.86	6.35
50529	6.12	4.80	4.32	9.47	0.283	235.9	630	580	33.46	9.75	23.64	23.20	5.47
LHV (MJ/kg)	36.16												

DATE	6-May-98		TEST	Matrix Diesel 1								
SOI (DBTDC)	IMEP (bar)	Indicated Power (kW)	Air Flow (g/s)	Fuel Flow (g/s)	ISFC (g/kWhr)	NOX (ppm dry)	NO (ppm dry)	AFR	Exhaust Flow (g/sec)	NOx (g/hr)	NOx (g/kg fuel)	NOx (g/kW-h)
9.18	4.566	4.11	9.5	0.255	223.5	830	760	37.25	9.76	31.21	34.00	7.60
7.16	4.955	4.46	9.49	0.275	222.1	740	680	34.51	9.77	27.82	28.10	6.24
5.44	4.9	4.41	9.49	0.272	222.1	640	580	34.89	9.76	24.17	24.68	5.48
3.46	4.75	4.27	9.48	0.27	227.5	510	470	35.11	9.75	19.12	19.68	4.48
1.86	4.78	4.30	9.51	0.276	231.1	410	390	34.46	9.79	15.25	15.35	3.55
10.2	4.62	4.16	9.46	0.262	226.9	980	880	36.11	9.72	36.98	39.21	8.90
42.03												
.												

			FUEL	MK-1 Diesel										
			DATE	28-May-98										
TEST NO.	LOAD (Nm)	POWER (kW)	SOI (DBTC)	IMEP (bar)	Indicated Power (kW)	Peak Pressure (bar)	Peak Location (DABC)	Air Flow (g/s)	Fuel Flow (g/s)	NOX (ppm dry)	NO (ppm dry)	AFR	Exhaust Flow (g/sec)	Indicated NOx (g/kW-h)
50306	16.5	4.14	9.18	5.36	4.82	88	184.6	9.1	0.308	1075	990	29.55	9.41	8.07
50305	16.6	4.17	9	5.4	4.86	87.3	186	9.09	0.309	1075	970	29.42	9.40	8.06
50303	16.5	4.14	8.16	5.36	4.82	85.9	185	9.09	0.308	990	920	29.51	9.40	7.40
50304	16.7	4.20	8.16	5.46	4.91	84.7	185	9.09	0.308	1000	930	29.51	9.40	7.33
50307	16.8	4.22	7.14	5.47	4.92	83	186	9.1	0.309	990	890	29.45	9.41	7.34
50308	16.7	4.20	7.14	5.44	4.89	83	186	9.1	0.309	980	890	29.45	9.41	7.28
50301	16.9	4.25	6.12	5.52	4.97	79.3	186.9	9.12	0.309	840	780	29.51	9.43	6.12
50309	16.9	4.25	6.12	5.54	4.98	79.9	186.9	9.1	0.31	910	840	29.35	9.41	6.60
503010	17.2	4.32	6.12	5.6	5.04	80	186.9	9.09	0.311	920	840	29.23	9.40	6.62
50302	17.0	4.27	5.52	5.51	4.96	78.6	187	9.12	0.309	850	790	29.51	9.43	6.20
503011	17.2	4.32	5.1	5.62	5.06	77.3	187.2	9.11	0.312	860	800	29.20	9.42	6.14
503012	17.3	4.35	5.1	5.64	5.07	77.4	186.8	9.11	0.312	850	790	29.20	9.42	6.05
503014	17.4	4.37	4.52	5.53	4.97	75.9	187.9	9.1	0.313	810	750	29.07	9.41	5.88
503013	17.3	4.35	4.1	5.65	5.08	74.9	187.4	9.09	0.314	800	740	28.95	9.40	5.69
503015	17.3	4.35	3.06	5.64	5.07	72.1	187.9	9.1	0.317	730	680	28.71	9.42	5.19
503016	17.3	4.35	3.06	5.67	5.10	72.1	187.8	9.1	0.317	720	680	28.71	9.42	5.07
503017	17.0	4.27	2.04	5.6	5.04	69.1	188.4	9.1	0.316	660	610	28.80	9.42	4.74
503018	17.1	4.30	2.04	5.55	4.99	70.6	188.4	9.1	0.316	660	610	28.80	9.42	4.78
(a) LHV (MJ/kg)	43.07													

		FUEL	237-04	9% water										
		DATE	31-May-98											
TEST NO.	LOAD (Nm)	SOI (DBTC)	IMEP (bar)	Indicated Power (kW)	Peak Pressure (bar)	Peak Pressure (DABC)	Air Flow (g/s)	Fuel Flow (g/s)	NOX (ppm dry)	NO (ppm dry)	AFR	Exhaust Flow (g/sec)	NOx (g/hr)	Indicated NOx (g/kW-h)
503106	15.7	10.2	5.25	4.72	88.5	184.4	9.08	0.349	840	790	26.02	9.43	30.24	6.40
503107	15.7	10.2	5.14	4.62	88.4	184	9.09	0.349	850	780	26.05	9.44	30.90	6.68
503104	16	9.18	5.28	4.75	85.8	185.1	9.11	0.35	800	740	26.03	9.46	29.07	6.12
503105	16	9.18	5.35	4.81	86.6	184.7	9.08	0.347	800	740	26.17	9.43	28.97	6.02
503101	16.4	8.16	5.42	4.88	85.5	185.5	9.14	0.348	760	720	26.26	9.49	27.46	5.63
503102	16.1	8.16	5.25	4.72	83.9	185.4	9.11	0.347	760	710	26.25	9.46	27.51	5.82
503103	16	8.16	5.38	4.84	84.2	185.5	9.11	0.349	770	720	26.10	9.46	27.87	5.76
503108	16	7.14	5.42	4.88	82.5	186.2	9.09	0.349	740	680	26.05	9.44	26.89	5.52
503109	16	7.14	5.46	4.91	82.4	186.1	9.1	0.348	750	690	26.15	9.45	27.27	5.55
503110	16.2	6.12	5.46	4.91	79.7	186.9	9.1	0.351	700	650	25.93	9.45	25.37	5.17
503111	16.2	6.12	5.5	4.95	79.5	186.8	9.1	0.353	690	640	25.78	9.45	25.03	5.06
503112	16.3	5.1	5.48	4.93	77.1	186.8	9.09	0.353	640	590	25.75	9.44	23.24	4.71
503113	16.3	5.1	5.47	4.92	77.1	187	9.09	0.354	640	590	25.68	9.44	23.24	4.72
503115	16.3	4.46	5.52	4.97	75	187.6	9.1	0.354	600	560	25.71	9.45	21.72	4.37
503114	16.2	4.08	5.47	4.92	74.5	187.6	9.09	0.354	580	540	25.68	9.44	20.99	4.27
503116	16.1	3.06	5.43	4.88	71.8	188	9.11	0.354	510	480	25.73	9.46	18.42	3.77
503117	16.1	3.06	5.42	4.88	71.6	187.9	9.11	0.355	520	490	25.66	9.47	18.78	3.85
503118	15.9	2.04	5.41	4.87	68.5	188.4	9.07	0.355	470	440	25.55	9.43	16.94	3.48
(a) LHV (MJ/kg)	37.61													

		FUEL	239-02	6% Water										
		DATE	1-Jun-98											
TEST NO.	LOAD (Nm)	SOI (DBTC)	IMEP (bar)	Indicated Power (kW)	Peak Pressure (bar)	Peak Pressure (DABC)	Air Flow (g/s)	Fuel Flow (g/s)	NOX (ppm dry)	NO (ppm dry)	AFR	Exhsust Flow (g/sec)	NOx (g/hr)	Indicated NOx (g/kW-h)
60101	16.1	8.16	5.44	4.89	85.1	185.3	9.08	0.338	860	800	26.86	9.42	31.05	6.34
60102	16.1	8.16	5.5	4.95	84.2	185.6	9.08	0.337	860	810	26.94	9.42	30.90	6.25
60103	16.2	7.14	5.52	4.97	82.4	186.2	9.09	0.337	830	780	26.97	9.43	29.88	6.02
60104	16.4	7.14	5.44	4.89	82.5	186.1	9.09	0.337	840	780	26.97	9.43	30.37	6.21
60105	16.4	6.12	5.55	4.99	80.1	187.1	9.09	0.338	800	750	26.89	9.43	28.83	5.77
60106	16.5	6.12	5.53	4.97	80	187	9.08	0.339	800	750	26.78	9.42	28.80	5.79
60107	16.6	5.1	5.56	5.00	77.5	187.5	9.08	0.339	750	700	26.78	9.42	27.05	5.41
60108	16.5	5.1	5.58	5.02	77.6	187.6	9.08	0.34	750	700	26.71	9.42	27.05	5.39
60109	16.5	5.1	5.57	5.01	77.6	187.7	9.08	0.341	750	700	26.63	9.42	27.05	5.40
60110	16.6	4.3	5.61	5.05	75.13	187.8	9.09	0.343	700	650	26.50	9.43	25.33	5.02
60111	16.5	4.1	5.58	5.02	74.87	187.9	9.09	0.341	690	640	26.66	9.43	24.97	4.97
60113	16.4	3.06	5.63	5.06	72.2	188.4	9.07	0.341	620	580	26.60	9.41	22.32	4.41
60112	16.4	3.06	5.55	4.99	71.9	188.4	9.07	0.341	620	580	26.60	9.41	22.32	4.47
60114	16.2	2.56	5.43	4.88	69.9	188.4	9.07	0.343	550	520	26.44	9.41	19.73	4.04
60115	16.4	2.05	5.53	4.97	69.7	189	9.07	0.343	550	520	26.44	9.41	19.73	3.97
(a) LHV (MJ/kg)	39.66													

	FUEL	236-02	6% water									
	DATE	9-Jun-98										
TEST NO.	SOI (DBTC)	IMEP (bar)	Indicated Power (kW)	Peak Pressure (bar)	Peak Pressure (DABC)	Air Flow (g/s)	Fuel Flow (g/s)	NOX (ppm dry)	NO (ppm dry)	AFR	NOx (g/hr)	Indicated NOx (g/kW-h)
60903	9.18	5.56	5.00	88.2	185.3	9.24	0.354	980	880	26.1	36.49	7.30
60904	9.18	5.68	5.11	88.8	185.4	9.22	0.346	980	890	26.6	36.24	7.09
60905	9.18	5.76	5.18	89	185.4	9.21	0.349	970	890	26.4	35.72	6.89
60906	9.18	5.62	5.06	89	185.1	9.21	0.349	970	900	26.4	35.57	7.04
60911	8.16	5.74	5.16	86.4	185.3	9.21	0.347	950	870	26.5	35.00	6.78
60912	8.16	5.7	5.13	86.8	185.1	9.21	0.346	930	850	26.6	34.28	6.69
60901	7.14	5.75	5.17	83.94	186.2	9.27	0.35	870	810	26.5	32.07	6.20
60902	7.14	5.84	5.25	83.9	186	9.26	0.355	830	780	26.1	30.48	5.80
60909	7.14	5.89	5.30	84.1	186.2	9.21	0.351	900	820	26.2	33.23	6.27
60910	7.14	5.82	5.24	83.8	186.3	9.2	0.349	890	810	26.4	32.83	6.27
60918	7.14	5.56	5.00	83	186.1	9.22	0.336	870	800	27.4	32.00	6.40
60919	7.14	5.7	5.13	81.7	186.3	9.22	0.338	910	840	27.3	33.43	6.52
60913	6.12	5.74	5.16	81	186.6	9.21	0.347	820	750	26.5	30.22	5.85
60914	6.12	5.87	5.28	81	186.6	9.21	0.347	820	750	26.5	30.22	5.72
60908	5.1	6.01	5.41	77.5	187.3	9.21	0.355	760	690	25.9	28.11	5.20
60907	4.1	5.95	5.35	76.8	187.1	9.21	0.355	760	700	25.9	27.96	5.22
60916	3.06	5.89	5.30	73	187.6	9.21	0.347	680	630	26.5	24.95	4.71
60917	3.06	5.79	5.21	73.4	187.8	9.21	0.347	650	600	26.5	23.88	4.58
(a) LHV (MJ/kg)	39.34											

MK-1 Heat Release Results

		MK-1	LHV = 43.07 MJ/kg	AFRs = 15.06			
File	SOI (DBTC)	Peak Pressure (bar)	Peak Pressure Location (DATC)	Peak Mass Burning Rate (1/CAD)	Peak Mass Burning Rate Location (DATC)	SOC (q) (DATC)	Ignition Delay (q) (CAD)
50313	4	74.2	8	0.089	2	0	4
50309	6	79.5	8	0.07	3	-2	4
50310	6	79.6	7	0.068	3	-2	4
50303	8.1	85.5	6	0.078	1	3.7	4.2
50304	8	84.3	6	0.07	1	3.7	4.3
		237-04	LHV = 37.61 MJ/kg	AFRs = 13.32			
503114	4	73.7	8.5	0.087	2	0	4
503110	6.1	79.1	8	0.077	2	-2	4.1
503111	6.1	78.7	8	0.075	2	-2	4.1
503101	8.1	84.7	6	0.077	-1	-3.9	4.2
503103	8.1	83.4	7	0.084	-1	-3.7	4.4
		239-02	LHV = 39.66 MJ/kg	AFRs = 13.9			
60111	4	74.2	9	0.078	2	-0.7	3.3
60110	4.1	74.4	9	0.079	1	-0.9	3.2
60105	6.1	79.65	8	0.069	-1	-2.3	3.8
60106	6.1	79.58	8	0.068	-1	-2.3	3.8
60101	8.1	83.5	6	0.072	-1	-4	4
60102	8.1	84.6	6	0.06	-1	-4	4.1

	FUEL	GO-11	DATE	30-Nov-98	13-Dec-98								
	Water	0.00											
TEST NO.	LOAD (Nm)	POWER (kW)	SOI (DBTC)	IMEP (bar)	Indicated Power (kW)	Air Flow (g/s)	Fuel Flow (g/s)	NOX (ppm dry)	NO (ppm dry)	CO2 (%)	AFR	Indicated NOx (g/kW-h)	NOx (g/MJ fuel)
1130G04	18.3	4.60	4.08	5.86	5.27	9.23	0.329	720	680	7.75	28.05	4.98	0.518
1130G05	18.3	4.60	4.08	5.81	5.23	9.23	0.329	720	680	7.77	28.05	5.02	0.518
1130G06	18.3	4.60	4.08	5.82	5.24	9.24	0.329	730	690	7.79	28.09	5.08	0.526
1128G03	17.8	4.47	6.12	5.67	5.10	9.27	0.32	860	800	7.64	28.97	6.20	0.642
1128G04	18	4.52	6.12	5.69	5.12	9.25	0.32	860	800	7.64	28.91	6.16	0.640
1128G05	17.8	4.47	6.12	5.73	5.15	9.25	0.32	860	800	7.64	28.91	6.12	0.640
1130G01	18	4.52	6.12	5.67	5.10	9.25	0.321	860	800	7.67	28.82	6.19	0.638
1130G02	18.4	4.62	6.12	5.77	5.19	9.24	0.323	850	790	7.70	28.61	6.00	0.627
1130G03	18.3	4.60	6.12	5.74	5.16	9.25	0.326	850	790	7.72	28.37	6.04	0.622
1213G01*	18.1	4.55	6.12	5.62	5.06	9.23	0.323	850	790	7.79	28.58	6.16	0.626
1213G02*	18.2	4.57	6.12	5.74	5.16	9.22	0.322	850	790	7.79	28.63	6.02	0.627
1213G03*	18	4.52	6.12	5.57	5.01	9.21	0.322	850	790	7.79	28.60	6.20	0.627
1130G07	18.3	4.60	8.16	5.78	5.20	9.21	0.329	1000	920	7.89	27.99	7.06	0.725
1130G08	18.3	4.60	8.16	5.79	5.21	9.21	0.329	1000	920	7.82	27.99	7.05	0.725
1130G09	18.3	4.60	8.16	5.76	5.18	9.21	0.328	1000	920	7.8	28.08	7.08	0.727
(a) LHV (MJ/kg)	42.76												

	FUEL	251-02	DATE	4-Dec-98		NOX (LS Diesel)	840						
	Water	0.09				Reference	840						
TEST NO.	LOAD (Nm)	POWER (kW)	SOI (DBTC)	IMEP (bar)	Indicated Power (kW)	Air Flow (g/s)	Fuel Flow (g/s)	NOX *(ppm dry)	NO* (ppm dry)	CO2 (%)	AFR	Indicated NOx (g/kW-h)	NOx (g/MJ fuel)
124A09	17.5	4.40	4.2	5.53	4.975	9.12	0.36	660	620	7.79	25.33	4.80	0.494
124A10	17.5	4.40	4.2	5.54	4.984	9.12	0.36	660	620	7.79	25.33	4.80	0.494
124A01	17.9	4.50	6	5.56	5.002	9.2	0.36	720	680	7.82	25.56	5.25	0.542
124A02	17.9	4.50	6	5.64	5.074	9.19	0.36	720	680	7.70	25.53	5.17	0.542
124A03	17.4	4.37	6.12	5.54	4.984	9.19	0.356	730	690	7.70	25.81	5.33	0.555
124A04	17.2	4.32	6.12	5.54	4.984	9.19	0.36	730	690	7.70	25.53	5.33	0.549
124A05	17.7	4.45	8.14	5.63	5.065	9.14	0.363	830	770	7.77	25.18	5.98	0.620
124A06	17.5	4.40	8.16	5.6	5.038	9.14	0.36	830	770	7.77	25.39	6.01	0.625
124A07	17.5	4.40	8.16	5.57	5.011	9.14	0.36	830	760	7.77	25.39	6.07	0.628
(a) LHV (MJ/kg)	37.34												

		FUEL	QF-240	DATE	13-Dec-98		NOX (LS Diesel)	920						
		Water	0.06				Reference	840						
TEST NO.	LOAD (Nm)	POWER (kW)	BMEP (bar)	SOI (DBTC)	IMEP (bar)	Indicated Power (kW)	Air Flow (g/s)	Fuel Flow (g/s)	NOX* (ppm dry)	NO* (ppm dry)	CO2 (%)	AFR	Indicated NOx (g/kW-h)	NOx (g/MJ fuel)
1213B01	17.7	4.45	4.94	4.08	5.65	5.083	9.29	0.353	657	603	7.60	26.32	4.81	0.492
1213B02	17.7	4.45	4.94	4.08	5.67	5.101	9.29	0.353	657	603	7.60	26.32	4.79	0.492
1213B03	18	4.52	5.03	4.08	5.63	5.065	9.29	0.353	657	603	7.60	26.32	4.82	0.492
1213B04	18	4.52	5.03	6.12	5.62	5.056	9.23	0.35	767	712	7.60	26.37	5.57	0.573
1213B05	18	4.52	5.03	6.12	5.71	5.137	9.21	0.352	767	712	7.60	26.16	5.48	0.568
1213B07	17.9	4.50	5.00	8.16	5.62	5.058	9.21	0.357	858	776	7.79	25.80	6.29	0.633
1213B08	18	4.52	5.03	8.16	5.62	5.056	9.21	0.354	849	767	7.79	26.02	6.22	0.632
1213B09	18	4.52	5.03	8.16	5.62	5.056	9.21	0.354	849	767	7.79	26.02	6.22	0.632
(a) LHV (MJ/kg)	39.06													

	FUEL	285-01	DATE	6-Jan-99		NOX (LS Diesel)	920							
	water	0.06				Reference	840							
TEST NO.	LOAD (Nm)	POWER (kW)	SOI (DBTC)	IMEP (bar)	Power (kW)	Air Flow (g/s)	Fuel Flow (g/s)	NOX* (ppm dry)	NO* (ppm dry)	CO 2 (%)	AFR	Exhaust Flow (g/sec)	NOx (g/kW-h)	NOx (g/MJ fuel)
106C07	17.7	4.45	4.08	5.59	5.03	9.35	0.338	657	603	7.40	27.66	9.69	4.88	0.512
106C08	17.7	4.45	4.08	5.56	5.00	9.36	0.337	657	603	7.40	27.77	9.70	4.91	0.514
106C01	17.7	4.45	6.12	5.59	5.03	9.39	0.331	787	694	7.37	28.37	9.72	5.74	0.615
106C02	17.5	4.40	6.12	5.58	5.02	9.34	0.339	776	703	7.47	27.55	9.68	5.79	0.605
106C03	17.5	4.40	6.12	5.51	4.96	9.3	0.335	776	703	7.40	27.76	9.64	5.84	0.609
106C06	17.6	4.42	6.12	5.58	5.02	9.3	0.336	776	703	7.40	27.68	9.64	5.76	0.608
106C09	17.9	4.50	10.14	5.62	5.06	9.22	0.351	1004	858	7.70	26.27	9.57	7.50	0.782
106C10	17.9	4.50	10.2	5.5	4.95	9.27	0.349	1004	867	7.70	26.56	9.62	7.68	0.768
(a) LHV (MJ/kg)	39.37													

Sample Filter Results GO-11 Fuels Nov.-Dec. 98

251-02	9% Water									
Filter Group	SOI	IMEP (bar)	Power(kW)	Deposited Mass (mg)	Sampling Time (min)	Average Pressure (kPa)	Mass Dilution Ratio	Exhaust Mass Flow (kg/s)	Mass Deposited/ Mass Exhaust (mg/kg)	TPR (g/kWhr)
2512	2	5.5	4.95	2.7	17	88.1	11.9	0.00947	92.20	0.66
2514	4	5.5	4.95	2.5	19	88.5	11.9	0.00947	78.96	0.54
2516	6	5.5	4.95	2.5	22	89.5	11.8	0.00948	69.54	0.46
2518	8	5.45	4.90	2.9	22	89.3	12.1	0.00947	79.71	0.55
2519	10	5.41	4.87	2.3	16	87.8	12.1	0.00948	88.41	0.62
285-01	6% Water									
Filter Group	SOI	IMEP (bar)	Power(kW)	Deposited Mass (mg)	Sampling Time (min)	Average Pressure (kPa)	Mass Dilution Ratio	Exhaust Mass Flow (kg/s)	Mass Deposited/ Mass Exhaust (mg/kg)	TPR (g/kWhr)
2852	2	5.5	4.95	3.3	23	84.5	12.1	0.00947	94.47	0.63
2854	4	5.57	5.01	3	22	85	11.9	0.00946	85.20	0.58
2856	6	5.51	4.96	2.9	24	86.7	12	0.0095	74.64	0.51
2858	8	5.58	5.02	3	21	85.6	12	0.00943	89.38	0.62
GO-11	Base									
Filter Group	SOI	IMEP (bar)	Power(kW)	Deposited Mass (mg)	Sampling Time (min)	Average Pressure (kPa)	Mass Dilution Ratio	Exhaust Mass Flow (kg/s)	Mass Deposited/ Mass Exhaust (mg/kg)	TPR (g/kWhr)
GO2	2	5.77	5.19	3.5	19	88.7	11.2	0.00954	106.77	0.69
GO4	4	5.76	5.18	3.7	22	89.5	11.4	0.00953	98.19	0.63
GO6	6	5.64	5.07	3.4	22	92.3	11.2	0.00955	83.69	0.57
GO8	8	5.55	4.99	3.3	22	96.6	11	0.00947	76.23	0.52
GO10	10	5.55	4.99	3.5	22	89	11	0.00944	87.75	0.60
QF-240	6% Water									
Filter Group	SOI	IMEP (bar)	Power(kW)	Deposited Mass (mg)	Sampling Time (min)	Average Pressure (kPa)	Mass Dilution Ratio	Exhaust Mass Flow (kg/s)	Mass Deposited/ Mass Exhaust (mg/kg)	TPR (g/kWhr)
242	2	5.65	5.08	3.1	21	83	12	0.00951	95.25	0.64
244	4	5.6	5.04	3.1	22	86	12	0.00948	87.75	0.59
246	6	5.64	5.07	2.8	22	85.8	12	0.00950	79.44	0.54
248	8	5.58	5.02	2.6	19	85.6	12	0.00950	85.61	0.58
2410	10	5.42	4.88	2.8	20	84.3	12	0.00951	88.94	0.62

SMPS Number and Volume Concentration Results for Range 2 (February 1999)

SOI	No.Conc. (#/cm3) 10^6	Vol Conc. (nm3/cm3) 10^13	Diameter (nm)	SOI	No.Conc. (#/cm3) 10^6	Vol Conc. (nm3/cm3) 10^13	Diameter (nm)
	251-02 (9%)	251-02 (9%)			285-01 (6%)	285-01 (6%)	
4.2	149	62	118	4.08	154	65	121
4.2	147	62	117	4.08	150	63	117
6.12	125	45	113	6.12	129	49	114
6.12	127	46	111	6.12	131	51	113
8.16	140	60	125	8.16	140	62	119
8.16	142	62	123	8.16	141	61	118
Water	0.09			Water	0.06		

SOI	No.Conc. (#/cm3) 10^6	Vol Conc. (nm3/cm3) 10^13	Diameter (nm)	SOI	No.Conc. (#/cm3) 10^6	Vol Conc. (nm3/cm3) 10^13	Diameter (nm)
	GO-11	GO-11			QF-240 (6%)	QF-240 (6%)	
4.08	159	73	127	4.08	151	64	120
4.08	157	71	131	4.08	152	66	117
6.12	138	56	113	6.12	133	51	111
6.12	142	58	114	6.12	131	51	110
6.12	140	57	115	8.16	145	64	117
8.16	132	53	111	8.16	142	59	115
8.16	131	52	109				
				Water	0.06		
Water	0						

TSI Scanning Mobility Particle Sizer

FILENAME: 221C8.000
NOTEFILE:
RESOLUTION: 32 channels/decade
SAMPLE TIME: 13:49:07
SAMPLE DATE: Sun 21 Feb 1999
SAMPLE No: 1, SCANS/SAMPLE: 1
CHARGE CORRECTION: on

SCAN VOLTAGE: 10 V, 10965 V
SCAN RANGE: 19.81 nm to 964.66 nm
VIEW RANGE: 21.29 nm to 897.69 nm
tf: 11.0 s, td: 5.8 s
tup: 100.0 s, tdwn: 60.0 s
Qsh: 2 lpm, Qa: .2 lpm
IMPACTOR D50: 1008 nm

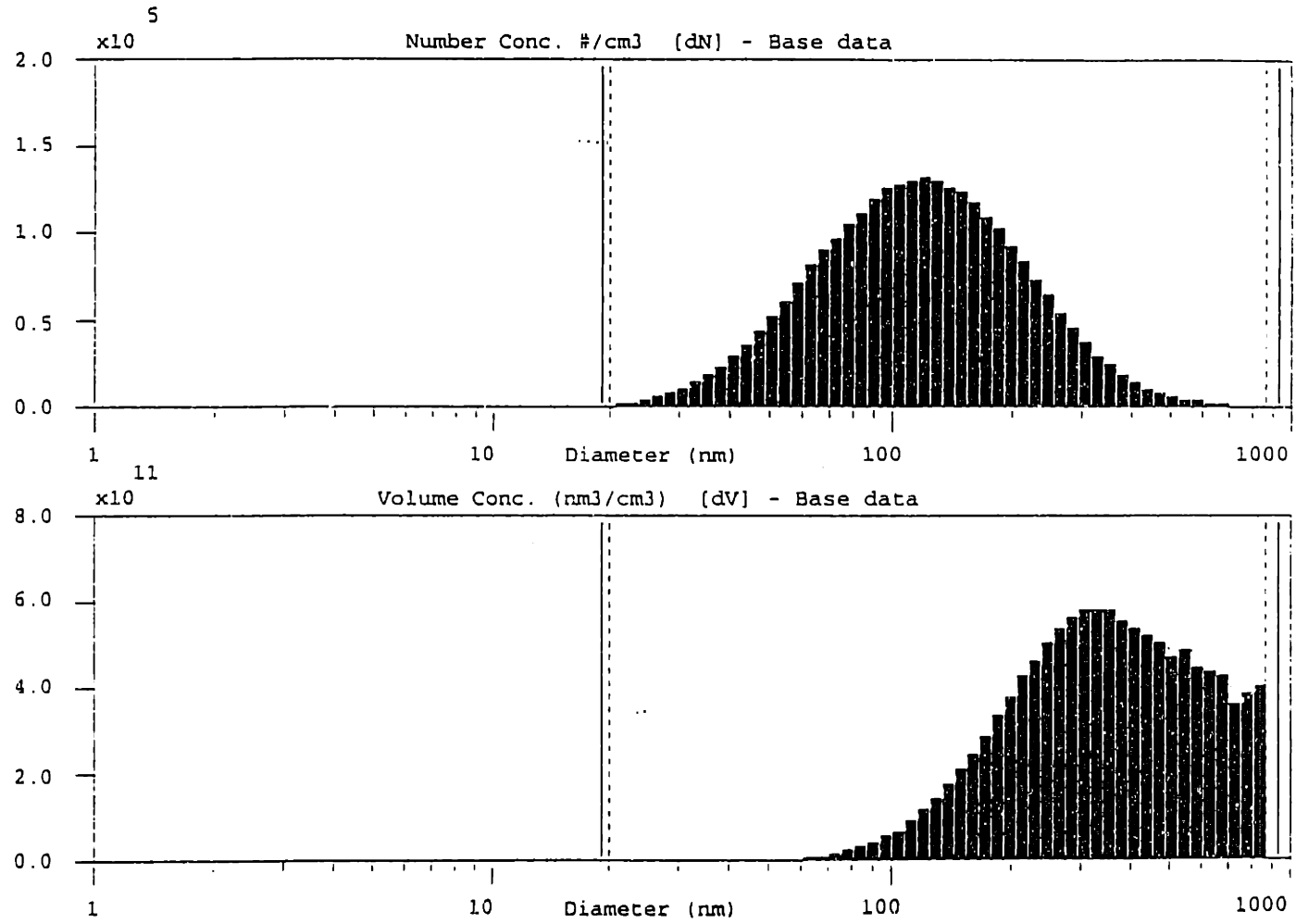

TSI Scanning Mobility Particle Sizer

FILENAME: 221C8.000
NOTEFILE:
RESOLUTION: 32 channels/decade
SAMPLE TIME: 13:49:07
SAMPLE DATE: Sun 21 Feb 1999
SAMPLE No: 1, SCANS/SAMPLE: 1
CHARGE CORRECTION: on

SCAN VOLTAGE: 10 V, 10965 V
SCAN RANGE: 19.81 nm to 964.66 nm
VIEW RANGE: 19.81 nm to 897.69 nm
tf: 11.0 s, td: 5.8 s
tup: 100.0 s, tdwn: 60.0 s
Qsh: 2 lpm, Qa: .2 lpm
IMPACTOR D50: 1008 nm

Particle Size Statistics:	No Assumption(1)	Lognormal Assumption(2)
Number Count:		
median (nm)	117.263	117.263
mean (nm)	140.801	140.853
geometric mean (nm)	117.157	
mode (nm)	119.709	81.272
standard deviation	93.360	
geo. standard deviation	1.832	1.832
skewness	0.226	
coeff. of variation (%)	66.306	
Total Concentration (#/cm3)	2.8562E+06	
Surface Area:		
median (nm)	243.472	244.113
mean (nm)	286.264	
geometric mean (nm)	242.128	293.224
mode (nm)	245.824	
standard deviation	169.141	
geo. standard deviation	1.803	
dia. of average surface (nm)		169.190
Total Concentration (nm2/cm3)	2.5610E+11	
Volume:		
median	343.501	352.215
mean	386.202	
geometric mean	335.870	423.073
mode	305.053	
standard deviation	196.589	
geo. standard deviation	1.732	
dia. of average volume (nm)		203.228
Total Concentration (nm3/cm3)	1.2219E+13	

1 The statistics in 'No Assumptions' column are calculated based on the number size distribution. The validity of the statistics depends on the completeness of the distribution as well as the appropriateness of the calculation. For example: standard deviation and geometric standard deviation cannot both be valid since they are appropriate only for normal and lognormal distributions, respectively.

2 The statistics in the 'Lognormal Assumption' are calculated based on the number median and geometric standard deviation of the sampled data. The remaining values are derived from the Hatch-Choate conversion equations for lognormal distributions.

APPENDIX D

MODELLING

1) Location of Modeling Files

Folder: \Fogo\users\suilivan\thesis\model

Files:		
	215g11.gtm, 221b3.gtm:	model files
	215g11.dat, 221b3.dat:	input files
	215g11.plt, 221b3.plt:	plot files
	215g11.prn, 221b3.prn:	experimental pressure data
	215g11h.prn, 221b3h.prn:	experimental heat release data
	215g11.xls, 221b3.xls:	output files

2) Sample Input Data File – 215g11.dat

```
|===DATA FILE for GTpowerS [Version 4.3.1]
  PROJECT: 215g11.gtm :GTpowerS
| DATE:    Saturday, July 03, 1999
| TIME:    20:24:07
| CREATOR: GT-ISE [Version 4.3.1]
|===RUN
SPECIFICATIONS=============================================================
TimeControl--------------------------------------------------------------
[4.3.1]
 Periodic [ncyc] New 1 AutoStep 1 ign ign [edriver] |TIMCYC DURATN
ISTATE TSMAX TSFIX SSTOL TRLTVAR USRTOL MAINDRV
 None None ign |IRESTR IRESTW IRESTINC
FlowControl--------------------------------------------------------------
[4.3.1]
 def Off Ign ign Off off def def |TSMULT HTFLAG HTSS DTHT FLFLAG REALGAS
CFTRANS HGTRANS
Optimization-------------------------------------------------------------
[4.3.1]
 Off ign ign ign ign ign def def off |DRVOPT OPTVAR PARTNAME OPTVAL
OPTIND RANGE RESOLUTION DAMPING MAXOPT IOPTPLOT
|===PLOT
SPECIFICATIONS=============================================================
PlotPoints---------------------------------------------------------------
-------
 100 |NPTSMX
PlotData-----------------------------------------------------------------
-------
|I/O CMPTYP CMP VARIABLES XLOC
 pf cyl {65544} {temp}
 pf cyl {65544} {NOx}
|===REFERENCE
OBJECTS====================================================================
Driver-------------------------------------------------------------------
[4.2.0]
|NAME TYPE CYCDEG DRVFREQ DRVPROF THETAB THETAE
 partc frequency 720.0 [rpm] ign [ic-eo] 0
EngCylCombDIJet----------------------------------------------------------
[4.2.9.4]
|NAME OVIMEP CMBEND AXZONE
 cmb1 1.7 130 100
 5 0.8 1.2 0.5 1.2 1 1 1 |ASPECT TBMULT CBAIR CAAIR CWALL WALLJT ENTAMP
ENTEXP
 def [evap-mult] [tboil10] [tboil50] [tboil75] [smd-mult] 1.35 1.19 1.01
0.85 0.74 [comb-mult] |TDRAG DVMULT TMP10 TMP50 TMP75 SMDMULT SMD1 SMD2
SMD3 SMD4 SMD5 CMBMULT
 standard ign [delay-mult] [delay-press-exp] [activa-temp] |KDELAYTYP
KDELAYMOD CIGN1 CIGN2 CIGN4
 model3 1 1 [no] |SOOTMDL SFMULT SCMULT NOXMULT
EngCylDataComp-----------------------------------------------------------
[4.0.6]
 DataComp 1 on {pres htrl} {ign ign} |NAME NCDCOMP COMPARE EXT_DATA
FACT_NORM
 THET1> [file1] <
 DATA1> [file2] <
 THET2> [file4] <
 DATA2> [file3] <
EngCylFlow---------------------------------------------------------------
[4.1.1.2]
|NAME FLWTYPE FLWMOD DOHEAD DCHEAD HHEAD SWLRAT TMBRAT UPRIME LRATIO
PCUPNAME
 flw1 standard ign def 0 1e-020 [rswirl] def def def pcup
```

```
EngCylGeom-------------------------------------------------------------
[4.2.1.1]
|NAME BORE STROKE RODLEN PINOFF COMPRAT HCLEAR
 cylg1 80.26 88.9 155.6 0 [CRatio] 0.5
EngCylHeatTr-----------------------------------------------------------
[4.2.0]
|NAME HTRTYP HTMULT AHEAD APIST MULTRAD HGFILE
 htr1 woschni 1 1 1.21 ign ign
EngCylJetOutput--------------------------------------------------------
[4.0.6]
 jetout 1 off {smd} |NAME NCJPLOT XYPLOT XY_PLOTS
 0.1 0.3 0.5 0.7 0.9 |AXIP1 AXIP2 AXIP3 AXIP4 AXIP5
 0.5 0.5 0.5 0.5 0.5 |RADIP1 RADIP2 RADIP3 RADIP4 RADIP5
 off 5 {phb liqfue tzb} |CONTOUR DUMPFREQ XYZ_PLOTS
 off 0.5 zone {phb} |SPATIAL RADLOC XAXIS SPAT_PLOTS
EngCylPistCup----------------------------------------------------------
[4.2.0]
|NAME DCPIST HCPIST DOPIST HHPIST
 pcup 32 15.2 32 7.6
EngCylTWall------------------------------------------------------------
[4.0.3]
|NAME THEAD TPIST TCYL
 tw1 520 520 400
EngFrictionCF----------------------------------------------------------
[4.2.9.1]
|NAME CFA CFB CFC CFD
 fric1 0.32 0.001 0.08665 0.0009
FPropBasicOld----------------------------------------------------------
[4.2.1.1]
|NAME FILENAME EVAPFLUID
 fuelg [fuelg] ign
 fuelli [fuelli] ign
 h2o <h2og.prp> ign
 n2 <n2.prp> ign
 o2 <o2.prp> ign
FPropMixtureCombust----------------------------------------------------
[4.2.1.1]
|NAME STBURN FLBASIC FMI
 air noburn {n2 [n2] o2 [o2] h2o [h2o]}
 resi1 burn {air 0.97 fuelli 0.03}
FStateInitOld----------------------------------------------------------
[4.2.1.4]
|NAME PRES TEMP FLUID FMI
 ptambexh 1.5 1000 {air 1}
 ptambint [imap] [imat] {air 0.97 resi1 0.03}
 ptivc [imap] [imat] {air 0.97 resi1 0.03}
 ptvolef 1.01 298 {air 1}
InjectionProfile-------------------------------------------------------
[4.2.1.2]
 injprf 0.21 4 0.7 |NAME DNOZZ NHOLES CNOZZ
 presprof [SOI] [fuelmass] |TYPE THINJ FUELMG
 THET> 0 [inj-mid1] [inj-mid2] [inj-duration] <
 PROF> [inj-open-press] [inj-mid-press1] [inj-mid-press2] [inj-close-
press] <
ValveCam---------------------------------------------------------------
[4.2.1.7]
 val1 44 1 2.3341 0 180 |NAME VDIA VSTRAN VSTRLF VLASH VTMNG
 THET> -18 0 50 90 <
 LIFT> 0 3.6 3.6 0 <
 L/DI> 0 0.0866 0.2887 <
 CD11> 0 0.2809 0.5231 <
```

```
 CD22> 0 0.2809 0.5231 <
 CSWL> ign <
 CTMB> ign <
|++++++++++++++++++++++++++++++++++++
 val2 40 1 2.5667 0 180 |NAME VDIA VSTRAN VSTRLF VLASH VTMNG
 THET> -90 -60 0 30 <
 LIFT> 0 2.63 2.63 0 <
 L/DI> 0 0.1155 0.2887 <
 CD11> 0 0.2948 0.5497 <
 CD22> 0 0.2948 0.5497 <
 CSWL> ign <
 CTMB> ign <
|===COMPONENT
OBJECTS=============================================================
EndEnvFixedOld-----------------------------------------------------
[4.2.1.3]
|NAME PTCini PTYPE
 exh-env ptambexh total
 int-env ptambint total
EngCylinder--------------------------------------------------------
[4.2.1.7]
|NAME CYLSTART CYLGEOM PTCini PTCvolef COMBcopy OUTPUT
 cylinder [ivc] cylg1 ptivc ptvolef ign last
 tw1 flw1 htr1 cmb1 ign |TWAL FLOW HEATTR COMB SCAV
EngineCrankTrain---------------------------------------------------
[4.2.1.4]
|NAME ENGTYP NCYLS CONFIG VANGLE SPLDOPT RPM FWINER INSTTRQ FRIC ANGSTRT
 engn1 4-stroke 1 in-line ign speed [rpm] ign off fric1 [ivc]
|CYLINDER# FINTRVL CYLGEOM CYLCSLD
 1 0 cylg1 ign
Pipe----------------------------------------------------------------
[4.2.1.7]
|NAME D1 D2 PIPEL DXP ROUGH CFR TWAL HEATC CHT CP1 CP2 FLEXW PTCini UI
PNUM
 pepipe 32 32 76 80 def 0 470 ign 2 0 0 ign ptambexh 0 1
 pipipe 36 36 60 50 def 0 350 ign 2 0 0 ign ptambint 0 1
|===CONNECTION
OBJECTS=============================================================
InjectorConn-------------------------------------------------------
[4.2.9.7]
|NAME TYPE PRFNAME DRIVER ENGINE DIST1 DIST2 #INJ MRATIO TEMPINJ FUELLIQ
FVAP LCONTROL SMOKELIM
 injector proffx injprf * engn1 ign ign ign ign [tfuel] fuelli 0 ign ign
OrificeConn--------------------------------------------------------
[4.2.9.14]
|NAME ONUM PLUG DIA CD1 CD2 LCONTROL HEATCC
ValveConn----------------------------------------------------------
[4.2.9.8]
|NAME ONUM VALNAME CMPCAM CMPENG PAIR# HEATCC
 ve1 1 val2 * engn1 ign ign
 vi1 1 val1 * engn1 ign ign
|===PARTS/MAP=========================================================
=======
PartsList----------------------------------------------------------
-------
|PART# TEMPLATE OBJECT NAME OVERRIDES
 65544 EngCylinder cylinder cylinder
 65545 EngineCrankTrain engn1 engine
 65556 EndEnvFixedOld exh-env exh-en1
 65548 EndEnvFixedOld exh-env exh-en2
 65549 EndEnvFixedOld int-env int-en1
```

```
 65547 EndEnvFixedOld int-env int-en2
 65554 Pipe pepipe pepipe1
 65539 Pipe pepipe pepipe2
 65551 Pipe pipipe pipipe1
 65540 Pipe pipipe pipipe2
SystemMap-------------------------------------------------------------
-------
|PART# TEMPLATE OBJECT CMP1 CMP2 NAME OVERRIDES
 65550 OrificeConn def 65549.1 65551.1 1
 65538 OrificeConn def 65547.1 65540.1 2
 65555 OrificeConn def 65554.2 65556.1 4
 65541 OrificeConn def 65539.2 65548.1 5
 65546 EngCylConn ign 65544.5 65545.1 crnk
 65553 ValveConn ve1 65544.4 65554.1 eval1 CMPCAM=1
 65542 ValveConn ve1 65544.3 65539.1 eval2 CMPCAM=1
 65557 InjectorConn injector 65544.0 ign injector DRIVER=1
 65552 ValveConn vi1 65551.2 65544.1 ival1 CMPCAM=1
 65543 ValveConn vi1 65540.2 65544.2 ival2 CMPCAM=1
|===RUN
CASES=========================================================================
Parameters------------------------------------------------------------------
-------
 activa-temp=3500 comb-mult=.95 CRatio=18.8 delay-mult=1.05 delay-press-
exp=-1.25 edriver=partc
 evap-mult=.3 file1=<215G11.prn> file2=<215G11.prn> file3=<215G11h.prn>
file4=<215g11h.prn> fuelg=<dieselgg.prp>
 fuelli=<diesellg.prp> fuelmass=11.8 h2o=0 ic-eo=442 imap=1.2 imat=355
 inj-close-press=250 inj-duration=11 inj-mid-press1=500 inj-mid-
press2=500 inj-mid1=2 inj-mid2=2.1
 inj-open-press=400 ivc=-139 n2=.79 ncyc=1 NO=.12 o2=.21
 rpm=2400 rswirl=1 smd-mult=0.7 SOI=-9.5 tboil10=453 tboil50=536
 tboil75=567 tfuel=340
End-------------------------------------------------------------------------
-------
```